LA-5781-PR
Progress Report

C. 3

Quarterly Report

Advanced Plutonium Fuels Program

April 1 through June 30, 1974

and

Eighth Annual Report, FY 1974

Compiled by

R. D. Baker

los alamos
scientific laboratory
of the University of California
LOS ALAMOS, NEW MEXICO 87544

This report presents the status of the Advanced Plutonium Fuels Program. The four most recent reports in this series, unclassified, are:

<div align="center">

LA-5390-PR   LA-5582-PR

LA-5477-PR   LA-5660-PR

</div>

In the interest of prompt distribution, this progress report was not edited by the Technical Information staff.

TABLE OF CONTENTS

ABSTRACT

This is the 31st quarterly and eighth annual report on the Advanced Plutonium Fuels Program at the Los Alamos Scientific Laboratory.

Most of the investigations discussed here are of the continuing type.
·Results and conclusions described may therefore be changed or augmented
as the work continues. Published reference to results cited in this report
should not be made without obtaining explicit permission to do so from the
person in charge of the work.

PROJECT 401

EXAMINATION OF FAST REACTOR FUELS

Person in Charge: R. D. Baker
Principal Investigators: J. W. Schulte
                         K. A. Johnson
                         G. R. Waterbury

I. INTRODUCTION

This project is directed toward the examination and comparison of the effects of neutron irradiation on LMFBR Program fuel materials. Unirradiated and irradiated materials are examined as requested by the Fuels and Materials Branch of DRRD. Capabilities are established and are being expanded for providing conventional preirradiated and postirradiation examinations. Nondestructive tests are conducted in a hot cell facility specifically modified for examining irradiated prototype fuel pins at a rate commensurate with schedules established by DRRD.

Characterization of unirradiated and irradiated fuels by analytical chemistry methods were continued and additional methods were modified and mechanized for hot cell application. Macro- and microexaminations were made on fuel and cladding using the shielded electron microprobe, radiochemistry, gamma scanner, mass spectrometers, and other analytical facilities. New capabilities were applied in gamma scanning, analyses to assess spatial distributions of fuel and fission products, mass spectrometric measurements of burnup and fission gas constituents, chemical analyses, and measurement of carbon and oxygen in irradiated fuels.

Microstructural analyses of unirradiated and irradiated materials was continued using optical and electromicroscopy, and autoradiographic and x-ray techniques. New etching and mounting techniques were developed for high burnup materials.

II. EQUIPMENT DEVELOPMENT

A. In-Cell Equipment
   (R. W. Basinger, G. R. Brewer. F. J. Fitzgibbon, M. E. Lazarus, J. M. Ledbetter, P. A. Mason, F. H. Newbury, O. Serna, W. T. Wood)

   1. System for Obtaining Weight and Density of Fuel Pins. A system has been installed to measure in air or in a suitable fluid the weights of irradiated fuel pins up to 61 in. in length in a vertical position. Using the weights in air and in a fluid, the density of irradiated fuel pins can be determined.

   The system consists of a 1000-g analytical balance, with a sensitivity of 0.1 mg, mounted on a cell roof plug directly above a small hole through the plug. A piano wire is attached to the balance and hangs into the operating cell. The fuel pins are weighed by attaching them to a holding device on the end of the piano wire and suspending them in a 152-mm (6-in.) diameter tube installed in the cell. The fill and drain system to permit using a suitable fluid in the submersion of the fuel pins for density determination has been completed and installed. The unit is now operational for irradiated pins.

   2. Sodium Distillation Furnace. The furnace was completed, and thermocouples were attached to both the heating plate and a "dummy" uranium carbide fuel sample mounted in the usual metallography grinding gauge and cup. A temperature of 305°C was attained by the "dummy" fuel sample while maintaining the heating plate at 450°C. To permit heating the fuel samples to the desired 450°C during distillation, the "dummy" sample will be included in

the assembly to provide a true test of the furnace capability.

Figure 401-1 is a photo of the furnace after a distillation operation. Note the deposition of sodium on the concave surface of the liquid-N_2 cold trap. The "dummy" fuel sample with attached thermocouple is also visible on the remotely replaceable heating plate assembly.

3. Electro-Optical Profilometer

a. **Modification and Programs for Current System.** Several modifications have been made to the optical profilometer system in the past year. These changes provide better measurements on bowed rods, a uniform reference position located near the bottom of the fuel elements, and the capability to obtain temperature profiles on any fuel element within the dimensional capacity of the profilometer. A spiral trace capability (requested by GE) for relatively straight fuel elements has also been added to the system and is now undergoing initial testing.

Two computer programs are now available for processing profilometry data. The first provides trace outputs on 35-mm film and on Calcomp graph paper, and a magnetic tape output of corrected data. It also provides a printout of data averaged over any specified length of fuel element together with the standard deviation of the numbers averaged. The second program was developed specifically for HEDL. It utilizes the magnetic tape, generated by the first computer program, to perform the following operations:

(1) Averages $0°$, $45°$, $90°$, $135°$ and $180°$ outputs.

(2) Subtracts the $180°$ run from the $0°$ run, which gives an indication of instrument drift and of errors introduced in the data by element bow in the $0° - 180°$ plane.
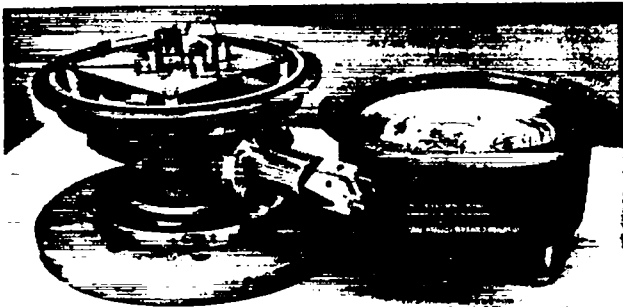
(3) Prints the maximum at each 2.5 mm (0.1 in.) length average.

(4) Prints the minimum at each 2.5 mm (0.1 in.) length average.

(5) Subtracts the minimum from the maximum.

(6) Subtracts a preirradiated constant, provided by the Experimenter, from the average.

(7) Obtains percent change of (6).

(8) Subtracts a postirradiated plenum average from the average.

(9) Obtains a percent change of (8).

b. **Improvements in Program are:**

(1) An electronic centering system for measuring severely bowed fuel elements.

(2) A Parity Error read circuit to ensure the magnetic tape profilometer data are valid while the measurements are being taken. (We presently have to process the results through the Central Computer Facility to determine data validity.)

(3) A microcomputer system to provide automatic system operation, produce standard length tape records, and automatically correct data for bow error.

(4) A second Optical Profilometer system to provide a capability for failed elements.

4. Fission Gas Sampling System.
In order to improve the accuracy of the void volume measurements obtained from fuel pins, a new drilling system was designed for pins up to 9.5 mm (0.375 in.) in diameter. The improved device utilizes a smaller chamber to house the drill. The preceding unit had the flexibility of puncturing capsules or pins from 3.2 to 32 mm (0.125 to 1.25 in.) in diameter, and thus the drill housing had to be large. The new device has been used successfully on several fuel pins.

A request has been received to double-puncture through a 29 mm (1.125-in.) diameter capsule which is NaK filled. The NaK must be frozen during the puncturing operation. Equipment is presently being designed to satisfy this request.

Fig. 401-1. Sodium Distillation Furnace.

5. Fuel Pin Sectioning. Assembly of a new saw was completed as a backup unit for the saw installed in the Disassembly Cell. A new design for a vacuum attachment was installed on the saw to permit more efficient retrieval of dust during sectioning of fuel pins.

A newly designed jig is being fabricated for more accurate positioning of the saw used in sectioning fuel pins. The jig incorporates a micrometer indicator to locate the sectioning cuts with an error less than ± 0.025 mm (0.001 in.). The present requirement of referencing all cuts to the lower welded seam of the fuel clad infers that this position must be established visually which increases the error to ± 0.254 mm (0.010 in.) for the saw cuts relative to the actual clad-end adapter interface.

6. Methods for Preserving Orientation

a. Fuel Pin Striping Fixture. A fixture to permit striping fuel pins with a solid paint line at 0° and a dashed line at 30° has been designed and fabricated. This design will provide improved retention of the pin orientation.

b. Fuel Pin Scribing Fixture. A fixture to permit marking GE fuel pins with scribe marks along the length of the pin at 0°, 90°, and 135° has been designed and built. The scribe marks are easily visible on the macrophotographs and provide a check on the orientation of the transverse metallography samples.

c. Chamfer Tool for Metallography Samples. A tool for chamfering one end of sectioned fuel samples has been designed and constructed. The chamfer readily distinguishes top from bottom on longitudinal metallographic samples.

7. Pulsed Eddy Current Scanner. An indexing mechanism has been incorporated into the Pulsed Eddy Current Scanner to permit the rotational orientation of fuel pins.

8. Data-Logger. A Data-Logger has been ordered which will automatically record thermocouple (TC) output in $^\circ$C. The unit has a capacity of 40 points. Presently, measurements are made by measuring the TC output on a potentiometer and then calculating the temperature using suitable tables.

The Data-Logger will be extremely useful in fuel element length measurements, where the temperature must

be measured every 5 cm (2 in.) along the fuel element. The Length Gauge is shown in Figs. 401-2 and 401-3. Note the holes, spaced at 5-cm (2-in.) intervals, in the aluminum fuel element holders where the TC measurements are made. Measurements are presently made by a single TC inserted in one of the holes until equilibrium is established. The measurement is then repeated in each of the remaining holes. When the Data-Logger is ready for use, TC Assemblies, up to a 30 TC assembly for a 150-cm (60-in.) pin, will be used. Measurements can be printed by the Logger on paper at a rate of 2 measurements/s. The Data-Logger, besides saving time, will eliminate possible errors that can be made when adjusting and reading the potentiometer and when calculating temperatures.

9. Improved Packaging of Fuel Sections. Sections which have been removed from an irradiated fuel pin are placed in a stainless steel sleeve for either storage or intercell transfer. The identity of the specimen is scribed on the sleeve. The ends of the sleeve are secured with socket head set screws. For storage, the loaded sleeves are placed in a stainless steel tube which is sealed in an inert atmosphere with solder joints. Intercell movement is effected with the usual transfer devices.
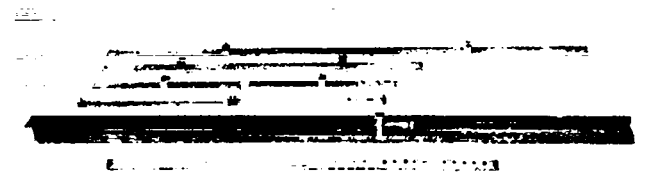

Fig. 401-2. Length Gauge.

Fig. 401-3. Length Gauge - Closeup (of Readout Unit).

10. **Improvements Made in the Metallography Cells.** Another filter assembly was built and installed in the Slurper Drains of the Metallography Cells. The filter utilizes a disposable package concept for easier replacement. Teflon O-rings are used to eliminate previous problems of swelling encountered with neoprene and viton O-rings.

A bell jar assembly utilizing a heating plate was fabricated to permit potting of metallography samples in a new epoxy resin. A temperature of $80^{\circ}C$ is required for proper curing.

Two new fixtures were fabricated and installed to improve efficiency in preparing metallographic samples.

A newly designed macrophotography Loading Device was fabricated and placed in service.

A Vacuum Potting Box, with design requirements furnished by the metallographer, was fabricated and prepared for installation.

A micrometer stand for verification of the grinding depth obtained during metallograph sample preparation has been designed and fabricated.

11. **Miscellaneous Equipment.**

a. A second trunnion fixture for loading the radiography cask has been placed in service. This eliminates the necessity for transferring the fixture between the Wing 9 and DP-West Facilities.

b. The radiography cart was overhauled. The lead screw shaft end was modified, machined, and new drive gears installed with dowel pins for more reliable operation.

c. An additional set of collimators was fabricated to provide a 1.3-mm (0.050-in.) slit for gamma scanning.

d. A Boom Hoist Assembly was designed to assist unloading fuel capsules in two of the hot cells at the DP-West Facility.

e. Preparations are being made for the installation of the General Electric "oxygen potential" instrument in a hot cell at Wing 9. The equipment is scheduled for arrival at LASL in August 1974.

f. Preliminary design studies have been conducted on the installation of an electro-optical profilometer in the replacement disassembly alpha box. Fuel pins will be measured within the inert atmosphere of the alpha box permitting the profiling of breached pins if desired.

B. **Development Work and Maintenance of Manipulators**
(W. R. Carter, E. L. Mills, P. A. Mason)

Two minimanipulators used in the metallography blister were overhauled; one was modified to permit easier installation.

Five AMF manipulators required tape replacement; eleven manipulator boots were replaced.

Ten AMF manipulators were modified to permit installation of the new design seal packages which will provide better control of atmosphere and contamination. (Refer to next section on "Inert Atmospheres" for a description of seal package.)

Manipulators utilizing the newly designed through-tube seal packages were installed in the cell containing the Na-Distillation Furnace Assembly to provide an improved capability for controlling the purity of the inert atmosphere.

C. **Inert Atmosphere Systems**
(R. W. Basinger, P. A. Mason)

The design of the manipulator through-tube seal package was improved. Compared to the previous design, an improvement of > 50 times ΔP is attainable for a given boot purge flow rate. The design of an assembly for sealing the exterior of the through-tube of the manipulator to the alpha box penetration ports has been completed utilizing an inflatable inner tube.

With the installation in the Disassembly Cell of manipulators incorporating the new design of through-tube seal packages, the air leakage due to diffusion through the booting material has been eliminated. This reduced the overall air leak-rate into the cell sufficiently to permit operating the recirculating purifier. Levels of 3 to 10 ppm O_2 and < 1 ppm H_2O are being currently maintained for the Disassembly Cell atmosphere.

Figure 401-4 displays both the internal seal package and the external inflatable seal packages in use on some manipulators.

A certified bottle of Ar with 10 ppm O_2 was obtained to allow a verification of the accuracy of the built-in calibrator unit of the Delphi Oxygen Analyzers. The two methods agreed well within the certified accuracy of

Fig. 401-4. AMF Manipulator Through-Tube Seal
Assemblies.

10 ± 0.05 ppm for the standard gas. The analyzers in
service will be recalibrated on a monthly basis with the
standardized gas, in addition to the weekly calibration
performed with the built-in test unit.

In an effort to reduce the operating costs of maintain-
ing the inert atmosphere cells, N_2 gas has been substituted
for the Ar gas previously used. The N_2 gas contains ap-
proximately 0.7 ppm O_2 and < 1 ppm H_2O. The carbide
fuels will continue to be stored in an Ar atmosphere as
requested.

Installation of manipulators incorporating the new
through-tube seal package in the Metallography Cells has
been delayed due to a shortage of manipulator boots. A
shipment of boots received recently, contained a design
change unsuitable for our use. The boots were returned
to the factory. A replacement shipment is expected soon.

D. Shipping Casks
(F. J. Fitzgibbon, J. W. Schulte)

Modifications have been made to both casks (designated
AEC-AL USA/5885/BLF) to permit handling at the EBR-
II facilities, HFEF-North, and HFEF-South. The required
tests were performed at HFEF-South to demonstrate com-
patibility. Personnel from ANL adapted a lifting fixture
to permit use of the LASL cask inserts (approximating
2R containers). Shipments of fuel pins in the modified
casks have already been made using a threaded pipe in-
sert, a 19-hole insert, and a 6-hole insert.

The T-2 casks have been loaded and unloaded success-
fully several times using special fixtures to handle the
cask inserts.

The small (900 kg) "Analytical Sample" cask was used
on 3 occasions to ship irradiated fuel specimens to HEDL.

Minor design changes are currently being considered
to assure that the Rover casks survive the 30-ft-drop test
required in Chapter 0529 of the AEC manual. The casks
are scheduled for "recertification" in FY 1975.

III. ANALYTICAL CHEMISTRY

A. Gamma Scanning
(J. R. Phillips, T. K. Marshall, J. R. Netuschil,
J. N. Quintana)

The axial burnup profiles of six, low-burnup (< 1 at.%)
(U,Pu)O_2 fuel pins were determined using precision gamma
scanning by measuring the relative axial isotopic distri-
butions of ^{95}Zr. The ^{95}Zr isotope was selected because
of its high gamma-ray activity, uncomplicated gamma-
ray spectra (724 and 756 keV), and especially its tendency
to remain with the fuel material. The burnup profiles
(Fig. 401-5) illustrated the effect of the axial reflectors
in EBR-II upon the axial neutron flux profile which was
slightly higher at the top and bottom due to the reflected
neutrons. The burnup profiles determined by gamma
scanning agreed within 3 to 5% with results obtained by
destructive mass spectrometric analyses.

Significant differences in the axial isotopic distributions
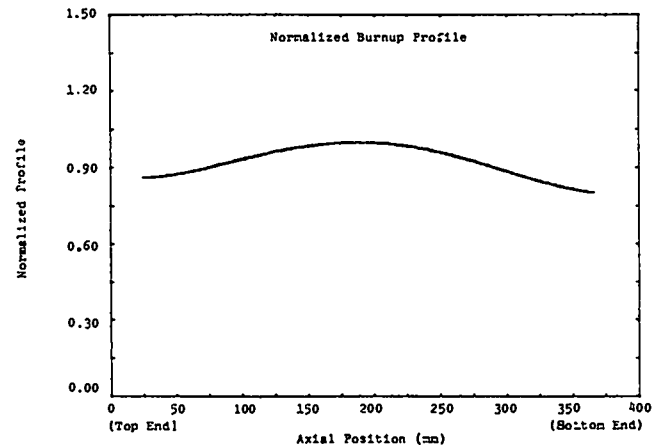of ^{103}Ru and ^{106}Ru isotopes in several (U,Pu)O_2 fuel pins

Fig. 401-5. Axial burnup profile obtained from the ^{95}Zr
isotopic distribution in a (U,Pu)O_2 fuel pin.

were found. The axial isotopic distributions of ^{103}Ru and ^{106}Ru isotopes for a failed (U,Pu)O$_2$ fuel pin irradiated in EBR-II at 11 at.% burnup (Fig. 401-6) showed that nearly 16.5% of the total ^{103}Ru activity was located in the three spikes at the 1228-, 1233-, and 1376-mm positions, but 29.4% of the total ^{106}Ru activity was at several locations between 1228 and 1376 mm. The difference in the two distributions resulted from the large differences in the half-lives of the two Ru isotopes: ^{103}Ru(39.6d) and ^{106}Ru(369d). The ^{103}Ru axial distribution reflects the axial locations where Ru was being deposited possibly in the form of metallic inclusions at the conclusion of the most recent irradiation cycle. The ^{106}Ru (longer half-life) shows the locations where Ru was deposited in the earlier irradiation cycles. Analysis of the two Ru isotope distributions should allow the fuel engineer to assign relative times to the formation of Ru deposits within the fuel matrix.
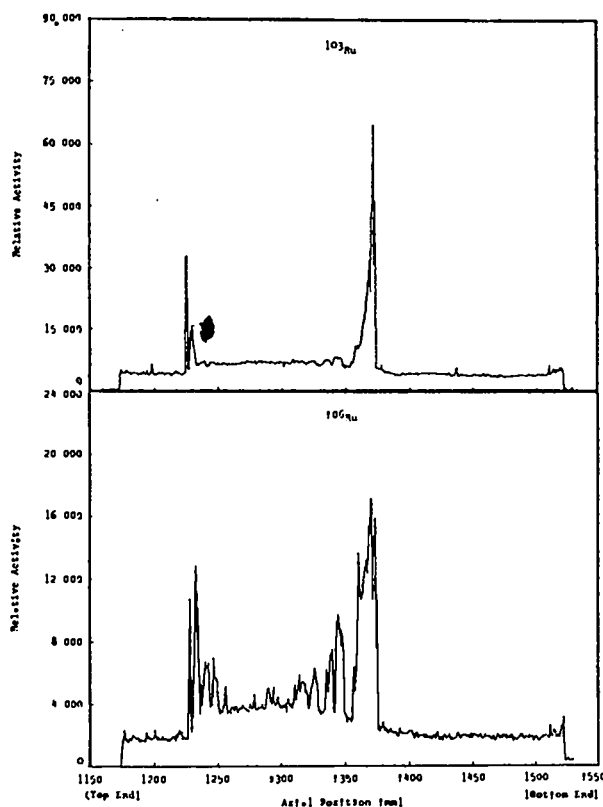
Fig. 401-6. The axial isotopic distribution of ^{103}Ru and ^{106}Ru for an irradiated (U,Pu)O$_2$ fuel pin.

Precision gamma scanning was applied to the nondestructive quantitative determination of fission products in irradiated (U,Pu)C and (U,Pu)O$_2$ fuel pins. The quantitative determination of gamma-ray emitting isotopes was made possible by a detailed calibration of the gamma scanning system including: measurement of the effective collimating slit, detector surface response functions, and the development of a computer code for simulation of various source geometries. Following the nondestructive gamma scanning examinations of the irradiated fuel materials, the samples were dissolved remotely, and analyzed independently by well-proven radiochemical methods.

Three sections of irradiated (U,Pu)C fuel pins having undergone about 9.5 at.% burnup were analyzed for ^{106}Ru-^{106}Rh, ^{137}Cs, and ^{144}Ce-^{144}Pr. The comparison of the gamma scanning results with the destructive radiochemical results are presented in Table 401-I. The absolute average deviation for all three fission products was 3.2% for the three (U,Pu)C fuel sections.

Three irradiated (U,Pu)O$_2$ fuel sections were similarly analyzed for ^{106}Ru-^{106}Rh, ^{137}Cs, ^{144}Ce-^{144}Pr, and ^{95}Zr. The results for these four fission products are presented in Table 401-II. The ^{106}Ru-^{106}Rh, ^{137}Cs, and ^{144}Ce-^{144}Pr gamma scanning results compare very well with the radiochemical results with average differences of 4.3%, 4.0%, and 2.9%, respectively. One exception is the second set of ^{106}Ru-^{106}Rh results which were significantly different. This particular section was scanned diametrically to determine the radial isotopic distributions of the fission products. The radial distribution of ^{106}Ru-^{106}Rh indicated that a significant amount (about 20% of the total ^{106}Ru-^{106}Rh activity) was deposited around the central void of the fuel probably in the form of metallic ingots. It appears that during the handling of the sample after gamma scanning, the ^{106}Ru-^{106}Rh deposits were dislodged and lost. The possibility of loss of sample material is eliminated when nondestructive gamma scanning is used to examine the fuel material, and the sample remains available for reanalysis to check the results if necessary.

TABLE 401-I

Gamma Scanning and Radiochemical Quantitative Results for Three (U, Pu) Carbide Sections

Isotope	Gamma Scanning* (Atoms)**	Radiochemical* (Atoms)**	Difference
^{106}Ru- ^{106}Rh			
	$1.74 \pm 0.04 \times 10^{18}$	$1.80 \pm 0.05 \times 10^{18}$	3.1 %
	$2.08 \pm 0.04 \times 10^{18}$	$2.13 \pm 0.04 \times 10^{18}$	2.6 %
	$1.69 \pm 0.03 \times 10^{18}$	$1.76 \pm 0.06 \times 10^{18}$	3.6 %
		Average	3.1 %
^{137}Cs			
	$5.27 \pm 0.06 \times 10^{19}$	$5.40 \pm 0.06 \times 10^{19}$	2.5 %
	$6.12 \pm 0.06 \times 10^{19}$	$5.80 \pm 0.06 \times 10^{19}$	5.5 %
	$4.89 \pm 0.06 \times 10^{19}$	$4.97 \pm 0.06 \times 10^{19}$	1.6 %
		Average	3.2 %
^{144}Ce- ^{144}Pr			
	$4.66 \pm 0.08 \times 10^{18}$	$4.78 \pm 0.09 \times 10^{18}$	2.5 %
	$5.76 \pm 0.08 \times 10^{18}$	$5.45 \pm 0.08 \times 10^{18}$	5.8 %
	$4.58 \pm 0.08 \times 10^{18}$	$4.58 \pm 0.08 \times 10^{18}$	0.0 %
		Average	2.8 %

* The ± value associated with each measurement represents the deviation due to only the counting statistics.

** The number of atoms was computed using the appropriate half-lives and branching ratios.

The ^{95}Zr results show a constant bias of about 9.3%, with the gamma scanning results being lower than the radiochemical results. This bias is attributed to the method of extrapolation used to determine the surface response function for the 724-keV gamma ray of ^{95}Zr. The 661.6-keV gamma ray of ^{137}Cs was used as the reference standard for the 622-keV (^{106}Ru- ^{106}Rh) and 695-keV (^{144}Ce- ^{144}Pr) gamma rays. The method of interpolation of surface response functions appeared to be satisfactory for the two adjacent gamma rays; however, an additional factor will be incorporated in the extrapolation to the 724-keV gamma ray of ^{95}Zr.

This nondestructive method for the quantitative determination of fission products does not require the use of irradiated fuel standards, eliminating the major obstacle to quantitative gamma scanning. The detailed calibration of the system along with the computer code for simulation of service geometrics is all that is necessary for quantitative gamma scanning. The development of quantitative gamma scanning adds another dimension to provide nondestructively more detailed information about the behavior of fission products within irradiated fuel materials.

B. Sealed-Reflux Dissolution System
(J. W. Dahlby, R. R. Geoffrion)

A new method using a sealed-reflux dissolution system was developed for dissolving difficult soluble irradiated materials. More than 60 irradiated fuel-clad samples ranging from 0.003 to 12.5 at.% burnup have been successfully dissolved using this method. In this method, the sample is reacted in a covered beaker with HNO_3, HCl, HF, or with mixtures of these acids, and any undissolved residue is washed into a fused-silica tube (Fig. 401-7) with water. The tube and water are heated to approximately

TABLE 401-II

Gamma Scanning and Radiochemical Quantitative Results for Three (U, Pu) Carbide Sections

Isotope	Gamma Scanning[*] (Atoms)[**]	Radiochemical[*] (Atoms)[**]	Difference
^{106}Ru–^{106}Rh			
	$1.17 \pm 0.03 \times 10^{18}$	$1.12 \pm 0.03 \times 10^{18}$	5.0 %
	$1.34 \pm 0.03 \times 10^{18}$	$9.55 \pm 0.12 \times 10^{17}$	40.1 % (Reject)
	$1.28 \pm 0.03 \times 10^{18}$	$1.25 \pm 0.02 \times 10^{18}$	3.6 %
		Average	4.3 %
^{137}Cs			
	$3.50 \pm 0.04 \times 10^{19}$	$3.61 \pm 0.04 \times 10^{19}$	3.1 %
	$5.68 \pm 0.05 \times 10^{19}$	$5.83 \pm 0.05 \times 10^{19}$	2.8 %
	$4.17 \pm 0.05 \times 10^{19}$	$4.44 \pm 0.05 \times 10^{19}$	6.0 %
		Average	4.0 %
^{144}Ce–^{144}Pr	$2.34 \pm 0.06 \times 10^{18}$	$2.40 \pm 0.03 \times 10^{18}$	2.8 %
	$2.54 \pm 0.08 \times 10^{18}$	$2.45 \pm 0.03 \times 10^{18}$	3.9 %
	$2.39 \pm 0.08 \times 10^{18}$	$2.44 \pm 0.03 \times 10^{18}$	1.9 %
		Average	2.9 %
^{95}Zr	$1.36 \pm 0.10 \times 10^{16}$	$1.52 \pm 0.03 \times 10^{16}$	10.8 %
	$1.37 \pm 0.07 \times 10^{16}$	$1.49 \pm 0.03 \times 10^{16}$	8.0 %
	$1.28 \pm 0.08 \times 10^{16}$	$1.41 \pm 0.03 \times 10^{16}$	9.1 %
		Average	9.3 %

[*] The ± value associated with each measurement represents the deviation due to the counting statistics.

[**] The number of atoms was computed using the appropriate half-lives and branching ratios.

85°C to evaporate the slurry to dryness with the aid of an air stream directed on the liquid. An acid mixture consisting of 2 ml of 12$\underline{M}$ HCl, 1 drop of 15$\underline{M}$ HNO$_3$, and 1 drop of 0.41$\underline{M}$ HF is added, and the tube is then sealed with a rubber stopper and clamped. The tube is placed in a metal block (Fig. 401-8) and heated to 150°C until the sample is dissolved. Internal pressures in the tube range up to 0.8 MPa (115 psi). Dissolution times range from a few hours for samples having up to 8 at.% burnup to 24 h for samples having up to 12.5 at.% burnup. Small samples (100 mg) of oxide fuels can be added directly to the fused-silica tube for dissolution.

Other acid systems have also been tested as well as larger containers in which up to 500 mg samples can be dissolved. This technique has also been successfully applied to the dissolution of high fired PuO$_2$, ThO$_2$,

and highly irradiated (Np-Zr-Ca-Pu) oxide materials. Major advantages of the sealed-reflux dissolution system are its simplicity and its ability to release pressures above approximately 1 MPa without loss of sample. This essentially eliminates the possibility of the tube rupturing due to high pressure surges.

C. Determination of Retained Fission Gases in Irradiated Fuels
(R. M. Abernathey, J. W. Dahlby, R. R. Geoffrion)

Measurement of the quantities of gaseous fission products in the fuel pin plenum relative to that retained in the (U,Pu)O$_2$ fuel matrix is important in investigations of gas-release mechanisms. The measurement of the gaseous fission products in the fuel pin plenum is routinely done at LASL in postirradiation examinations of fuel pins. Specialized equipment was assembled to collect and measure
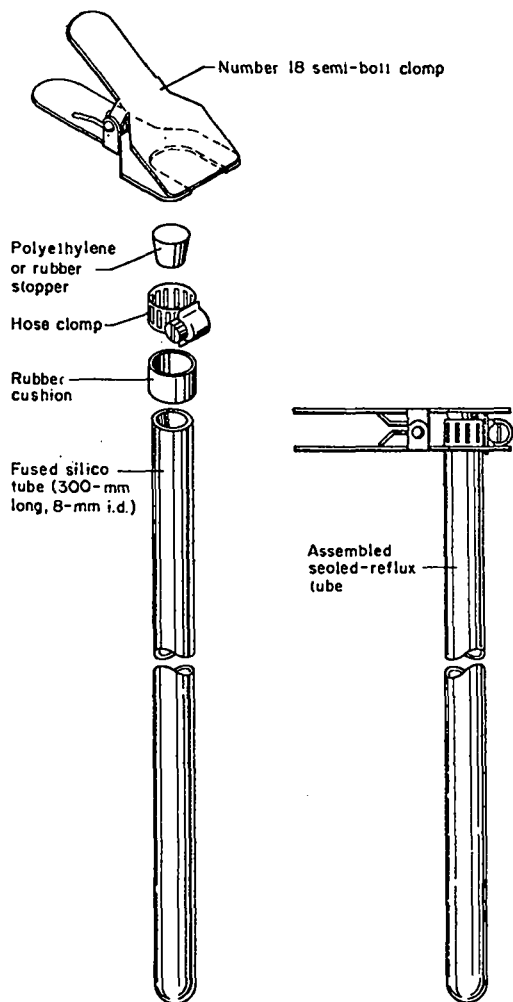
Fig. 401-7. Sealed-reflux dissolution tube and accessories.

Fig. 401-8. Heating block for sealed-reflux dissolution system.

the retained fission gases in irradiated $(U,Pu)O_2$ fuel materials.

In this method, the $(U,Pu)O_2$ fuel section is dissolved remotely in a HNO_3-HF acid mixture to release the fission gases. Known amounts of Kr and Xe enriched in nonfission product isotopes are added to the fission gases which are collected, purified, and analyzed mass spectrometrically for total quantities and isotopic distributions.

Five 2-g cross sections of $(U,Pu)O_2$ fuel with < 1 at.% burnup were analyzed by this technique. The isotopic distributions of the retained fission gases relative to the plenum fission gases were significantly different with the

^{83}Kr, ^{131}Xe, and ^{132}Xe isotopes being higher in abundance in the retained fission gas samples. The precursors of the Kr and Xe isotopes in these chains have the longest half-lives and possibly tend to remain in the fuel matrix.

D. Electron Microprobe Automation

(W. F. Zelezny, W. B. Hutchinson, L. C. Haynes)

The shielded electron microprobe was automated using a small digital computer (PDP-11) to perform the following operations: setting of two spectrometers, translation of the specimen stage, monitoring of the aperture current, and the control of the timer, scalers, and pulse-height analyzers for two x-ray readout channels. More than 20 programs have been written for automated data acquisition and processing for the examination of irradiated specimens. Program capabilities include: the computer-controlled movement of the spectrometers to the correct setting for the desired element upon typing in the chemical symbol, and the option of peak-seeking to determine precise spectrometer settings. The acquired data are transmitted to the Central Computing Facility for obtaining graphical plots for analysis reports.

The automation of the electron microprobe has improved the system reliability by eliminating possible

human error, and has reduced the data acquisition and processing time by nearly 50% for the examination of irradiated fuel samples.

E. Determination of Oxygen Potential in Irradiated Oxide Fuels
(G. C. Swanson, J. W. Dahlby)

The oxygen potential of reactor oxide fuels is an important parameter affecting actinide migration, fuel-clad interaction, and other important fuel properties. A solid-state, electrochemical oxygen potential meter was ordered from the General Electric Company for use in measuring oxygen potential of irradiated oxide fuels. The equipment is expected to be delivered early next fiscal year. Representatives of GE have visited LASL twice to verify dimensions, to establish installation procedures, and to specify necessary ancillary equipment. All equipment to install and use with the meter is on hand.

IV. MICROSTRUCTURAL ANALYSIS
(J. H. Bender, D. D. Jeffries, K. A. Johnson, J. L. Lehmann, L. N. Sanchez)

Scanning electron microscope techniques, fully applicable to routine use, were applied to moderate (< 200 mr/hr at a meter) beta-gamma radioactive LMFBR claddings. The resolution of the SEM for nonirradiated materials has been improved to 10 nm this year.

Mounting and specimen impregnation methods and materials were improved during the year. The polyester base mounting material has proven to be a slightly superior mounting and reimpregnation material. However, in higher burnup (> 5-7 at.%) and in regions containing large deposits of fission products, it is still not as reliable as could be desired. Development efforts will continue in this area.

The results of the grinding experiments and other developments have been applied to the hot cell metallographic grinding with a significant increase in throughput rate at this step.

Ion gun etching development has continued this year with the solution to the small etched spot problem being achieved through a combination of a minor gun design change and somewhat different operating conditions.

Major revisions were made during the year to the microstructural analysis quality assurance documentation

and overcheck system. These efforts have resulted in significant improvements in the product quality and in catching defects at much earlier stages.

An additional darkroom has been put into full operation during the year. It contains an autoprocessor for developing films and negatives. Films and processes have been intensively tested, and integrated implementation of superior systems (materials, processes, and techniques) has started.

V. REQUESTS FROM DRRD

A. Examination of Irradiated Materials
(R. M. Abernathey, K. A. Johnson, M. E. Lazarus, R. A. Morris, J. R. Phillips, J. W. Schulte, G. R. Waterbury, W. F. Zelezny)

During the 1974 fiscal year, 114 irradiated fuel elements were received as listed in Table 401-III.

General Electric Company. During the 1974 fiscal year, 55 irradiated fuel elements were received. Examinations performed on 56 fuel elements, received between March 21, 1973, and June 20, 1974, are listed in Table 401-IV.

Secondary fission gas samples, taken from eight F20 series fuel pins, have been shipped to GE for analysis. Samples from the remaining F20 fuel pins will be shipped as containers become available.

Fission gas samples from four irradiated fuel pins were sent to NRTS for analysis of Xe isotopes.

Ten irradiated structural assemblies (L-16 Series) were shipped to ANL-West following nondestructive

TABLE 401-III

IRRADIATED FUEL ELEMENTS RECEIVED IN FY 1974

Fiscal Year Quarter	Advanced Fuel Type	Oxide Fuel Type
1st	2	15
2nd	--	25
3rd	--	34
4th	15	23
Total	17	97

Hanford Engineering Development Laboratory. During the 1974 fiscal year, 42 irradiated fuel elements were received. Examinations performed on 46 irradiated fuel elements, received between February 1, 1973, and March 21, 1974, are listed in Table 401-V.

TABLE 401-IV

POSTIRRADIATION EXAMINATIONS OF CAPSULES AND PINS FROM GE

Examination	No. of Capsules	No. of Pins
1. Visual Inspection	28	39
2. Preliminary Measurements	55	52
3. Profilometry, Optical	30	49
4. Profilometry, Mechanical	—	4
5. Radiography	18	24
6. Gamma Scan[a]	57	--
7. Gas Sampling and Analysis	50	34
8. Na Removal	42	—
9. Clad Removal	42	—
10. Photography, Full Length	8	56
11. Photography, Maximum Bow	16	26
12. Photography, Incremental	5	57
13. Wire Wrap Removal	3	58
14. Eddy Current	3	34
15. Weight	21	--
16. Balance Point	21	--
17. Diameter Measurement, Micrometer	--	4
18. Sectioning	—	49
19. Density Measurement[b]	—	28 (71 samples)
20. Profilometry, Capsule Clad	4	--
21. Length Measurement	—	3
22. Photography, Sectioned Faces	—	2
23. Atom % Burnup	—	30 (40 samples)
24. Shielded Electron Microprobe	—	10 (15 samples)
25. O_2 in Clad	—	7 (12 samples)
26. Total Cs	—	3 (6 samples)
27. ^{134}Cs by Radiochemistry	—	3 (6 samples)
28. ^{137}Cs by Radiochemistry	—	3 (6 samples)
29. ^{134}Cs/^{137}Cs by Gamma Scan	--	1 (3 samples)
30. Na Analysis	—	1
31. Leach of Clad Plenum	--	3 (6 samples)
32. Shipment of Solutions to HEDL	--	2
33. Microstructural Analysis[c]	--	30 (98 samples)

[a] 208 Gross gamma scans, 61 complete spectral scans, and 541 isotopic distributions of fission and activation products were determined.

[b] There were also 10 unirradiated samples on which the density was determined.

[c] The optical microscopy includes macrophotography, alpha autoradiography, beta-gamma autoradiography, and as-polished and etched photomicroscopy, (including mosaics). The hot cell operations were conducted in an inert (N_2) atmosphere. Specimens from other experimenters were examined in a like manner.

TABLE 401-V

POSTIRRADIATION EXAMINATIONS OF CAPSULES AND PINS FROM HEDL

Examination	No. of Capsules	No. of Pins
1. Visual Inspection	3	28
2. Preliminary Measurements	9	43
3. Profilometry, Optical	--	6
4. Radiography	21[a]	23
5. Gamma Scan[b]	36	--
6. Gas Sampling and Analysis	3	3
7. Na Removal	3	--
8. Clad Removal	3	--
9. Photography, Full Length	9	25
10. Photography, Maximum Bow	9	24
11. Photography, Incremental	9	25
12. Wire Wrap Removal	--	8
13. Eddy Current	--	4
14. Sectioning	--	16
15. Na Melting and Pressuring Tests	--	2
16. Atom % Burnup	--	10 (24 samples)
17. Shielded Electron Microprobe	--	7 (15 samples)
18. Retained Fission Gas	--	1 (5 samples)
19. Microstructural Analysis	--	17 (69 samples)

[a] One GETR capsule assembly is included.

[b] 107 Gross gamma scans, 39 complete spectral scans, 4 TWODIMS, and 293 isotopic distributions of fission and activation products were determined. Also axial burnup profiles over the enriched fuel columns of 6 capsules were determined from gamma scan data.

The following materials were sent to HEDL as special shipments:

1. Fuel sections from two irradiated fuel pins

2. Residues from solutions of six pin sections and one 6.4-mm cross-section sample

3. Seventeen pins from the HEDL P-20 Series, following nondestructive (and some destructive) testing at LASL.

4. Two inserts from the Rover casks.

Los Alamos Scientific Laboratory. In this section, examinations of carbide and nitride fuel elements are discussed. The technical evaluation of these elements is being carried out by LASL personnel under the Advanced Fuels Program.

1. BMI Experiments -- In the 1974 fiscal year, three irradiated fuel elements were received. Examinations performed on seven fuel elements received between October 11, 1972, and May 6, 1974, are listed in Table VI.

TABLE 401-VI

POSTIRRADIATION EXAMINATIONS OF CAPSULES AND PINS FROM BMI

	Examination	No. of Capsules	No. of Pins
1.	Visual Inspection	2	2
2.	Preliminary Measurements	3	2
3.	Profilometry, Optical	2	2
4.	Profilometry, Mechanical	--	2
5.	Radiography	2	2
6.	Gamma Scan[a]	2	--
7.	Gas Sampling and Analysis	4	3
8.	Na Removal	4	--
9.	Clad Removal	4	--
10.	Photography, Full Length	3	2
11.	Photography, Incremental	--	4
12.	Eddy Current	--	2
13.	Sectioning	--	2
14.	Density Measurements	--	2 (2 samples)
15.	Atom % Burnup	--	2
16.	Electron Microprobe	--	1
17.	Microstructural Analysis	--	5 (24 samples)

TABLE 401-VI (continued)

[a]Eight gross gamma scans, one complete spectral scan, and 15 isotopic distributions of fission and activation products were determined.

BMI capsules 1-4 and 2-5 were returned to NRTS for re-insertion.

2. Gulf United Experiments -- During the 1974 fiscal year, 10 irradiated fuel elements were received. Examinations performed on 13 irradiated fuel elements, received between September 10, 1971, and May 6, 1974, are listed in Table 401-VII.

TABLE 401-VII

POSTIRRADIATION EXAMINATIONS OF CAPSULES AND PINS FROM GU

	Examination	No. of Capsules	No. of Pins
1.	Visual Inspection	8	2
2.	Preliminary Measurements	12	3
3.	Profilometry, Optical	2	1
4.	Radiography	6	1
5.	Gamma Scan[a]	7	--
6.	Gas Sampling and Analysis	--	1
7.	Photography, Full Length	4	1
8.	Photography, Incremental	2	1
9.	Wire Wrap Removal	1	1
10.	Eddy Current	1	1
11.	Sectioning	--	1
12.	Atom % Burnup	--	5
13.	Electron Microprobe	--	2
14.	Microstructural Analysis	--	2 (5 samples)

[a]Twenty-eight gross gamma scans, 9 complete spectral scans, and 79 isotopic distributions of fission and activation products were determined.

3. Los Alamos Scientific Laboratory Experiments -- During the 1974 fiscal year, three fuel elements were received. Examinations performed on six irradiated fuel elements, received between October 11, 1972, and May 6, 1974, are listed in Table 401-VIII.

TABLE 401-VIII

POSTIRRADIATION EXAMINATION OF CAPSULES AND PINS FROM LASL

	Examination	No. of Capsules	No. of Pins
1.	Visual Inspection	1	1
2.	Preliminary Measurements	2	1
3.	Profilometry, Optical	1	1
4.	Profilometry, Mechanical	1	--
5.	Radiography	3[a]	--
6.	Gamma Scan[b]	1	--
7.	Gas Sampling and Analysis	2	1
8.	Na Removal	2	--
9.	Clad Removal	2	--
10.	Photography, Full Length	1	2
11.	Photography, Incremental	--	2
12.	Eddy Current	--	1
13.	Sectioning	--	2
14.	Density Measurements	--	1
15.	Na Melting and Pressurizing Tests	--	1
16.	Atom % Burnup	--	1
17.	Electron Microprobe	--	3
18.	Microstructural Analysis	--	3 (13 samples)

---

[a]This includes 2 TREAT capsule assemblies.

[b]Four gross gamma scans, and 4 isotopic distributions of fission and activation products were determined.

Density measurements (3 in-cell and 22 out-of-cell) were made on 13 unirradiated archive cladding samples.

4. WARD Experiments -- During the 1974 fiscal year, one irradiated fuel element was received. Experiments performed on three irradiated fuel elements, received between February 21, 1973, and May 6, 1974, are listed in Table 401-IX.

Other Examinations -- Thirteen samples were analyzed for tritium, and lithium was determined on two samples for Gulf General Atomic.

TABLE 401-IX

POSTIRRADIATION EXAMINATION OF CAPSULES AND PINS FROM WARD

	Examination	No. of Capsules	No. of Pins
1.	Preliminary Measurements	1	--
2.	Profilometry, Optical	1	--
3.	Gamma Scan[a]	1	--
4.	Gas Sampling and Analysis	--	1
5.	Photography, Full Length	--	3
6.	Photography, Maximum Bow	--	1
7.	Photography, Incremental	--	2
8.	Sectioning	--	1
9.	Density Measurements	--	2 (6 samples)
10.	Atom % Burnup	--	2
11.	Microstructural Analysis	--	2 (8 samples)

---

[a]Four gross gamma scans, one complete spectral scan, and 4 isotopic distributions of fission and activation products were determined.

VI. QUALITY ASSURANCE

A. General

1. A meeting was held June 5, 1974, with the AEC-DRRD Postirradiation Examination Program representatives. Included in this meeting was a discussion of the existing quality assurance programs and FY 1975 quality assurance plans.

2. Two Quality Assurance Specialists have been hired for the Postirradiation Examinations. One will report to work July 1, 1974, and the second who will be assigned primarily to microstructural analysis will report sometime after July 1, 1974. These two men will perform an independent quality assurance overcheck of work in the Postirradiation Examination area.

B. Chemical Analysis

1. An audit was conducted which included all areas and all sections performing chemical analysis, microprobe examinations, and gamma scanning. An audit report has been prepared. Corrective actions have been taken on all discrepancies found during this audit.

2. Sodium samples have been submitted to HEDL for analysis. It is planned that this work will be done using procedures prepared by HEDL that are consistent with the requirements of the LASL-DRRD Quality Assurance Program.

C. Hot Cell Examinations

All quality assurance procedures used in Hot Cell Examinations have been revised and check lists have been prepared for all critical operations. These have been submitted to the experimentors for review and will be in effect early in the next quarter. The revision updates each operation and eliminates the reference to Standard Operating Procedures.

Corrective Action for LASL-2, which is an Unusual Occurrence involving a bent element, has been completed. The final report has been prepared and submitted to AEC.

D. Microstructural Analysis

Quality Assurance surveillance has been established in the microstructural analysis operations. It is planned to initiate an independent quality assurance overcheck function as soon as manpower is available.

VII. PUBLICATIONS

1. M. E. Lazarus, "Fission Gas and Void Volume Measuring System," Proceedings of the 21st Conference on Remote Systems Technology, Amer. Nucl. Soc., 11, 1973.

2. M. E. Lazarus, "Technical Note: Use of Profilometer System at LASL," Proceedings of the 21st Conference on Remote Systems Technology, Amer. Nucl. Soc., 111, 1973.

3. M. E. Lazarus, and P. A. Mason, Jr., "Technical Note: Cold Trap for Removal of Impurities From Inert Gas Systems Used With Shielded Dry Boxes," Proceedings of the 21st Conference on Remote Systems Technology," Amer. Nucl. Soc., 113, 1973.

4. J. H. Bender, C. Baker, and K. A. Johnson, "A New Etch for LMFBR Materials," presented at the Sixth Annual Technical Meeting of the International Metallographic Society, Beverly Hills, CA, 1973.

5. K. A. Johnson, "BASIC Saltykov," presented at the Sixth Annual Technical Meeting of the International Metallographis Society, Beverly Hills, CA, 1973.

6. J. L. Lehmann and K. A. Johnson, "Ion Gun Etching of Metallographic Specimens," presented at the Sixth Annual Technical Meeting of the International Metallographic Society, Beverly Hills, CA, 1973.

7. K. A. Johnson, J. L. Lehmann, and D. D. Jeffries, "Metallographic Grinding Efficiency," presented at the Sixth Annual Technical Meeting of the International Metallographic Society, Beverly Hills, CA, 1973.

8. C. S. MacDougall, T. K. Marshall, G. M. Matlack, and G. R. Waterbury, "Determination of Oxygen, Hydrogen, and Tritium in Irradiated Reactor Fuels and Cladding Materials," presented at the 17th Conference on Analytical Chemistry in Nuclear Technology, Gatlinburg, TN, October 23-25, 1973.

9. T. K. Marshall, J. R. Phillips, B. K. Barnes, and G. R. Waterbury, "New Techniques in Two-Dimensional Gamma Scanning," presented at the 17th Conference on Analytical Chemistry in Nuclear Technology, Gatlinburg, TN, October 23-25, 1973.

10. J. W. Dahlby, T. K. Marshall, G. R. Waterbury, G. C. Swanson, "Measurement of Oxygen-to-Metal Atom Ratios in Uranium and Plutonium Oxides," Los Alamos Scientific Laboratory report LA-5329 (August 1973).

11. J. R. Phillips, G. R. Waterbury, N. E. Vanderborgh, "Distributions of ^{134}Cs and ^{137}Cs in the Axial UO_2 Blankets or Irradiated (U,Pu)O_2 Fuel Pins," J. Inorg. Nucl. Chem., 36, 17-23, January 1974.

12. J. R. Phillips, N. E. Banderborgh, G. R. Waterbury, "Application of Modern Gamma Scanning Techniques," Invited paper presented at the 76th Annual Meeting of the American Ceramic Society, Chicago, Ill., May 1, 1974.

13. C. S. MacDougall, T. K. Marshall, G. M. Matlack, G. R. Waterbury, "Determination of Carbon, Hydrogen, and Tritium in Irradiated Reactor Fuels and Cladding Materials," Los Alamos Scientific Laboratory report LA-5497 (May 1974).

14. J. R. Phillips, G. R. Waterbury, N. E. Vanderborgh, T. K. Marshall, "Quantitative Determination of Fission Products in Irradiated Fuel Pins Using Nondestructive Gamma Scanning," submitted to Analytical Chemistry for publication.

PROJECT 463

HIGH PERFORMANCE LMFBR FUEL MATERIALS

Person in Charge: R. D. Baker
Principal Investigator: J. L. Green

I. INTRODUCTION

The primary objective of this program is the overall
evaluation of the most promising of the candidate fuel
systems for advanced LMFBR application. Emphasis
currently is placed on the study of the relative merits of
stainless steel clad nitride and carbide fuels under con-
ditions that appropriately exploit the potential of these ma-
terials to operate to high burnup at high power densities.
The major portion of the program is the evaluation of the
irradiation performance of these fuel element systems.
A continuing series of irradiation experiments is being
carried out under steady-state conditions in fast reactor
environments to assess the effects of damage and burnup
on stainless-steel-clad carbide and nitride fuel elements.
These experiments are designed to investigate fuel swell-
ing, interactions between the fuel and clad and thermal
bonding medium, fission gas release, and the migration
of fuel material and fission products as a function of burn-
up and irradiation conditions. In addition, experiments
are being considered which would allow the study of the
effects of rapid, overpower, reactor transients on car-
bide and nitride fuel assemblies. Contiguous efforts are
necessary in the development of fuel material preparation
and fabrication procedures as well as the techniques re-
quired for the characterization of fuel materials both be-
fore and after irradiation.

A second objective in the program is the determin-
ation of thermophysical, mechanical and chemical proper-
ties and characteristics of plutonium-containing ceramics
that are required for their evaluation and use as fuel
materials. A broad range of capabilities in this area has

been developed including the study of (1) phase relation-
ships using differential thermal analysis, (2) thermal
transport, (3) thermal stability and compatibility, (4)
vapor pressure using mass spectrometry, (5) heat con-
tent using drop calorimetry, (6) elastic properties using
sonic modulus measurements, (7) hot hardness and its
temperature dependence, (8) structure and phase rela-
tionships using high temperature x ray and neutron dif-
fraction, (9) thermal expansion, and (10) compressive
creep rate as a function of temperature and stress. Sev-
eral of these techniques are available for use with irradi-
ated fuels.

II. IRRADIATION TESTING

The objective of the irradiation testing program is the
overall evaluation of the most promising of the candidate
fuel systems for advanced LMFBR application. The ir-
radiation experiments are carried out under conditions
that take advantage of the potential of these materials to
operate to high burnup at high power densities.

A. Fuel Synthesis and Fabrication
(K. W. R. Johnson, J. G. Reavis, H. G. Moore,
R. W. Walker, C. Baker, D. W. Kelley,
J. Mascarenas, W. C. Robbins, D. Scarafiotti)

1. Carbide Fuel Production

Carbide fuel pellets previously synthesized at
LASL have been high-purity single-phase $U_{0.80}Pu_{0.20}C_{0.97}$
having densities $\geq$ 93% of theoretical. New irradiation ex-
periments require fuels of comparable purity having ses-
quicarbide concentrations which vary from 1 to 17 vol%
and having minimum densities of 98% of theoretical. One
means of achieving this higher density is by the use of

nickel sintering aid. The carbothermic process was designated as the process to be used for this synthesis because of the commercial attractiveness of the process and because of the experience gained from previous scoping experiments.[1] The steps of this process are:

1. Blend and comminute UO_2, PuO_2 and C powders in a ball mill.

2. Press the blended powder into pellets.

3. Heat the pellets in vacuum to remove CO.

4. Comminute in a Spex mill.

5. Add Ni powder, blend and comminute in a ball mill.

6. Press into pellets.

7. Sinter.

8. Characterize.

To establish optimum processing parameters, a 225-g batch of $U_{0.8}Pu_{0.2}C_{1+x}$ was carried through step 4 above. Sufficient carbon was added initially to give a product which contained 13 vol% sesquicarbide. The powder was divided into four equal batches and blended with 0, 0.10, 0.15, and 0.20 wt% Ni powder by ball milling for 16 h. The Ni-containing batches were sintered at two different temperatures. Shown in Table 463-I are the sintering results. The amount of Ni found in the sintered pellets was generally about 0.05 wt% less than the amount added. This loss was subsequently shown to be due to the preferential sticking of the Ni powder to the surfaces of new process equipment. Density values listed in Table 463-I show essentially no variation due to changes in the

Ni concentration. Pellets sintered at 1800°C were essentially the same density as pellets of similar composition which were sintered at 1550°C.

Pellet batch No. 7, which was fabricated without Ni sintering aid, had a significantly lower pellet density. In this batch, the vol% M_2C_3 as measured by image analysis was not representative of the actual M_2C_3 concentration because of the state of aggregation of the second phase. In the absence of Ni, much of the M_2C_3 exists as platelets and the image analysis apparatus did not respond to the narrow grain boundary network. The presence of Ni appears to promote agglomeration of the M_2C_3 into more nearly equiaxed grains which are more readily measured by the apparatus.

Using the values of processing parameters indicated by these test batches, five additional developmental batches of high-density carbide fuel pellets containing M_2C_3 and Ni sintering aid were prepared on the 225-g scale. These batches met the criteria of > 98% of theoretical density, 1-17% M_2C_3 and pellet integrity. Characterization of these batches is not complete at this time.

2. Preparation of Single-Phase UC Insulator Pellets

The LASL specification for UC insulator pellets requires that, at a 500X magnification of the microstructure, no sesquicarbide or higher carbides be detectable. A review of the microstructure of previous UC preparations indicated that this stringent microstructural requirement necessitated additional developmental work. Although arc-cast material is capable of meeting this specification, it is possible that the presence of higher carbides is disguised by an extremely fine state of subdivision, leaving the high carbon activity associated with these carbides.

Accordingly, ingots with initial compositions of $UC_{0.98}$, $UC_{1.00}$ and $UC_{1.02}$ were prepared and subjected to a variety of processing conditions. The process was similar to the LASL arc-melting process used for the preparation of single phase $U_{0.80}Pu_{0.20}C_{0.97}$. Process variables which were investigated included time of H_2 treatment, comminution cycles, powder aging, prepressing and pressing pressures, sintering time and temperature. The process which evolved from this investigation

TABLE 463-I

DENSITIES OF SINTERED $U_{0.8}Pu_{0.2}C_{1+x}$
PELLETS CONTAINING Ni ADDITIONS

Batch No.	Ni Added, wt.%	Sinter Time, h	Sinter Temp, $^{\circ}$C	Ni Conc. By Anal, wt.%	Density %TD[a]	vol% M_2C_3[b]
1	0.10	1	1550	0.06	98.4	13
2	0.10	1	1800	0.03	98.6	15
3	0.15	1	1550	0.10	98.7	17
4	0.15	1	1800	0.12	--	--
5	0.20	1	1550	0.16	98.2	13
6	0.20	1	1800	0.14	98.0	13
7	0.00	8	1850	---	92.7	> 6

[a]Based on theoretical density of 13.45 g/cm^3 for MC and 12.72 g/cm^3 for M_2C_3

[b]Values by image analysis of photomicrographs

and which is capable of producing pellets which meet all UC specifications is as follows:

1. Arc melt U and graphite chunks combined to give a C/U atomic ratio of 0.98, using a graphite electrode and copper hearth.

2. Solution treat the ingots at 1600°C for 16 h.

3. Grind the ingots in a Spex mill to -250 mesh.

4. Pass H_2 over shallow trays (~ 6 mm deep) of powder for 65 h at 800°C.

5. Press the powder at 210 000 kPa without prepressing.

6. Sinter 8 h at 1800°C under flowing Ar, using about 2 h to heat to 1800°C, cooling at about 25°C/min to 1400°C, holding 2 h, and cooling at about 25°C/min to room temperature.

These conditions are not necessarily optimum and may be altered in the future. .

Two additional 225-g batches of UC insulator pellets were prepared by the use of this process. All specifications were met by 86 pellets while 18 pellets were 0.025 mm below the diametral dimensional minimum.

3. Nitride Fuel Development

The primary aim of experiments in this effort was to develop a method for production of high-purity, high-density, single-phase $U_{0.8}Pu_{0.2}N$ fuel pellets and UN insulator pellets on a 250-g scale. Equipment to synthesize, grind, press, and sample nitrides was set up in an inert atmosphere glovebox, and the sintering furnace was put into operation in another inert atmosphere glovebox. The equipment was designed so that it could be used for the synthesis and fabrication of either nitride or carbide pellets.

Two batches of UN were prepared on a 100-g scale by reaction of chunks of U metal with N_2 in the temperature range 800-1065°C. This reaction was found to be slow. Consequently, two additional batches of UN were prepared by first breaking down the chunks of uranium to a fine powder by forming the hydride in the temperature range 25-300°C, and decomposing it by heating above 400°C in vacuum. This reaction was rapid (after a variable and somewhat unpredictable induction period), as was the reaction between N_2 and the metal powder produced.

The optimum temperature range of nitride formation appeared to be 400-600°C. This two-step process requires much less time for completion than did the direct reaction between N_2 and chunks of metal. Weight changes indicated that the product of this process was U_2N_3.

The U_2N_3 was pressed into pellets and heated in vacuum to the temperature range 1350-1500°C to convert it to UN. Continued heating of some of these pellets through a 2100°C sintering cycle produced pellets having densities in the range 77-85% of theoretical, and having widely variable diameters. For the remaining material, the process included grinding and pressing. The UN produced in the vacuum decomposition was ground 3-5 min in an oscillatory mill, and the resulting powder was pressed into pellets which were sintered 16-18 h at 2100°C under ~ 78 KPa N_2. The pellets were cooled to ~ 1500°C under N_2, then in vacuum to room temperature.

Densities and microstructural appearance of these pellets were sufficiently good that a procedure was set up for preparation of UN from U metal and (U,Pu)N from U-Pu alloy on a 250-g scale. The procedure was:

1. Form metal powder by allowing U or U-Pu alloy to react with pure H_2, then thermally decompose the product hydride (2 cycles required).

2. React the metal powder with N_2 at 650-900°C to form a sesquinitride.

3. Sieve the powder through 170-mesh screen to remove any unreacted metal.

4. Press the powder into large pellets.

5. Heat the pellets in vacuum at 1400°C to form the mononitride.

6. Grind the powder, then sieve through 325 mesh screen.

7. Press the powder into pellets.

8. Heat the pellets in vacuum to 1500°C, then in a nitrogen atmosphere for 8 h at 2200°C. Cool in N_2 to 1500°C, then in vacuum to ambient temperature.

9. Characterize product.

A series of six test experiments were run on a 100- to 250-g scale with small variations in the listed values of process parameters. The values and densities of the

pellets produced are listed in Table 463-II.

TABLE 463-II

PREPARATION PARAMETERS AND DENSITIES
OF UN AND $U_{0.8}Pu_{0.2}N$ PELLETS

Expt. No.	No. of Hydride Cycles	Decomp. Temp., °C	Sintering Time, h	Sintering Temp., °C	Density % T.D.[a]
UN-3	1	1500	18	2150	92.1
UN-4	3	1340	15	2150	93.8
UN-5	3	1400	16	2150	92.6
UN-6	2	1500	16	2150	92.6
(U,Pu)N-1	2	1100	20	2000	77
(U,Pu)N-2	2	1370	16	2100	87

[a] Based on T.D. = 14.32 g/cm^3

Although high-density UN pellets were prepared, additional work will be required to produce $U_{0.8}Pu_{0.2}N$ pellets of comparable density. Microstructural examination of the pellets indicated that they were consistently single phase.

A developmental batch of UN insulator pellets was made, using specifications expected to be applied for irradiation experiments. Major detected impurities were 50 ppm Pu, 80 ppm C, 225 ppm O_2, 50 ppm Mo, and 120 ppm W. The observed immersion density was 12.80 Mg/m^3 (89% T.D.)

4. Carbide Grain Growth Studies

Grain size may be one of the factors influencing the behavior of reactor fuels during irradiation. If grain size is to be investigated as an experimental parameter, a method must be developed to produce various controlled grain sizes in $U_{0.8}Pu_{0.2}C$.

A series of experiments has been started to determine the effectiveness of additional sintering to increase grain size. The starting material for this series was a batch of $U_{0.8}Pu_{0.2}C$ pellets which were originally sintered 8 h at 1800°C and annealed 4 h at 1400°C. Small batches of these pellets were thermally cycled. The densities of the pellets were then measured and the microstructures were examined. Average grain sizes of the

original and the thermally cycled pellets were estimated by use of the comparison procedure described in ASTM Procedure E-112. The thermal cycles used and the grain size and density of the initial and product pellets are listed in Table 463-III.

The results shown in Table 463-III indicate that little or no change of either grain size or density was produced by the thermal cycling in this series of experiments. The precision of this method of grain size estimation is approximately ± 5 μm, and none of the grain size changes observed are greater than this. Similarly, it does not appear that significant changes in density have occurred.

5. BCL Nitrides

Eight full batches and one partial batch of $U_{0.8}Pu_{0.2}N$ pellets supplied by BCL were subjected to complete chemical and physical overcheck analyses. Physical characterizations and microstructural examinations were completed and chemical analyses are nearly complete.

6. Equipment Development

During FY 74 three inert atmosphere recirculating gloveboxes were put into service, bringing the total number of recirculating gloveboxes in the fuel synthesis facilities to six. Each glovebox and each purifier was somewhat different in design features and each presented

TABLE 463-III

EVALUATION OF THE EFFECT OF ADDITIONAL
SINTERING OF $U_{0.8}Pu_{0.2}C$

Expt. No.	Additional Thermal Cycle	Estimated Grain Size, μm	Density % T.D.
0	None	36	93.1
1	0.1 h at 2100°C	37	93.1
1a	0.1 h at 2100°C + 16 h at 1400°C	41	93.0
2	0.5 h at 2000°C	38	93.2
2a	0.5 h at 2000°C + 16 h at 1400°C	34	92.4
3	2 h at 1900°C	32	92.6
3a	2 h at 1900°C + 16 h at 1400°C	38	92.5
4	Cycled 1400-1800°C, 9 cycles	37	93.3

unique problems. The equipment contained in these boxes has all been checked out and put into service.

The original gas handling system for the hydride-nitride furnace was cumbersome and could not readily be modified to meet new safety standards. A new manifold was designed, fabricated, and installed and proved to be superior to the original installation. On completion and approval of a standard operating procedure, this system was used in the previously described nitride development work. After a brief period of operation, the drive motor on the new centrifugal mill used to grind nitrides failed to function properly. Special silver-doped graphite brushes designed for use in an inert atmosphere were ordered and installed to correct the problem. Preliminary observations suggest that considerable time may be saved by using the centrifugal mill rather than the older grinding equipment.

The centerless grinder used for reduction of fuel pellet diameters was modified to provide more precise control of the advance mechanism and thus a smoother grinding operation. In addition, a dust collection system was adapted to the apparatus in order to reduce powder scattering, minimize cross contamination, and facilitate material accountability. A pellet feed and collection system was also fabricated and installed on the apparatus. The apparatus was installed in a recirculating inert atmosphere glovebox and used to successfully grind pellets of UN, UC, and (U,Pu)C.

All measuring and test equipment was brought into the Q.A. recall system by completing calibrations and calibration procedures. Preventative maintenance activities and routine replacement of components due to normal attrition were continued. The fuel synthesis and fabrication operations were audited by the LASL Quality Assurance Manager. All suggestions and recommended corrective actions stemming from the audits were accomplished.

B. Fuel Element Fabrication
   (K. W. R. Johnson, D. G. Clifton, G. E. Meadows,
   J. R. Ruhe, H. E. Strohm, L. L. Marriott,
   W. J. Heyman)

   1. Welding Development
      An automatic programable welder was put into operation and basic parameters for welding end plugs to

cladding were established. Preliminary welds indicated the welding fixtures were incapable of reproducibly positioning the work piece and the welding torch. New fixtures capable of very accurately positioning the work piece and welding torch were designed and fabricated. Test welds indicated complete reproducibility and > 100% weld penetration.

   2. Xenon Tagging
      A xenon tagging device was fabricated and calibrated. Two dummy prototypic fuel element volumes were loaded with Xe and He, then analyzed. These analyses confirmed that the tagging technique satisfied the EBR-II requirement of a minimum of 1 ml (STP) of Xe.

   3. Sodium and Sodium Bonding
      The sodium loop of the fuel fabrication facility was reactivated after a prolonged shutdown period. Samples of the sodium were sent to HEDL for chemical analysis. Work was initiated to establish an "on-site" sodium analysis capability.

      Sodium bonding operations involve the use of a heated centrifuge and a bonding furnace to promote sodium wetting. Extensive developmental work was performed on these apparatuses to determine operating characteristics and to calibrate associated instrumentation. The efficacy of this operation was demonstrated when elements from the C-BMI-5 and O-N1 series which contained bond defects between the cladding and the (UPu)N fuel were successfully rebonded. The sensitivity of the eddy current apparatus was significantly improved by modifying the sensor carriage head.

   4. Associated Activities
      A wire wrap machine was designed and components were purchased or fabricated. Assembly of this machine is approximately 35% complete.

      Detailed Quality Assurance procedures were written for the various processes involved in the fabrication of sodium-bonded, more advanced plutonium fuel elements. Raw materials for fabrication of this type of element were ordered. Most of these materials have been delivered and overchecked.

C. EBR-II Irradiation Testing
   (J. O. Barner, J. F. Kerrisk, T. W. Latimer,
   R. L. Petty)

The purpose of the EBR-II testing program is the evaluation of the steady-state irradiation behavior of high-performance fuel element systems for application in advanced LMFBR reactors. Several series of carbide- and nitride-fueled experiments have been initiated in the past several years. The main objectives of the irradiations are: (1) the development of fuel element designs for use with each fuel type; (2) the determination of the irradiation behavior of the fuel materials; (3) a comparison of sodium and helium bonding; (4) a comparison of different cladding alloys; and (5) the evaluation of the overall irradiation performance of the fuel element systems. The majority of the experiments under test or that have been completed have been encapsulated. Most of the experiments that are currently available for irradiation or that are being designed are singly clad.

1. Experiment Description and Status

Fourteen series of experiments have been originated. The description and status of these series are summarized in Tables 463-IV to 463-XI. In order to better define the status of those experiments which are undergoing postirradiation examination, the following steps are referenced in the tables:

a. Capsule Examination

    a.1 Visual Examination

    a.2 Preliminary Measurements (radiation measurements, etc.)

    a.3 Profilometry

    a.4 Photography

    a.5 Radiography

    a.6 Eddy Current Test

    a.7 Gamma Scan

    a.8 Cover Gas Analysis

    a.9 Deencapsulation

b. Element Examination

    b.1 Visual Examination

    b.2 Profilometry

    b.3 Photography

    b.4 Eddy Current Test

    b.5 Fission Gas Analysis

    b.6 Sectioning

    b.7 Autoradiography

    b.8 Metallography

    b.9 Burnup

    b.10 Clad Density

    b.11 Special Tests

    b.12 Data Reduction

    b.13 Report Preparation

All hot cell examinations are done by Project 401 personnel under the guidance of Project 463 personnel.

Table 463-IV describes the K1, K2, and K3 series tests. In these experiments single-phase, high-purity, uranium-plutonium monocarbide pellets are sodium bonded to Type 316 stainless steel cladding. In general, the operating linear power ratings of the capsules are relatively high (approximately 85 kW/m). Three tests at very high power (> 125 kW/m) were included to determine the effect of high thermal stresses and high fuel temperatures on fuel element behavior. Indications of element cladding failure were found at EBR-II in several experiments from these series (five in subassembly X119B, one from X142, and two from X152), using γ-scanning for ^{133}Xe. Examinations of these experiments in the LASL hot cells confirmed the failures. Complete postirradiation examination of the failed experiments is continuing.

One unfailed experiment, K-44, recently completed irradiation in subassembly X182 after reaching a maximum burnup of 7.1 at.%. A second unfailed experiment, K-39B, will be reconstituted into a new subassembly upon approval of a data package which is being prepared.

Table 463-V describes the Series U1300 experiments. These experiments contain two-phase, uranium-plutonium carbide fuel pellets which are helium bonded to either Type 316 stainless steel or Incoloy 800 cladding. Two methods for the accommodation of fuel swelling were investigated in this series, i.e., the introduction of internal porosity by the use of either low-density solid fuel pellets or high-density cored pellets. These experiments reached their goal burnup of 10 at.% in subassembly X142 after operation at moderate linear power ratings (52-70 kW/m). Indications of element cladding failure for three experiments were found at EBR-II using γ-scanning for ^{133}Xe. These element failures have been confirmed by γ-scanning for ^{137}Cs at LASL. Three of these experiments have completed postirradiation examination and

TABLE 463-IV

SERIES K1, K2, AND K3 ENCAPSULATED CARBIDE EXPERIMENTS

Expmt. No.	Fuel Type[a]	Fuel Density, % Theo.[b]	Bond and Diametral Gap, mm	Clad Type[c]	Clad O.D. x I.D., mm	Max. Linear Power, kW/m[h]	Maximum Centerline Temp., °C[h]	Goal Burnup, at.%[d]	Maximum Current Burnup at.%[d]	Status
				Series K1						
K-36B	MC	90	Na-0.38	SA-316SS	7.62 x 7.11	82[†]	990[†]	6	5.85[*]	b.12[e]
K-37B	MC	90	Na-0.38	SA-316SS	7.62 x 7.11	85	1000	6	2.9	a.7[e,f]
K-38B	MC	90	Na-0.38	SA-316SS	7.62 x 7.11	85	1000	6	5.8	a.7[e,f]
K-39B	MC	90	Na-0.38	SA-316SS	7.62 x 7.11	85	1000	10	5.8	EBR-II, Un-assigned
K-42B	MC	90	Na-0.38	SA-316SS	7.62 x 7.11	85[†]	1000[†]	6	4.46[*]	Completed[g]
				Series K2						
K-49	MC	95	Na-0.51	SA-316SS	7.62 x 7.11	130[†]	1270[†]	5	3.74[*]	b.12[e]
K-50	MC	95	Na-0.51	SA-316SS	7.62 x 7.11	130	1300	6.5	3.6	a.9[e]
K-51	MC	95	Na-0.51	SA-316SS	7.62 x 7.11	130	1300	8	3.5	a.9[e]
				Series K3						
K-43	MC	94	Na-0.51	SA-316SS	7.62 x 7.11	80	1000	8	5.6	b.3[e]
K-44	MC	94	Na-0.51	SA-316SS	7.62 x 7.11	80	1000	8	7.1	b.5
K-45	MC	94	Na-0.51	SA-316SS	7.62 x 7.11	80	1000	5	2.37[*]	b.9[e]
K-46	MC	94	Na-0.51	SA-316SS	7.62 x 7.11	80[†]	965[†]	5	2.39[*]	b.12[e]

[a] $M = (U_{0.8}Pu_{0.2})$
Series 1 and 3 experiments are 93% enriched in ^{235}U.
Series 2 experiments are 97% enriched in ^{233}U.

[b] Theoretical density of MC = 13.45 Mg/m^3.

[c] SA = Solution annealed.

[d] Burnup values marked with [*] were measured using the ^{148}Nd method. Remaining values were computed from EBR-II data.

[e] Element cladding failure indicated.

[f] Damaged during reconstitution of X152.

[g] Reported in LA-4669-MS.

[h] Linear power & centerline temperature marked with [†] are beginning-of-life values computed using measured burnup results. Remaining values based on EBR-II power adjustment factor of 0.91.

---

evaluation of the results is continuing. Destructive examination of U97 and U98, in addition to profilometry and fission gas analysis of U106, U110, U113, and U114 are planned for FY 1975.

The Series U1950 experiments are described in Table 463-VI. In these experiments, either two-phase or single-phase carbide fuel is helium bonded to Type 304 or 316 stainless steel or to Incoloy 800 cladding. Fuel densities range from 77 to 99% theoretical. These experiments are currently within one at.% of their goal burnup after operation at low linear power (38 to 44 kW/m). During interim examination at EBR-II after run 58, ^{137}Cs was detected by γ-scanning in the sodium reservoir of

capsule U136. Release of fission gas from a breached helium-bonded element would be expected. However, no ^{133}Xe was detected in the capsule plenum. The lack of fission gas in the capsule and the presence of ^{137}Cs in the capsule sodium present a contradictory picture and the failure of the element in capsule U136 can only be considered tentative and of a low degree. None of the other capsules indicated fuel element failure during the examinations at EBR-II. All 19 capsules were reconstituted into subassembly X055B which is currently being irradiated.

The Series U1930 and U1960 experiments are described in Table VII. Experimental parameters include

TABLE 463-V

SERIES U1300 ENCAPSULATED CARBIDE EXPERIMENTS

Expmt. No.	Fuel Type[a]	Fuel Density % Theo.[b]	Bond and Diametral Gap, in.	Clad[d] Type	Clad O.D. x I.D., in.	Max. Linear Power, kW/ft[g]	Maximum Centerline Temp., °C	Goal Burnup at.%	Current Peak Burnup, at.%[e]	Status
U93	MC+5% M_2C_3	86	He-0.10	SA-316SS	7.66 x 6.10	59[t]	1750	11	9.64*	b.12
U94	MC	85	He-0.18	SA-316SS	7.73 x 6.86	70[t]	1680	11	9.42*	b.12
U97	MC+5% M_2C_3	86	He-0.10	SA-INC-800	7.60 x 6.10	54	1750	11	10.0	b.8
U98	MC+5% M_2C_3	86	He-0.18	SA-INC-800	7.60 x 6.86	65	1680	11	9.6	a.7[f]
U105	MC+5% M_2C_3	77	He-0.20	SA-INC-800	7.61 x 6.10	52[t]	1900	11	9.69*	b.12
U106	MC+5% M_2C_3	77	He-0.20	SA-INC-800	7.72 x 6.86	59	1820	11	9.9	a.7[f]
U110	MC+10% M_2C_3	99°	He-0.33	SA-INC-800	7.73 x 6.86	65	1960	10	9.2	a.7
U113	MC+10% M_2C_3	98°	He-0.28	SA-INC-800	7.61 x 6.10	50	1880	11	10.2	a.7
U114	MC+15% M_2C_3	98°	He-0.18	SA-INC-800	7.72 x 6.86	66	1570	10	9.5	a.7[f]

[a] $M = (U_{0.85}Pu_{0.15})$.

[b] Theoretical density of MC = 13.45 Mg/m^3.
Theoretical density of M_2C_3 = 12.72 Mg/m^3.

[c] Cored pellet with nominal 2.0 mm diameter axial hole.

[d] SA = Solution annealed.

[e] Burnup values marked with * were measured using the ^{148}Nd method. Remaining values were computed from EBR-II data.

[f] Element cladding failure indicated.

[g] Linear power marked with [t] are beginning-of-life values computed using measured burnup results.
Remaining values based on EBR-II power adjustment factor of 0.91.

fuel type, fuel density, bond type, and cladding type. The operating linear power ratings for the experiments are relatively high (73-100 kW/m). Nondestructive examination of the eleven experiments listed in part A of Table 463-VII showed that fuel elements U194 and U200 had failed. Destructive examination of this group of experiments has been completed. Data reduction and interpretation are continuing.

The experiments listed in part B of Table 463-VII completed irradiation in subassembly X182. Prior to their irradiation in X182, elements U188, U190, U193, and U196 had not failed after maximum burnups of 8.5 at.% and elements U199, U201, U207, and U209 had not failed after maximum burnups of 5.5 at.%. After an accumulation of approximately an additional 2 at.% burnup, elements U190 and U199 have not failed. However, U188, U193, U196, U201, U207, and U209 have failed as evidenced by γ-scanning at EBR-II. Five of the capsules –

U188, U190, U193, U199, and U209 – were accidentally damaged at EBR-II while being transferred between the air cell and the argon cell in FEF-S. The capsules were dented and bent 3-5° approximately 12 inches from the bottom ends. A sixth capsule, U207, sustained only slight damage. All of the experiments in this group were returned to LASL for examination.

The experiments listed in part C of Table 463-VII were used as replacement capsules in order to allow irradiation to be continued to the desired burnup in lead experiments from other series. Only a cursory postirradiation examination is planned for these elements. Nondestructive examinations of these experiments are complete. Element U203, in addition to elements U260 and U262 from part D of Table 463-VII will be reconstituted into a new subassembly upon approval of a data package which is being prepared. Capsule U261 was rejected because of a sodium bond defect in the capsule–element annulus.

TABLE 463-VI

SERIES U1950 ENCAPSULATED CARBIDE EXPERIMENTS

Expmt. No.	Fuel Type[b]	Fuel Density, % Theo.[c]	Bond and Diametral Gap, mm	Clad Type[e]	Clad O.D. x I.D., mm	Max. Linear Power, kW/m[g]	Maximum Centerline Temp., °C	Goal Burnup, at.%	Maximum Current Burnup at.%[g]	Status
U129	MC	86	He-0.41	SA-316SS	7.70 x 6.60	38	1750	11	10.5	EBR-II, X055B
U130	MC	77	He-0.25	SA-316SS	7.70 x 6.60	39	1500	11	10.6	EBR-II, X055B
U131	MC	85	He-0.36	SA-316SS	7.70 x 6.60	38	1490	11	10.3	EBR-II, X055B
U132	MC	85	He-0.36	SA-316SS	7.70 x 6.60	38	1490	11	10.2	EBR-II, X055B
U133	MC	85	He-0.36	SA-316SS	7.70 x 6.60	38	1490	11	10.0	EBR-II, X055B
U134	MC	85	He-0.36	SA-316SS	7.70 x 6.60	38	1490	11	10.1	EBR-II, X055B
U135	MC	85	He-0.36	SA-INC-800	7.67 x 6.60	38	1470	11	10.3	EBR-II, X055B
U136	MC	85	He-0.36	SA-INC-800	7.67 x 6.60	40	1470	11	9.9	EBR-II, X055B[f]
U137	MC+20% M_2C_3	97	He-0.36	SA-316SS	7.70 x 6.60	40	1440	10	8.9	EBR-II, X055B
U138A[a]	MC+20% M_2C_3	98	He-0.36	SA-316SS	7.44 x 6.60	44	1440	8	5.9	EBR-II, X055B
U139	MC+20% M_2C_3	97	He-0.36	SA-INC-800	7.72 x 6.60	44	1440	10	9.1	EBR-II, X055B
U140	MC	90	He-0.36	SA-INC-800	7.72 x 6.60	41	1460	10	9.6	EBR-II, X055B
U141	MC	91	He-0.25	SA-316SS	7.70 x 6.60	43	1460	10	9.5	EBR-II, X055B
U142	MC	91	He-0.25	SA-316SS	7.72 x 6.60	43	1460	11	9.6	EBR-II, X055B
U143	MC+20% M_2C_3	96[d]	He-0.36	SA-INC-800	7.67 x 6.60	38	1390	11	9.8	EBR-II, X055B
U144	MC+20% M_2C_3	96[d]	He-0.36	SA-316SS	7.72 x 6.60	39	1390	11	9.9	EBR-II, X055B
U145	MC	90	Na-0.76	SA-304SS	7.75 x 6.86	40	820	10	9.4	EBR-II, X055B
U146A[a]	MC+20% M_2C_3	99	Na-0.76	SA-304SS	7.62 x 6.86	41	810	8	5.8	EBR-II, X055B
U147	MC+20% M_2C_3	97	Na-0.76	SA-INC-800	7.72 x 6.86	42	810	10	9.5	EBR-II, X055B

[a] Capsules 138 and 146 were removed at 4.0 at.% burnup for TREAT testing. Duplicates replaced the originals.

[b] $M = (U_{0.85}Pu_{0.15})$; U is 60% enriched in ^{235}U.

[c] Theoretical density of MC = 13.49 Mg/m^3.
Theoretical density of M_2C_3 = 12.76 Mg/m^3.

[d] Cored pellet with nominal 2.0 mm diameter axial hole.

[e] SA = Solution annealed.

[f] Possible element cladding failure indicated.

[g] Computed using EBR-II power adjustment factor of 0.91.

Table 463-VIII describes the Series WF experiments. These sodium-bonded, carbide capsules were designed to evaluate the effects of (1) various amounts of sesquicarbide in the fuel, (2) linear power rating, and (3) cladding cold work on element performance. The amount of sesquicarbide reported to be in the fuel varies from 0 to 24 vol%. One experiment, W6F, was determined to have an element cladding failure after a maximum burnup of 5.4 at.%. This was the first failure in this series and was determined by γ-scanning at EBR-II. W6F was returned to LASL for examination. Two other experiments, W4F

and W8F, have completed postirradiation examination. Irradiation of the remaining five capsules will continue to a goal burnup of 10 at.%.

Table 463-IX describes the Series B-1, B-2, and B-3 experiments. These capsules are fueled with single-phase, uranium-plutonium mononitride. All the elements in Series B-1 and B-2 are sodium bonded and clad with either Type 304 or 316 welded stainless steel tubing. Operating linear power ratings for the experiments are relatively high (79-110 kW/m). Capsules B-1-4, B-2-1, B-2-3 and B-2-5 have been examined using γ-scanning

TABLE 463-VII

SERIES U1930 AND U1960 ENCAPSULATED CARBIDE EXPERIMENTS

Expmt. No.	Fuel Type[a]	Fuel Density, % Theo.[b]	Bond and Diametral Gap, mm	Clad Type[d]	Clad O.D. x I.D., mm	Max. Linear Power, kW/m[h]	Maximum Centerline Temp., °C[h]	Goal Burnup at.%	Maximum Current Burnup at.%[g]	Status
A										
U187	$MC+5\%M_2C_3$	86	He-0.18	SA-316SS	7.72 x 6.60	77†	1930	5	4.60*	b.12
U189	$MC+5\%M_2C_3$	85	He-0.25	SA-INC-800	7.67 x 6.60	81†	1930	~5	4.80*	b.12
U191	MC	92	Na-0.76	SA-304SS	7.72 x 6.91	84†	1010†	5	4.50*	b.12
U192	MC	92	Na-0.76	SA-304SS	7.75 x 6.91	73†	940†	5	4.3	b.12
U194	$MC+10\%M_2C_3$	98	Na-0.84	SA-304SS	7.75 x 6.91	81†	980†	5	4.64*	b.12[e]
U195	$MC+10\%M_2C_3$	98	Na-0.84	SA-304SS	7.75 x 6.91	83†	990†	5	4.94*	b.12
U197	$MC+10\%M_2C_3$	98	Na-0.84	SA-INC-800	7.75 x 6.91	80†	1020†	5	4.90*	b.12
U198	$MC+10\%M_2C_3$	98	Na-0.84	SA-INC-800	7.75 x 6.91	84†	1000†	5	4.78*	b.12
U200	$MC+5\%M_2C_3$	86	He-0.23	SA-304SS	7.32 x 6.60	83†	2040	5	4.72*	b.12[e]
U206	$MC+5\%M_2C_3$	90	He-0.25	SA-316SS	7.44 x 6.58	90†	2080	5	4.96*	b.12
U208	$MC+10\%M_2C_3$	97°	He-0.30	SA-316SS	7.44 x 6.58	87†	1910	5	5.00*	b.12
B										
U188	$MC+5\%M_2C_3$	85	He-0.18	SA-316SS	7.72 x 6.60	90	1930	11	11.0	a.7[e,i]
U190	$MC+5\%M_2C_3$	85	He-0.28	SA-INC-800	7.67 x 6.60	90	1930	11	11.0	a.7[i]
U193	MC	92	Na-0.79	SA-304SS	7.75 x 6.91	94	1000	11	11.0	a.7[e,i]
U196	$MC+15\% M_2C_3$	98	Na-0.79	SA-304SS	7.75 x 6.91	97	1000	11	10.9	a.8[e]
U199	$MC+10\%M_2C_3$	98	Na-0.79	SA-INC-800	7.75 x 6.91	100	1000	11	8.2	a.7[i]
U201	$MC+5\%M_2C_3$	85	He-0.23	SA-304SS	7.32 x 6.60	90	2040	11	7.8	a.8[e]
U207	$MC+5\%M_2C_3$	90	He-0.25	SA-316SS	7.44 x 6.58	94	2090	11	7.9	a.8[e,i]
U209	$MC+10\%M_2C_3$	97c	He-0.30	SA-316SS	7.44 x 6.58	92	1910	11	7.9	a.7[e,i]
C										
U185	$MC+10\%M_2C_3$	97	He-0.28	SA-316SS	7.72 x 6.60	90	2190	3	2.7	a.7
U186	$MC+10\%M_2C_3$	97	He-0.28	SA-316SS	7.72 x 6.60	90	2190	3	2.7	a.7
U202	$MC+5\%M_2C_3$	85	He-0	SA-316SS	6.83 x 6.38	94	1270	3	2.5	a.7
U203	$MC+5\%M_2C_3$	85	He-0.05	SA-316SS	7.32 x 6.43	93	1260	3	2.5	LASL unassigned[j]
U204	$MC+10\%M_2C_3$	97c	He-0.05	SA-316SS	6.76 x 6.32	96	1130	3	2.6	a.7
U205	$MC+10\%M_2C_3$	97c	He-0.08	SA-316SS	7.21 x 6.35	95	1120	3	2.6	a.7
D										
U260	$MC+10\%M_2C_3$	98	He-0.48	20CW-316SS	7.57 x 6.71	90	2400	3	0	EBR-II, unassigned[j]
U261	$MC+10\%M_2C_3$	98	He-0.38	SA-316SS	7.49 x 6.60	--	--	--	0	Reject[f]
U262	$MC+10\%M_2C_3$	96	He-0.38	SA-INC-800	7.34 x 6.60	90	2260	3	0	EBR-II, unassigned[j]

[a] $M = (U_{0.85}Pu_{0.15})$.

[b] Theoretical density of MC = 13.45 Mg/m^3.
Theoretical density of M_2C_3 = 12.72 Mg/m^3.

° Cored pellet with nominal 2.0 mm diametral axial hole.

[d] SA = Solution annealed; 20 CW = 20% cold worked.

[e] Element cladding failure.

[f] EBR-II eddy current test indicates capsule bond discontinuity.

[g] Burnup values marked with * were measured using the ^{148}Nd method. Remaining values were computed using an EBR-II power adjustment factor of 0.91.

[h] Linear power and centerline temperature marked with † are beginning-of-life values computed using the measured burnup results. Remaining values are based on EBR-II power adjustment factor of 0.91.

[i] Damaged at EBR-II.

[j] To be reconstituted for further irradiation.

techniques for the detection of ^{137}Cs, and the elements are apparently intact. Further irradiation of B-1-4, B-2-1, and B-2-5 is planned. During the interim examination, capsules B-1-1, B-1-2, B-2-2, B-2-6, and B-2-7, were found to have failed as indicated by γ-scanning for ^{133}Xe at EBR-II.

TABLE VIII

SERIES WF ENCAPSULATED CARBIDE EXPERIMENTS

Expmt. No.	Fuel Type[a]	Fuel Density, % Theo.[b]	Bond and Diametral Gap, mm	Clad Type[c]	Clad O.D. x I.D., mm	Max. Linear Power, kW/m[f]	Maximum Centerline Temp., °C	Goal Burnup, at.%	Maximum Current Burnup at.%[e]	Status
W3F	$MC+15\% M_2C_3$	93	Na-0.64	SA-316SS	7.62 x 7.01	81	1000	10	5.5	EBR-II, un-assigned
W4F	$MC+10\% M_2C_3$	95	Na-0.69	SA-316SS	7.62 x 7.01	82[†]	950	6	5.32[*]	b.12
W5F	$MC+10\% M_2C_3$	91	Na-0.25	SA-316SS	6.35 x 5.84	60	925	10	5.4	EBR-II, un-assigned
W6F	$MC+10\% M_2C_3$	90	Na-0.28	SA-316SS	6.38 x 5.87	60	925	6	5.4	a.8[d]
W7F	$MC+5\% M_2C_3$	90	Na-0.69	20CW-316SS	7.62 x 7.01	81	1000	10	5.5	EBR-II, un-assigned
W8F	$MC+5\% M_2C_3$	94	Na-0.64	20CW-316SS	7.62 x 7.01	83[†]	950	6	5.82[*]	b.12
W10F	MC	89	Na-0.30	SA-316SS	6.38 x 5.87	60	925	10	5.4	EBR-II, un-assigned
W12F	$MC+25\% M_2C_3$	97	Na-0.33	SA-316SS	6.38 x 5.87	63	975	10	5.4	EBR-II, un-assigned

[a] $M = (U_{0.8}Pu_{0.2})$.

[b] Theoretical density of MC = 13.45 Mg/m^3. Theoretical density of M_2C_3 = 12.72 Mg/m^3.

[c] SA = Solution annealed, 20 CW = 20% cold worked.

[d] Element cladding failure indicated by gamma scanning.

[e] Burnup values marked with * were measured using the ^{148}Nd method. Remaining values were computed using EBR-II power adjustment factor of 0.91.

[f] Linear power marked with † are beginning-of-life values computed using the measured burnup results. Remaining values are based on EBR-II power adjustment factor of 0.91.

Series B-3 is similar to the B-1 and B-2 series except that three helium-bonded experiments are included and the average operating linear power ratings are slightly higher. The three helium-bonded elements have not failed at a maximum burnup of 6 at.%. Three of the failed sodium-bonded elements in the Series B-3 have completed postirradiation examination. Helium-bonded experiment B-3-7 was returned to LASL for destructive examination. The other two helium-bonded experiments will continue irradiation in a new subassembly.

The Series U5100 singly clad experiments are described in Table 463-X. In this group, either single-phase or two-phase carbide fuel is sodium bonded to Type 304 or 316 stainless steel or to Incoloy 800. In seven of the elements, a perforated shroud is incorporated primarily to test the retention of fuel fragments by close-fitting tubes. A secondary objective of the shroud is to study the effectiveness of the shroud alloy as a carbon getter.

An element failure was indicated in this series after a maximum burnup of 3 at.%. The interpretation of results from EBR-II reactor monitoring systems was that the size of the failure was very small. The subassembly was removed from the reactor on January 1, 1974. Examination of these elements at EBR-II indicated that one element, U248, had failed. The failure was detected by means of a weight loss of 4 g. All other elements had no weight losses. Visual examination of U248 revealed no obvious failure point. Neutron radiography at ANL West revealed that four pellets in element U246 had shifted upward; the displacement of the top pellet was 130 mm. No holddown springs were used in the elements of this series. Both U246 and U248 were returned to LASL for destructive examination. Radiographic examination of the seven elements having perforated shrouds around the fuel pellets has shown that this concept has been effective in containing the fuel fragments. It is planned to continue irradiation of the remaining 16 elements.

TABLE IX

SERIES B-1, B-2 AND B-3 ENCAPSULATED NITRIDE EXPERIMENTS

Expmt. No.	Fuel Type [a]	Fuel Density, % Theo. [b]	Bond and Diametral Gap, mm	Clad Type [d]	Clad O.D. x I.D., mm	Max. Linear Power, kW/m [h]	Maximum Centerline Temp., °C [h]	Goal Burnup, at.%	Maximum Current Burnup, at.% [e]	Status
					Series B-1					
B-1-1	MN	94	Na-0.48	SA-304SS	7.37 x 6.35	79[†]	1045[†]	5	5.70[*]	b. 12[f]
B-1-2	MN	94	Na-0.46	SA-304SS	7.37 x 6.35	81	1100	9	5.7	a. 7
B-1-4	MN	94	Na-0.30	SA-304SS	7.37 x 6.35	85	1100	10	2.7	LASL, unassigned[g]
					Series B-2					
B-2-1	MN	95	Na-0.53	SA-316SS	8.02 x 6.99	98	1230	10	5.7	EBR-II, unassigned[g]
B-2-2	MN	94	Na-0.51	SA-316SS	8.01 x 6.98	93[†]	1230	9	5.48[*]	b. 12[f]
B-2-3	MN	94	Na-0.51	SA-316SS	8.00 x 6.99	97	1230	12	8.5	b. 5
B-2-5	MN	94	Na-0.71	SA-316SS	8.00 x 7.21	97	1230	12	2.7	LASL, unassigned[g]
B-2-6	MN	94	Na-0.53	SA-316SS	8.03 x 7.49	109	1230	6	5.6	a. 7[f]
B-2-7	MN	94	Na-0.51	SA-316SS	8.03 x 7.49	110	1230	12	5.6	a. 7[f]
					Series B-3					
B-3-2	MN	88	Na-0.23	SA-316SS	8.01 x 7.22	110[†]	1235[†]	9	2.78[*]	b. 12[f]
B-3-3	MN	91	Na-0.25	SA-316SS	8.01 x 7.22	116	1280	12	2.8	a. 7[f]
B-3-4	MN	94	Na-0.33	SA-316SS	8.01 x 7.22	108[†]	1200[†]	12	2.70[*]	b. 12[f]
B-3-5	MN	90	Na-0.25	SA-316SS	8.01 x 7.48	118[†]	1255[†]	6	2.74[*]	b. 12[f]
B-3-6	MN	95[o]	He-0.13	SA-316SS	8.00 x 6.99	102	1920	10	6.0	EBR-II, unassigned[g]
B-3-7	MN	89	He-0.13	SA-316SS	8.00 x 6.99	102	1920	6	6.0	b. 5
B-3-8	MN	90[o]	He-0.13	SA-316SS	8.00 x 6.99	97	1870	10	6.0	EBR-II, unassigned[g]

[a] $M = (U_{0.8}Pu_{0.2})$.

[b] Theoretical density of MN = 14.17 Mg/m^3.

[o] Cored pellet with nominal 1.78 mm. diameter axial hole.

[d] Cladding is welded tubing.
SA = Solution annealed.

[e] Burnup values marked with [*] were measured using the [148]Nd method.
Remaining values were computed using an EBR-II power adjustment factor of 0.91.

[f] Element cladding failure indicated.

[g] To be reconstituted for further irradiation.

[h] Linear power and centerline temperature marked with [†] are beginning-of-life values computed using measured burnup results. Remaining values based on EBR-II power adjustment factor of 0.91.

The C-5 and O-N1 series of singly clad experiments are described in Table 463-XI. Single-phase nitride fuel is sodium bonded to 20% cold-worked Type 316 stainless steel cladding in all of the fuel elements in this group. Profilometry measurements of the C-5 series elements have been made using the same equipment that will be used for the postirradiation examination. Shipment of selected elements to EBR-II is pending LASL review of the experiments from a quality assurance standpoint.

The O-N1 series of singly clad experiments is similar to the C-5 series. The elements are fueled with $(U_{0.8}Pu_{0.2})N$ which is sodium bonded to 20% cold-worked Type 316 stainless steel cladding. Three elements have been rejected because of large fuel chips in the sodium annulus. The diameters of the elements have been measured on the same profilometer that will be used after irradiation. Eddy current examination of these elements indicates multiple sodium bond defects. The remaining four elements will be rebonded. It is planned that four fuel elements from Series O-N1 will be irradiated with selected elements from Series C-5.

TABLE X

SERIES U5100 SINGLY CLAD CARBIDE EXPERIMENTS

Expmt. No.	Fuel Type[a]	Fuel Density, % Theo.[b]	Bond and Diametral Gap, mm[c]	Clad Type[d]	Clad O.D. x I.D. mm	Max. Linear Power, kW/m[f]	Maximum Centerline Temp., °C	Goal Burnup at.%	Maximum Current Burnup at.%[f]	Status
U241	MC	94	Na-0.46	SA-304SS	7.87 x 7.14	107	1170	6	3.0	EBR-II, X156
U242	MC	93	Na-0.44	SA-304SS	7.87 x 7.14	107	1170	9	3.0	EBR-II, X156
U243	MC	93	Na-0.80	SA-304SS	7.87 x 7.14	101	1150	6	2.9	EBR-II, X156
U244	MC	93	Na-0.44	SA-304SS	7.87 x 7.14	107	1170	9	3.0	EBR-II, X156
U245	MC	93	Na-0.81	SA-304SS	7.87 x 7.14	101	1150	12	2.9	EBR-II, X156
U246	MC	93	Na-0.43	SA-316SS	7.87 x 7.14	109	1190	6	3.1	EBR-II, X156
U247	MC	93	Na-0.81	SA-316SS	7.87 x 7.14	101	1150	6	2.9	EBR-II, X156
U248	MC	93	Na-0.81	SA-316SS	7.87 x 7.14	109	1140	12	3.1	EBR-II, X156[e]
U249	MC	93	Na-0.43	SA-INC-800	7.85 x 7.14	109	1210	6	3.1	EBR-II, X156
U250	MC	93	Na-0.81	SA-INC-800	7.85 x 7.14	109	1140	6	3.1	EBR-II, X156
U251	MC	93	Na-0.81	SA-304SS	7.87 x 7.14	109	1140	12	3.1	EBR-II, X156
U252	MC	93	Na-0.64	SA-304SS	7.87 x 7.14	109	1140	12	3.1	EBR-II, X156
U253	MC	93	Na-0.66	SA-304SS	7.87 x 7.14	101	1140	12	2.9	EBR-II, X156
U254	MC	93	Na-0.66	SA-304SS	7.87 x 7.14	101	1140	12	2.9	EBR-II, X156
U256	MC+15%M_2C_3	96	Na-0.61	SA-304SS	7.85 x 7.14	101	1140	12	2.9	EBR-II, X156
U257	MC+15%M_2C_3	96	Na-0.58	SA-INC-800	7.85 x 7.14	100	1130	12	2.9	EBR-II, X156
U258	MC+15%M_2C_3	96	Na-0.58	SA-304SS	7.87 x 7.14	100	1140	6	2.9	EBR-II, X156
U259	MC+15%M_2C_3	96	Na-0.58	SA-INC-800	7.85 x 7.14	103	1150	12	3.0	EBR-II, X156

[a] $M = (U_{0.85}Pu_{0.15})$.

[b] Theoretical density of MC = 13.45 Mg/m^3.
Theoretical density of M_2C_3 = 12.72 Mg/m^3.

[c] Elements U252 through U259 contain slotted shroud tubes ~ 0.09 mm thick, made of V. Fe, 304SS, V, Ta, 304SS, and 304SS, respectively. The shroud thickness is not included in the bond gap value.

[d] SA = Solution annealed.

[e] Element cladding failure indicated.

[f] Computed using an EBR-II power adjustment factor of 0.91.

In addition to the experiments described above, two nitride-fueled thermal irradiation experiments from ORNL (43N1 and 43N2) will be examined. Results and status will be reported in future reports.

A series of singly clad elements is currently being designed to irradiate sodium-bonded carbide and nitride fuels under, as nearly as possible, identical conditions.

2. Postirradiation Examination Results

As indicated in the previous section, most of the elements undergoing postirradiation examination are in the intermediate stages of their examination. As a compromise between reporting piecemeal results on all elements as they are obtained and waiting for complete results on a related series of experiments before reporting, this section will report significant trends in examination results as they become apparent. These trends should be considered as preliminary, when reported in progress reports, since additional examination results may alter initial ideas. Final examination results will be reported in topical reports.

a. Effect of Experimental Parameters on the Failure Ratios of Helium-Bonded (U,Pu) Carbide Fuel Elements

A compilation of the experimental parameters of 74 helium-bonded (U,Pu) carbide fuel elements irradiated in EBR-II was made. All elements contained pelletized fuel and included 62 full-size (343 mm fuel stack) elements from UNC Series 1100, 1200, 1300, 1930, 1950, and 1960, 4 full-size elements from ANL, and 8 short (51-mm fuel stack) elements from UNC Series 1200. Of these, 54 have completed irradiation and 50 are presently

TABLE XI

SERIES C-5 AND O-N1 SINGLY CLAD NITRIDE EXPERIMENTS

Expmt. No.	Fuel Type[a]	Fuel Density, % Theo.[b]	Bond and Diametral Gap, mm	Clad Type[c]	Clad O.D. x I.D. mm	Max. Linear Power, kW/m	Maximum Centerline Temp., °C	Goal Burnup, at.%	Maximum Current Burnup at.%	Status
C-5-1	MN	93	Na-0.51	20CW-316SS	7.87 x 7.11	---	----	----	--	Reject[d,e]
C-5-2	MN	94	Na-0.51	20CW-316SS	7.87 x 7.11	---	----	----	--	Reject[d,e]
C-5-3	MN	95	Na-0.51	20CW-316SS	7.87 x 7.11	---	----	----	--	Reject[d,e]
C-5-4	MN	96	Na-0.53	20CW-316SS	7.87 x 7.11	---	----	----	--	Reject[g]
C-5-5	MN	96	Na-0.51	20CW-316SS	7.87 x 7.11	---	----	----	--	Reject[f]
C-5-6	MN	94	Na-0.53	20CW-316SS	7.87 x 7.11	82	1050	12	0	At LASL[h]
C-5-7	MN	95	Na-0.51	20CW-316SS	7.87 x 7.11	84	1060	12	0	At LASL[h]
C-5-8	MN	95	Na-0.76	20CW-316SS	7.87 x 7.11	82	960	12	0	At LASL[h]
C-5-9	MN	95	Na-0.51	20CW-316SS	7.87 x 7.11	84	980	12	0	At LASL[h]
C-5-10	MN	95	Na-0.51	20CW-316SS	7.87 x 7.11	83	970	12	0	At LASL[h]
C-5-11	MN	95	Na-0.51	20CW-316SS	7.87 x 7.11	83	970	12	0	At LASL[h]
C-5-12	MN	95	Na-0.76	20CW-316SS	7.87 x 7.11	81	970	12	0	At LASL[h]
C-5-13	MN	96	Na-0.76	20CW-316SS	7.87 x 7.11	82	950	12	0	At LASL[h]
C-5-14	MN	97	Na-0.76	20CW-316SS	7.87 x 7.11	81	1030	12	0	At LASL[h]
C-5-15	MN	96	Na-0.76	20CW-316SS	7.87 x 7.11	82	970	12	0	At LASL[h]
C-5-16	MN	96	Na-0.76	20CW-316SS	7.87 x 7.11	80	1030	12	0	At LASL[h]
C-5-17	MN	97	Na-0.76	20CW-316SS	7.87 x 7.11	---	----	----	--	Reject[e]
C-5-18	MN	95	Na-0.53	20CW-316SS	7.87 x 7.11	82	970	12	0	At LASL[h]
C-5-19	MN	94	Na-0.53	20CW-316SS	7.87 x 7.11	82	980	12	0	At LASL[h]
C-5-20	MN	96	Na-0.53	20CW-316SS	7.87 x 7.11	84	1050	12	0	At LASL[h]
O-N1-1	MN	91	Na-0.51	20CW-316SS	7.87 x 7.11	80	990	12	0	At LASL[h]
O-N1-2	MN	91	Na-0.51	20CW-316SS	7.87 x 7.11	---	----	----	--	Reject[d]
O-N1-3	MN	91	Na-0.51	20CW-316SS	7.87 x 7.11	80	1060	12	0	At LASL[h]
O-N1-4	MN	90	Na-0.51	20CW-316SS	7.87 x 7.11	80	1060	12	0	At LASL[h]
O-N1-5	MN	91	Na-0.51	20CW-316SS	7.87 x 7.11	---	----	----	--	Reject[d]
O-N1-6	MN	90	Na-0.51	20CW-316SS	7.87 x 7.11	---	----	----	--	Reject[d]
O-N1-8	MN	91	Na-0.51	20CW-316SS	7.87 x 7.11	81	980	12	0	At LASL[h]

[a] $M = (U_{0.8}Pu_{0.2})$.

[b] Theoretical density of MN = 14.17 Mg/m^3.

[c] 20CW = 20% cold worked.

[d] Fuel chips in bond.

[e] Air in plenum.

[f] Possible impurities present.

[g] Damaged.

[h] QA evaluation in progress.

unfailed. All but five were clad in Types 304 or 316 stainless steel or in Incoloy 800. Other experimental parameters are:

> Fuel density: 77 to 99% of theoretical
>
> Amount of $(U,Pu)_2C_3$: 0 to 20 vol%
>
> Thickness of cladding: 0.22 to 0.79 mm
>
> Fuel-cladding diametral gap: 0 to 0.41 mm.

Peak linear power: 38 to 96 kW/m.

Peak burnup: 2.0 to 11.0 at.%

Experimental parameters of all elements are shown in Table 463-XII. Grouping of the experiments was selected so that comparisons could be made of elements which had similar power and burnup combinations. The following classifications were adapted for these comparisons:

TABLE XII

UNFAILED He-BONDED (U.Pu) CARBIDE FUEL ELEMENTS

No.	$\%M_2C_3$	Fuel Density (% T.D.)[b]	Cladding Type	Cladding Thickness (mm.)	Original Diam. Gap (mm.)	Smear Density (% T.D.)[b]	Peak Lin. Power (kW/m)	Peak Burnup (at. %)
				38-60 kW/m				
NMP-1	0	87	Nb-1Zr	0.33	0.20	82	53	3.9
SMP-1	0	85	316SS	0.61	0.13	82	54	2.0
U86	15	99	INC800	0.56	0.25	91	42	6.2
U89D[a]	10	98	316SS	0.61	0.22	92	41	3.0
U90A[a]	10	98	INC800	0.56	0.17	93	51	2.7
U90D[a]	10	99	INC800	0.56	0.23	92	55	3.0
U93	5	86	316SS	0.78	0.10	83	59	9.6
U97	5	86	INC800	0.75	0.10	83	54	10.0
U105	5	77	INC800	0.76	0.20	72	52	9.9
U113	10	98[o]	INC800	0.76	0.28	79	50	10.2
U129	0	86	316SS	0.55	0.41	76	38	10.2
U130	0	77	316SS	0.55	0.25	70	39	10.3
U131	0	85	316SS	0.55	0.36	76	38	10.0
U132	0	85	316SS	0.55	0.36	76	38	9.9
U133	0	85	316SS	0.55	0.36	76	38	9.7
U134	0	85	316SS	0.55	0.36	76	38	9.7
U135	0	85	INC800	0.53	0.36	76	38	10.0
U137	20	97	316SS	0.55	0.36	87	40	8.6
U138	20	97	316SS	0.56	0.36	87	44	4.5
U138A	10	98	316SS	0.42	0.36	88	44	5.6
U139	20	97	INC800	0.56	0.36	87	44	8.8
U140	0	90	INC800	0.53	0.36	81	41	9.4
U141	0	91	316SS	0.55	0.25	84	43	9.2
U142	0	91	316SS	0.66	0.25	84	43	9.3
U143	20	96[c]	INC800	0.53	0.36	77	38	9.5
U144	20	96[c]	316SS	0.56	0.36	77	39	9.6
				60-80 kW/m				
U79	15	98	316SS	0.58	0.18	93	62	2.3
U87	10	99	INC800	0.56	0.15	94	64	3.3
U89A[a]	10	98	316SS	0.61	0.15	93	65	3.4
U89C[a]	10	98	316SS	0.61	0.15	93	62	3.3
U90B[a]	10	99	INC800	0.56	0.08	97	68	3.5
U90C[a]	10·	98	INC800	0.56	0.15	93	66	3.5
U92	---	85	316SS	0.43	0.20	81	67	7.1
U94	0	85	316SS	0.43	0.18	81	70	9.4
U96	---	85	INC800	0.43	0.18	81	66	7.0
U99	---	85	INC800	0.43	0.37	76	62	7.0
U104	---	77	INC800	0.38	0.20	72	60	7.3
U110	10	99[c]	INC800	0.43	0.33	81	65	9.2
U187	5	86	316SS	0.56	0.18	81	77	4.6

TABLE XII (continued)

80-100 kW/m

U80	15	98	V	0.56	0.15	93	92	3.3
U185	10	97	316SS	0.56	0.28	89	90	2.7
U186	10	97	316SS	0.56	0.28	89	90	2.7
U189	5	85	INC800	0.53	0.25	·79	81	4.8
U190	5	85	INC800	0.53	0.28	78	90	11.0
U202	5	85	316SS	0.23	0	85	94	2.5
U203	5	85	316SS	0.44	0.05	84	93	2.5
U204	10	97[c]	316SS	0.22	0.05	88	96	2.6
U205	10	97[c]	316SS	0.43	0.08	85	95	2.6
U206	5	90	316SS	0.43	0.25	83	90	5.0
U208	10	97[c]	316SS	0.43	0.30	79	87	5.0

FAILED He-BONDED (U,Pu) CARBIDE FUEL ELEMENTS

38-60 kW/m

HWMP-1	0	84	Hast.X	0.51	0.10	81	54	6.5
NMP-2	0	84	Nb-1Zr	0.33	0.10	82	56	6.6
U81	10	97	316SS	0.61	0.19	91	49	5.0
U82	10	99	316SS	0.61	0.14	95	47	4.7
U83	10	99	INC800	0.56	0.15	94	47	4.9
U84	10	98	316SS	0.61	0.23	91	45	5.9
U85	10	98	316SS	0.61	0.24	91	42	5.6
U106	5	77	INC800	0.43	0.20	72	59	9.9
U111	---	98[o]	INC800	0.79	0.25	79	55	7.4
U136	0	85	INC800	0.53	0.36	76	40	9.6

60-80 kW/m

U89B[a]	10	99	316SS	0.61	0.05	97	73	3.5
U98	5	86	INC800	0.38	0.18	82	65	9.6
U101	---	85	INC800	0.43	0.03	84	75	5.2
U107	---	98[c]	316SS	0.43	0.18	85	70	6.9
U108	---	98[c]	316SS	0.43	0.36	80	67	7.3
U109	---	98[c]	INC800	0.43	0.36	80	65	7.0
U112	---	98[c]	INC800	0.43	0.18	85	72	7.2
U114	15	98[o]	INC800	0.43	0.18	85	66	9.5

80-100 kW/m

U78	10	98	V-20Ti	0.53	0.13	94	92	3.2
U188	5	85	316SS	0.56	0.18	80	90	11.0
U200	5	86	304SS	0.36	0.23	80	83	4.7
U201	5	85	304SS	0.36	0.23	79	90	7.8
U207	5	90	316SS	0.43	0.25	83	94	7.9
U209	10	97[c]	316SS	0.43	0.30	79	92	7.9

---

[a] 51-mm Fuel Stack.

[b] Theoretical Density of (U,Pu)C - 13.45 Mg/m^3, (U,Pu)$_2$C$_3$ = 12.72 Mg/m^3.

[o] Contained 2.0-mm diametral hole.

[d] All cladding was solution annealed.

Low power: 38-60 kW/m (peak)

Intermediate power: 60-80 kW/m (peak)

High power: 80-100 kW/m (peak)

Low burnup: 2-4 at.% (peak)

Intermediate burnup: 4-8 at.% (peak)

High burnup: 8-11 at.% (peak)

(1) Density of the Fuel. Postirradiation exami-
nation of the fuel microstructure revealed a significant
difference between fuel elements containing high-density
(>95% of theoretical) fuel and those containing low-density
(77-91% of theoretical) fuel. The low-density fuels are re-
structured into three concentric zones. These zones
were: (1) a central zone which was relatively porous and
showed the greatest amount of swelling; (2) an intermediate
zone of relatively dense fuel; and (3) an outer zone of fuel
which showed little change from the as-fabricated struc-
ture. (See Fig. 463-1). Low-density fuel also has shown
the ability to swell into radial cracks which formed when
the fuel pellets cracked radially due to thermal stresses
and moved to contact the inside cladding surface. The
low-density fuel swelled into these cracks out to 0.5-0.8
of the fuel radius; in the central region no evidence of

the cracks remained.

High-density fuel did not restructure in any regular
or symmetric pattern. Typical as-fabricated micro-
structure of the high-density fuel consisted of large (100-
300 μm), dense grains, surrounded by smaller (5-50 μm)
grains. Photomosaics of different sections of high-density
fuel showed varied postirradiation microstructures. In
some sections, porosity occurred mainly in grain bound-
aries surrounding the large dense particles while in others,
the porosity was distributed mainly around the small
grains. (See Figs. 463-2 and 463-3). There was very
little tendency for the high-density fuel to swell into void
space provided by cracks in the fragmented fuel or by
central holes provided in the as-fabricated pellets of some
fuel elements.

Because of these observed microstructural differences,
the failure ratios of high- and low-density fuels were
grouped separately and are shown in Tables 463-XIII and
463-XIV. The failure ratio was quite low for all experi-
ments at low burnup - only 2 failures (both containing high-
density fuel) out of 20 experiments. At burnups over
4 at.%, the high-density-fueled elements had a failure

Fig. 463-1. Photomosaic of a low-density, helium-bonded
(U, Pu)C fuel element irradiated to 9.4 at.%
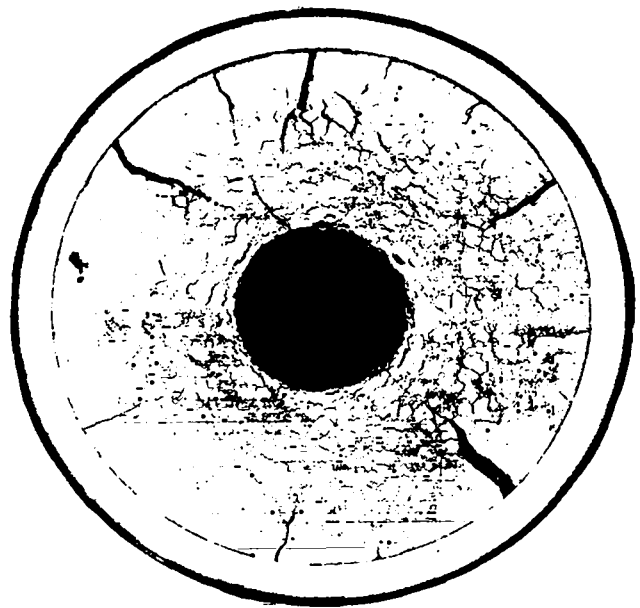at 70 kW/m. (Fuel element U94, Section G,
Mount No. 3C80).

Fig. 463-2. Photomosaic of an annular, high-density
helium-bonded (U, Pu)C fuel element ir-
radiated to 5.0 at.% burnup at 87 kW/m.
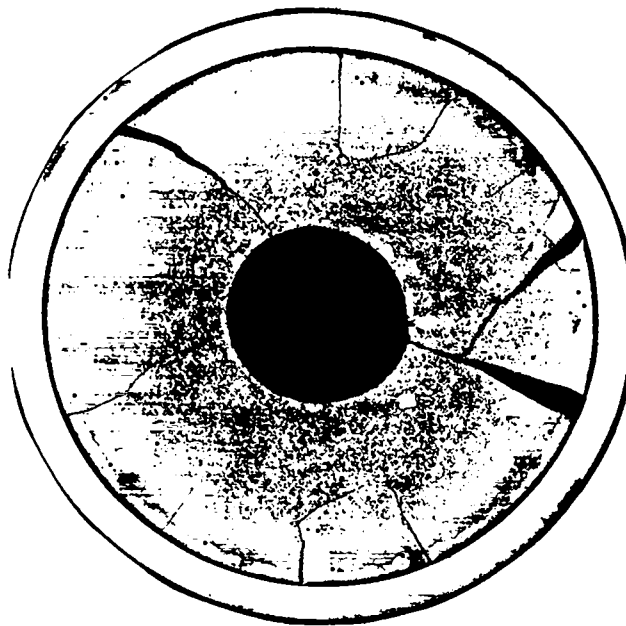(Fuel element U208, Section C. Mount No.
3C61).

Fig. 463-3. Photomosaic of an annular, high–density helium-bonded (U,Pu)C fuel element irradiated to 7.0 at.% burnup at 65 kW/m. (Fuel element U109, Section C, Mount No. 1B88).

TABLE 463-XIV

FAILURE RATIO FOR He-BONDED, HIGH-DENSITY (U,Pu) CARBIDE ELEMENTS

Grouping by Linear Power and Burnup

Power (kW/m)								
Burnup (at.%)	2-4	4-8	8-11	2-4	4-8	8-11	2-4	4-8	8-11
No. of experiments	0+3*	8	5	2+5*	4	2	6	2	0
No. of failures	0+0*	8	0	0+1*	4	1	1	1	0

*Elements having short (51 mm) fuel stacks.

(containing 1-5 vol% $(U,Pu)_2C_3$). The high–density fuel has been hyperstoichiometric, containing 10-20 vol% $(U,Pu)_2C_3$. Attempts have been made to determine the amount of $(U,Pu)_2C_3$ by chemical, x-ray, and metallographic analyses. However, in many cases, the amount of $(U,Pu)_2C_3$ calculated from the chemical analysis has not correlated well with the amount of $(U,Pu)_2C_3$ observed by metallography.

Since the amount of $(U,Pu)_2C_3$ was related to the fuel density in the experiments studied and since the original amount of $(U,Pu)_2C_3$ cannot be accurately determined, no meaningful correlation between the amount of $(U,Pu)_2C_3$ in the fuel and the failure ratio of these fuel elements can be made.

(3) **Type of Cladding.** The selection of Incoloy 800 was based on its somewhat better mechanical strength at elevated temperatures compared to Type 316 stainless steel. At 700°C, the tensile strengths of these alloys are about equal, but the yield strength (0.2%) of Incoloy 800 is 27 000 psi compared to 19 000 psi for Type 316 stainless steel. In a number of cases, fuel elements which were virtually identical except for the type of cladding were tested. In all cases, however, the Incoloy 800 cladding was 1 to 2 mils thinner than the comparable Type 316 stainless steel cladding. A list of these "pairs" is shown in Table 463-XV.

There is no clear indication from this comparison that either Incoloy 800 or Type 316 stainless steel is less likely to fail than the other under almost identical conditions. Quite possibly the difference in mechanical properties of the two types of cladding may not be great enough to show the effect of increased cladding strength on failure rate.

(4) **Thickness of Cladding** There were no fuel elements tested which had cladding thicknesses between 0.45

ratio of 12/22 while the low–density-fueled elements had a failure ratio of 10/32. Comparison of elements having a linear power over 60 kW/m and a burnup over 4 at.% showed that the high-density fueled elements had a failure ratio of 6/8 while the low–density-fueled elements had a failure ratio of 6/15. The higher failure ratios of the high-density-fueled elements are believed to be related to their relatively inconsistent postirradiation microstructural patterns and the inability for this fuel to swell into space provided by the original fuel-cladding gap.

(2) **Amount of $(U,Pu)_2C_3$ in the Fuel.** The low–density fuel which has been irradiated in the experiments thus far has been single-phase or slightly hyperstoichiometric

TABLE 463-XIII

FAILURE RATIO FOR He-BONDED, LOW-DENSITY (U,Pu) CARBIDE ELEMENTS

Grouping by Linear Power and Burnup

Power (kW/m)	35-60			60-80			80-100		
Burnup (at.%)	2-4	4-8	8-11	2-4	4-8	8-11	2-4	4-8	8-11
No. of experiments	2	2	15	0	6	2	2	5	2
No. of failures	0	2	2	0	1	1	0	3	1

TABLE XV

COMPARISON OF FAILURES IN He-BONDED (U, Pu) CARBIDE ELEMENTS CLAD IN TYPE 316 STAINLESS STEEL AND IN INCOLOY 800

(Each comparison is based on elements having the same design parameters and irradiation conditions)

	Type 316 Stainless Steel	Incoloy 800
(1)	U82 (failed)	U83 (failed)
(2)	U84 (failed, U85 (failed)	U86
(3)	U89B (failed)	U90B
(4)	U89C	U90C
(5)	U92	U96
(6)	U93	U97
(7)	U94	U98 (failed)
(8)	U107 (failed)	U112 (failed)
(9)	U108 (failed)	U109 (failed)
(10)	U131, U132, U133, U134	U135, U136 (failed)
(11)	U137	U139
(12)	U144	U143
(13)	U187	U189

and 0.50 mm, so the elements were split into two groups classified as < 0.45 mm and > 0.50 mm. The failure ratios of the elements having < 0.45 mm claddings were grouped by linear power and burnup and are shown for low-density-fueled elements in Table XVI and for high-density-fueled elements in Table XVII.

The overall failure ratio for elements in the thinner claddings and containing low-density fuel was somewhat lower (7/16) than that of elements containing high-density fuel (6/11). No failures occurred at low burnup for

TABLE XVI

FAILURE RATIO FOR He-BONDED, LOW-DENSITY (U, Pu) CARBIDE ELEMENTS HAVING CLADDING LESS THAN 0.45 mm THICK

Grouping by Linear Power and Burnup

Power (kW/m)	38-60			60-80			80-100		
Burnup (at.%)	2-4	4-8	8-11	2-4	4-8	8-11	2-4	4-8	8-11
No. of experiments	1	1	1	0	6	2	2	4	0
No. of failures	0	1	1	0	1	1	0	3	0

TABLE XVII

FAILURE RATIO FOR He-BONDED, HIGH-DENSITY (U,Pu) CARBIDE ELEMENTS HAVING CLADDING LESS THAN 0.45 mm THICK

Grouping by Linear Power and Burnup

Power (kW/m)	38-80			60-80			80-100		
Burnup (at.%)	2-4	4-8	8-11	2-4	4-8	8-11	2-4	4-8	8-11
No. of experiments	0	1	0	0	4	2	2	2	0
No. of failures	0	0	0	0	4	1	0	1	0

elements containing either low (0/3) or high (0/2) density fuel. At burnups over 4 at.%, low-density-fueled elements with < 0.45-mm-thick cladding had a failure ratio of 2/7 at intermediate power levels, but higher failure ratios at low (2/2) and high (3/4) power levels. Conversely, most of the high-density-fueled elements in thinner claddings failed (5/6) at intermediate powers.

The failure ratios of elements having > 0.50-mm-thick claddings are shown in Tables 463-XVIII and 463-XIX for the two groups of fuel densities. Most of the elements in the thicker claddings were irradiated at low power levels. Overall failure ratios for the elements having thicker claddings were lower than those having thinner claddings; the failure ratios for the low- and high-density-fueled elements were 3/20 and 8/27, respectively.

Many of the low-density-fueled elements were irradiated at low power, but the additional strength provided by thicker claddings appeared to be effective in reducing failures in elements containing this type of fuel.

TABLE 463-XVIII

FAILURE RATIO FOR He-BONDED, LOW-DENSITY (U,Pu) CARBIDE ELEMENTS HAVING CLADDING GREATER THAN 0.50 mm THICK

Grouping by Linear Power and Burnup

Power (kW/m)	38-60			60-80			80-100		
Burnup (at.%)	2-4	4-8	8-11	2-4	4-8	8-11	2-4	4-8	8-11
No. of experiments	1	1	14	0	1	0	0	1	2
No. of failures	0	1	1	0	0	0	0	0	1

TABLE 463-XIX

FAILURE RATIO FOR He-BONDED, HIGH-DENSITY (U,Pu) CARBIDE ELEMENTS HAVING CLADDING GREATER THAN 0.50 mm THICK

Grouping by Linear Power and Burnup

Power (kW/m)	38-60			60-80			80-100		
Burnup (at.%)	2-4	4-8	8-11	2-4	4-8	8-11	2-4	4-8	8-11
No. of experiments	0+3*	8	5	2+5*	0	0	4	0	0
No. of failures	0+0*	6	0	0+1*	0	0	1	0	0

*Elements having short (≤1 mm) fuel stacks.

Unfortunately, only four elements containing low–density fuel and having cladding over 0.50 mm have been irradiated at peak linear powers over 60 kW/m.

Elements containing high–density fuel appeared to be much less affected by the use of thicker claddings. There were no high–density-fueled elements in > 0.50-mm cladding irradiated at intermediate or high power to burnups over 4 at.%. However, a number of elements of this type were irradiated at low power but the results were anomalous; a failure ratio of 6/8 was found at intermediate burnup but no failures (0/5) were found at high burnup.

(5) Fuel-Cladding Gap. The fuel–cladding gap, besides influencing the fuel temperature, provides space into which the fuel can swell. The utilization of this space for fuel swelling is complicated by the breaking of the fuel pellets due to thermal stresses at startup. In all fuel elements that have been examined, the fuel has cracked generally in a radial direction and moved to contact the inside cladding surface. The space that was originally in the circumferential fuel –cladding gap was transferred to the space between the diametral and radial cracks. Low–density fuel swelled into these cracks out to 0.5-0.8 of the radius; in the central region, no evidence of the cracks remained. High–density fuel also swelled into these cracks but did not heal the cracks and, in general, did not utilize the space between the radial cracks to the degree that it was used by low–density fuel.

The low- and high–density-fueled elements are grouped by their original diametral fuel–cladding gap size and final burnup levels in Tables 463-XX and 463-XXI. The gap size groups were classified as small (<0.18 mm), intermediate (0.18-0.25 mm) and large (>0.25 mm).

At low burnup, only two failures occurred, both of which contained high–density fuel with gaps of 0.13 mm or less. At burnup levels over 4 at.%, elements containing either low–or high–density fuel showed a decreasing failure ratio with each increasing gap size range. For high–density-fueled elements at burnup levels over 4 at.%, the failure ratio was very high (9/10) for fuel–cladding gaps under 0.26 mm and significantly lower (3/12) for large gaps. Elements containing low–density fuel also had a low failure ratio (1/10) for fuel-cladding gaps over 0.25 mm at burnups greater than 4 at.%; equivalent elements with intermediate size gaps had a failure ratio of 6/17 but three of these failures occurred at burnups over 9-1/2 at.%.

In order to include the influence of cladding thickness with the fuel-cladding gap, all fuel elements having more than 4 at.% burnup are grouped by cladding thickness and fuel cladding gap in Tables 463-XXII and 463-XXIII. For elements containing high-density fuel, a low failure ratio (0/6) was indicated only for those which had thick (>0.50 mm) cladding and a large (>0.25 mm) fuel–cladding gap. Although most of the elements containing low–density fuel in thinner claddings had an intermediate gap

TABLE XXI

FAILURE RATIO FOR He-BONDED, HIGH-DENSITY (U,Pu) CARBIDE ELEMENTS

Grouping by Burnup and Fuel-Cladding Gap

Burnup (at.%)	2-4			4-8			8-11		
Diametral Gap (mm)	<0.18	0.18-0.25	>0.25	>0.18	0.18-0.25	>0.25	0.18	0.18-0.25	>0.25
No. of Experiments	5+6*	1+2*	2	2	7	8	0	1	8
No. of failures	1+1*	0+0*	0	2	6	3	0	1	0

*Elements having short (51 mm) fuel stacks

TABLE 463-XX

FAILURE RATIO FOR He-BONDED, LOW-DENSITY (U,Pu) CARBIDE ELEMENTS

Grouping by Burnup and Fuel-Cladding Gap

Burnup (at.%)	2-4			4-8			8-11		
Diametral Gap (mm.)	<0.18	0.18-0.25	>0.25	<0.18	0.18-0.25	>0.25	<0.18	0.18-0.25	>0.25
No. of Experiments	3	1	0	3	9	1	2	6	9
No. of failures	0	0	0	3	3	0	0	3	1

TABLE 463-XXII

FAILURE RATIO FOR He-BONDED, LOW-DENSITY (U,Pu) CARBIDE ELEMENTS WITH PEAK BURNUPS OVER 4 at.%

Grouping by Cladding Thickness and Fuel-Cladding Gap

Cladding Thickness (mm)	<0.45			>0.50		
Diametral Gap (mm)	>0.18	0.18-0.25	>0.25	<0.18	0.18-0.25	>0.25
No. of experiments	2	10	1	3	7	8
No. of failures	2	6	0	1	1	1

TABLE 463-XXIII

FAILURE RATIO FOR He-BONDED, HIGH-DENSITY (U,Pu) CARBIDE ELEMENTS WITH PEAK BURNUPS OVER 4 at.%

Grouping by Cladding Thickness and Fuel-Cladding Gap

Cladding Thickness (mm)	<0.45			>0.50		
Diametral Gap (mm)	<0.18	0.18-0.25	>0.25	<0.18	0.18-0.25	>0.25
No. of experiments	0	3	6	2	5	6
No. of failures	0	3	3	2	4	0

size, there was some indication that increased fuel-cladding gap sizes did reduce the failure ratio. The influence of the fuel-cladding gap size appeared to be much less for low-density-fueled elements which had claddings greater than 0.50 mm.

b. Fission Gas Release and Distribution

Sufficient postirradiation examination data are now available to calculate the fission gas release for 25 elements that are currently under examination. Of the 25 elements, data on 16 were reported in a previous progress report.[2] In addition, fission gas release results have been recalculated and reported here for three elements that had previously completed examination and been reported: U101,[3] U109,[3] and K-42B.[4] These data are used for comparative purposes.

The element data used to calculate fission gas release included 1) a measurement of the number of moles and an isotopic analysis of the fuel element plenum gas and the capsule plenum gas, 2) a mass spectrometric burnup determination from a sample taken at a known axial location along the fuel element, 3) fabrication data which specifies the amount of fuel, the fuel column length. and the isotopic content of the uranium and plutonium in the fuel, and 4) data specifying the element location in EBR-II and the reactor runs during which it was irradiated. Fission product yields were obtained from the 1972 compilation of Meek and Rider.[5] Relative fission rate data including axial and radial variation for ^{235}U, ^{238}U, ^{239}Pu, and ^{240}Pu were obtained from the EBR-II irradiation guide.[6] The fission rates of other fissionable isotopes were estimated as ratios to known fission rates:

$$^{233}U/^{235}U = 1.65,$$
$$^{241}Pu/^{239}Pu = 1.75, \text{ and}$$
$$^{242}Pu/^{239}Pu = 0.1.$$

The variation of fission rate data with changes in the EBR-II core configuration was also used. Since the information in the EBR-II irradiation guide is only approximate, the results of the calculations presented here must be considered as preliminary, until accurate run data are available.

Table 463-XXIV lists the measured Xe and Kr content of the fuel element plenum and capsule plenum , the measured isotopic content of Xe and Kr, and the total moles of gas in each plenum. Table 463-XXV summarizes the fission gas release and burnup results. The peak burnup and axial average burnup shown in Table 463-XXV were calculated from the measured burnup and its axial location. Two methods were used to calculate the amount of fission gas released from the fuel. In "Method A," the measured number of moles of gas in the fuel element plenum and in the capsule plenum, and the gas analyses, were used to calculate the amount of fission gas released from the fuel. This method uses direct experimental data without any subsidiary assumptions, but it is subject to error if fission gas is lost during sampling or is trapped in sodium voids. "Method B" assumes that the element and capsule were loaded with only He and Ar during fabrication under local atmospheric pressure and at 25°C. The total number of moles of gas in each plenum can be calculated using this assumption, in addition to the measured plenum volume of the element and capsule, and the He and Ar content of the gas after irradiation. Thus the two methods differ only in the way the amount of fission gas is determined. The number of moles of plenum gas shown in Table XXIV is based on the Method B calculation. A comparison of fission gas release calculated by the two methods (see Table 463-XXV) shows that there is either fair agreement or the Method A calculation gives a substantially lower result. In a number of cases where the Method A fission gas release is low, a calculation of the fuel element plenum pressure using the measured number of moles and the plenum volume results in a pressure below the initial loading pressure. This indicates a loss of plenum gas. In general, the Method B fission gas release is considered a better estimate.

Table 463-XXVI presents a detailed tabulation of the fission gas release results for the individual Kr and Xe isotopes. These results are from the "Method B" calculation. The ^{85}Kr (10.8 year half-life) results are not corrected for decay during or after irradiation. The systematic variation of the release fraction for some isotopes (^{83}Kr and ^{85}Kr are always lower than ^{84}Kr and ^{86}Kr) is probably due to differences in actual fission yields from tabulated values. The tabulated yields used are not

TABLE 463-XXIV

XENON AND KRYPTON COMPOSITIONS AND TOTAL MOLES OF PLENUM GAS

Element No. Ho Bonded Carbides	Plenum [a]	Total Moles of Gas [b]	Xe Content (Mole %)	Xe Isotopic Content (Mole %) [c] ^{131}Xe	^{132}Xe	^{134}Xe	^{136}Xe	Kr Content (Mole %)	Kr Isotopic Content (Mole %) ^{83}Kr	^{84}Kr	^{85}Kr	^{86}Kr
U 93 [d]	E	1.92×10^{-3}	71.3	14.99	21.91	34.29	28.76	11.2	15.6	28.8	6.08	50.5
	C	2.55×10^{-4}	-	-	-	-	-	-	-	-	-	-
U 94 [d]	E	4.65×10^{-3}	75.7	14.99	21.87	34.33	28.76	11.8	15.6	27.9	6.08	50.4
	C	1.90×10^{-4}	-	-	-	-	-	-	-	-	-	-
U 105 [d]	E	3.20×10^{-3}	78.5	14.94	21.89	34.36	28.76	12.2	15.66	27.89	6.05	59.40
	C	2.08×10^{-4}	-	-	-	-	-	-	-	-	-	-
U 187 [d]	E	1.35×10^{-3}	66.4	15.14	21.82	34.25	28.73	10.87	15.62	27.86	6.84	49.68
	C	2.27×10^{-4}	-	-	-	-	-	-	-	-	-	-
U 189 [d]	E	1.29×10^{-3}	65.7	15.12	21.83	34.24	28.77	11.16	15.61	27.78	6.82	49.79
	C	2.36×10^{-4}	-	-	-	-	-	-	-	-	-	-
U 200	E	1.27×10^{-3}	65.6	15.2	21.6	34.5	28.7	10.2	15.6	27.5	6.82	50.1
	C	3.84×10^{-4}	6.4	15.1	21.2	34.7	29.0	1.0	16.0	27.7	6.8	49.5
U 206 [d]	E	8.63×10^{-4}	57.0	15.22	21.84	34.21	28.71	8.93	15.64	27.60	6.86	49.90
	C	2.97×10^{-4}	-	-	-	-	-	-	-	-	-	-
U 208 [d]	E	9.33×10^{-4}	54.9	15.15	21.79	34.34	28.68	8.63	15.58	27.56	6.88	49.99
	C	2.85×10^{-4}	-	-	-	-	-	-	-	-	-	-
U 101 [f]	E	8.97×10^{-4}	55.0	15.26	21.77	34.30	28.67	8.92	15.58	27.47	7.05	49.89
	C	4.57×10^{-4}	28.6	14.99	21.63	34.66	28.72	4.64	15.48	27.56	7.02	49.95
U109 [f]	E	8.10×10^{-4}	49.9	15.03	21.84	34.27	28.86	7.54	15.52	27.72	6.37	50.40
	C	4.20×10^{-4}	29.0	14.93	21.98	34.28	28.86	4.61	15.60	27.51	6.85	50.04
Na Bonded Carbides												
K-36B	E	1.81×10^{-3}	57.7	14.99	22.00	34.16	28.82	8.84	15.71	27.77	6.49	50.03
	C	1.77×10^{-4}	0.09	89	8	3	<1	>0.002	(e)	(e)	(e)	(e)
K-42B [g]	E	8.70×10^{-4}	42.2	15.17	22.04	33.89	28.91	6.62	15.77	27.47	7.11	49.65
	C	1.62×10^{-4}	-	-	-	-	-	-	-	-	-	-
K-45	E	7.79×10^{-4}	20.9	14.75	21.88	34.40	28.96	3.28	15.7	27.6	6.74	50.0
	C	1.77×10^{-4}	0.23	73	11	11	4	>0.002	(e)	(e)	(e)	(e)
K-46	E	1.25×10^{-3}	27.4	14.74	22.01	34.33	28.90	4.28	15.61	27.44	6.94	50.00
	C	1.75×10^{-4}	0.08	86	8	5	1	>0.001	(e)	(e)	(e)	(e)
K-49 [b]	E	1.14×10^{-3}	35.6	15.94	23.37	29.60	31.05	9.01	17.4	28.1	7.58	46.9
	C	4.31×10^{-3}	32.3	17.80	22.67	29.00	30.47	7.44	17.2	27.9	7.72	47.1
U 191 [d]	E	4.84×10^{-4}	31.0	14.78	21.71	34.45	28.91	5.56	15.56	27.70	6.90	48.92
	C	1.97×10^{-4}	-	-	-	-	-	-	-	-	-	-
U 192 [d]	E	7.49×10^{-4}	55.0	14.90	21.62	34.53	28.91	9.33	15.54	27.61	6.89	49.96
	C	2.07×10^{-4}	-	-	-	-	-	-	-	-	-	-
U 194	E	1.67×10^{-3}	63.0	15.2	21.7	34.4	28.6	9.85	15.5	27.3	6.88	50.3
	C	1.95×10^{-4}	0.45	26.4	53.0	13.2	7.4	0.07	(e)	(e)	(e)	(c)
U 195 [d]	E	7.05×10^{-4}	55.7	14.82	21.76	34.45	28.93	9.35	15.62	27.64	6.87	49.87
	C	2.56×10^{-4}	-	-	-	-	-	-	-	-	-	-
U 197 [d]	E	1.14×10^{-3}	65.3	14.97	21.74	34.36	28.89	10.5	15.62	27.52	6.90	49.96
	C	2.45×10^{-4}	-	-	-	-	-	-	-	-	-	-
U 198 [d]	E	6.95×10^{-4}	58.6	14.73	21.72	34.55	28.06	9.43	15.63	27.61	6.87	49.89
	C	2.38×10^{-4}	-	-	-	-	-	-	-	-	-	-
W 41 [d]	E	9.03×10^{-4}	37.1	14.75	21.93	34.34	28.97	5.83	15.60	27.67	6.65	50.07
	C	1.27×10^{-4}	-	-	-	-	-	-	-	-	-	-
W8P [d]	E	8.52×10^{-4}	34.7	14.96	21.94	34.19	28.87	5.42	15.73	27.77	6.35	50.15
	C	1.40×10^{-4}	-	-	-	-	-	-	-	-	-	-
Na Bonded Nitrides												
B 1-1	E	3.72×10^{-4}	12.8	14.33	22.12	34.63	28.89	2.25	15.55	27.92	6.48	50.05
	C	4.18×10^{-4}	0.04	91	5	4	(c)	(c)	(c)	(c)	(c)	(e)
B 2-2	E	8.46×10^{-4}	25.70	14.73	21.82	34.35	29.08	4.0	15.6	27.5	6.75	50.1
	C	2.22×10^{-4}	3.86	17.25	22.31	33.51	26.89	0.58	17.1	27.8	6.75	48.3

TABLE 463-XXIV (continued)

B 3-2	E	7.80×10^{-4}	22.8	12.84	21.67	34.82	30.66	3.78	15.2	27.2	7.02	50.6
	C	2.01×10^{-4}	7.54	23.0	24.2	33.5	19.3	1.00	20.8	30.6	6.3	42.3
B 3-4	E	8.54×10^{-4}	31.4	14.35	21.97	34.57	29.11	5.15	15.84	27.47	6.99	49.70
	C	3.94×10^{-4}	11.25	15.63	22.04	33.92	28.40	1.52	15.72	28.50	6.74	49.05
B 3-5	E	5.83×10^{-4}	14.8	12.83	22.03	35.36	29.76	2.87	15.6	27.7	6.97	49.8
	C	4.61×10^{-4}	28.5	15.93	21.77	33.71	28.57	3.96	15.9	27.4	6.97	49.7

(a) E = Element Plenum; C = Capsule Plenum.
(b) Based on Method B Calculation.
(c) Small quantities of other Xe fission product isotopes not reported.
(d) Unfailed element – no fission gas in capsule plenum.
(e) Insufficient fission gas for an analysis.
(f) Failed elements reported previously by Gulf United Nuclear Fuels Corp. (Ref. 3)
(g) Unfailed element reported previously by Los Alamos Scientific Laboratory (Ref. 4)
(h) Element contained ^{233}U.

TABLE 463-XXV

FISSION GAS RELEASE SUMMARY

Element	Burnup, at.% Peak	Average	% Fission Gas Released[a] Method A	Method B
He Bonded Carbides				
U 93	9.64	8.68	12.5	16.3
U 94	9.42	8.48	1.7	34.9
U 105	9.89	8.91	8.2	34.0
U 187	4.60	4.15	22.1	20.4
U 189	4.80	4.33	20.6	18.7
U 200	4.72	4.26	15.9	18.1
U 206	4.96	4.48	9.6	9.6
U 208	5.00	4.51	10.5	10.3
U 101[b]	5.22	4.67	8.8	10.9
U 109[b]	7.04	6.31	4.1	7.2
Na Bonded Carbides				
K-36B	5.85	5.29	16.3	16.3
K-42B[c]	4.46	4.02	7.6	7.6
K-45	2.37	2.17	5.8	6.3
K-46	2.39	2.18	8.8	13.1
K-49	3.74	3.71	37.9	97.1
U 191	4.50	4.06	3.2	3.2
U 192	4.30	3.88	11.6	10.0
U 194	4.64	4.19	15.1	21.3
U 195	4.94	4.46	10.6	9.1
U 197	4.90	4.42	9.2	15.2
U 198	4.78	4.32	10.9	8.5
W 4F	5.32	5.09	8.5	8.1
W 8F	5.82	5.53	7.1	6.5
Na Bonded Nitrides				
B 1-1	5.70	5.16	0.72	0.86
B 2-2	5.48	5.21	4.1	4.5
B 3-2	2.78	2.65	6.9	7.1
B 3-4	2.70	2.57	5.8	11.5
B 3-5	2.33	2.21	8.4	8.6

[a] Calculation methods described in text.

[b] Elements reported previously by Gulf United Nuclear Fuels Corp. (Ref.3).

[c] Element reported previously by Los Alamos Scientific Laboratory (Ref. 4).

TABLE 463-XXVI

FISSION GAS RELEASE OF INDIVIDUAL ISOTOPES
(Method B Calculation)

| | % of Fission Gas Released | | | | | | | |
| | Kr | | | | Xe | | | |
Element	83	84	85(a)	86	131	132	134	136
He Bonded Carbides								
U 93	14.7	16.1	11.4	16.4	15.4	16.3	16.9	16.6
U 94	31.1	34.2	24.3	34.7	32.9	34.8	36.2	35.4
U 105	30.4	33.3	23.5	33.8	31.9	34.0	35.3	34.6
U 187	19.1	20.9	16.7	21.0	19.3	20.2	21.0	20.6
U 189	18.0	19.7	15.7	19.8	17.6	18.4	19.1	18.8
U 200	16.1	17.5	14.1	17.9	17.3	17.8	18.9	18.3
U 206	8.6	9.3	7.6	9.5	9.1	9.5	9.9	9.7
U 208(b)	9.3	10.1	8.2	10.3	9.8	10.3	10.7	10.5
U 101(b)	10.0	10.9	9.1	11.1	10.4	10.7	11.3	11.0
U 109(b)	6.3	6.9	5.3	7.0	6.8	7.2	7.4	7.3
Na Bonded Carbides								
K-36B	14.9	16.2	12.4	16.5	15.1	16.2	16.9	16.5
K-42B(c)	7.1	7.6	6.5	7.8	7.1	7.5	7.7	7.6
K-45	5.8	6.3	5.0	6.4	5.8	6.2	6.5	6.4
K-46	12.1	13.1	10.8	13.4	12.0	13.1	13.6	13.3
K-49	88.1	92.0	80.7	98.6	92.7	93.7	102.7	100.7
U 191	3.2	3.5	2.9	3.6	2.9	3.1	3.3	3.2
U 192	9.5	10.4	8.5	10.6	9.3	9.8	10.3	10.1
U 194	19.0	20.5	16.9	21.2	20.4	21.1	22.2	21.5
U 195	8.7	9.5	7.7	9.6	8.4	9.0	9.4	9.2
U 197	13.0	15.2	12.4	15.5	14.3	15.0	15.8	15.5
U 198	7.8	8.5	6.9	8.7	7.9	8.4	8.9	8.7
W 4F	7.4	8.1	6.4	8.3	7.4	8.0	8.4	8.2
W 8F	6.1	6.6	4.9	6.7	6.1	6.5	6.8	6.6
Na Bonded Nitrides								
B 1-1	0.87	0.96	0.73	0.97	0.77	0.85	0.88	0.85
B 2-2	4.1	4.5	3.6	4.6	4.1	4.5	4.7	4.6
B 3-2	6.8	7.4	6.1	7.6	6.0	7.0	7.4	7.4
B 3-4	10.9	11.7	9.7	11.9	10.3	11.4	11.9	11.6
B 3-5	8.2	8.9	7.3	9.0	7.9	8.5	8.9	8.8

(a)Not corrected for decay.

(b)Elements reported previously in Gulf United Nuclear Fuels Corp. (Ref. 3).

(c)Element reported previously in Los Alamos Scientific Laboratory (Ref. 4).

representative of the actual EBR-II neutron spectrum so that some differences can be expected. The data presented in Table 463-XXV represent weighted averages of the data in Table 463-XXVI, with each release percentage being weighted by the amount of that isotope present.

In the failed He-bonded carbide elements, no significant differences in the Xe or Kr isotopic distributions between fuel element and capsule were found. The total fission gas release percentages in Table 463-XXV combined with data from previously reported[2,7] He-bonded elements were used in an attempt to correlate fission gas release with fuel density, smear density, power level, and burnup.

In general, fission gas release was very low (~1%) for high-density (96-100% of theoretical) fuel. The greatest fission gas releases from high-density fuel were

from two elements which contained annular fuel pellets; these elements (U109 and U208) released 7.2 and 10.3%, respectively.

Low-density (77-90% of theoretical) fuel released a considerably greater amount of fission gas than high-density fuel; the releases ranged from 4.1 to 36.6% of theoretical. In these low-density-fueled elements, the percentage of fission gas release was found to increase with burnup. (See Fig. 463-4). In addition, the smear densities of the elements also appeared to have a significant effect on fission gas releases of low-density-fueled elements. Fig. 463-4 shows that a higher percentage gas release was attained for elements which had smear densities $\leq$ 81% theoretical fuel density than for elements which had smear densities $\geq$ 82% theoretical fuel density. The amount of fission gas release appeared to be independent of the original fuel density (if below 91% of theoretical) and also independent of power level within the range studied (52-90 kW/m).

These results indicate that the relative amount of fission gas released is related to microstructural changes in the fuel which result in a more open microstructure in the central portion of the fuel. (See Fig. 463-1). Fig. 463-4 also shows that the percentage of fission gas released reaches a constant value of about 35% between 7 and 10 at.% peak burnup for low-density-fueled elements
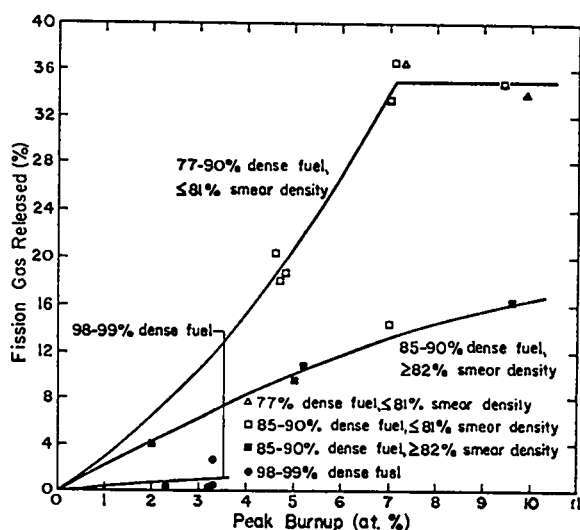
Fig. 463-4. Total fission gas release from helium bonded carbides vs peak burnup.

having smear densities $\leq$ 81%. These elements operated at 52-83 kW/m.

An examination of the Xe isotopic compositions found in the capsules of failed Na-bonded carbide and nitride elements (see Table 463-XXIV) indicated that the plenum gas in a number of capsules had a Xe isotopic composition that was grossly different from that in the element plenum (K-36B, K-45, K-46, U194, and B-1-1). No variations of this nature have been found in failed He-bonded elements. This observation indicates that the distribution of fission gas between the element and capsule is probably being influenced by the fuel element Na bond. In order to more completely examine the fission gas distribution between the element and capsule, a number of parameters have been calculated from the data of Table 463-XIV. Table 463-XXVII lists three groups of calculated parameters, 1) the ratio of total capsule fission gas to total element fission gas, 2) the ratio of total Kr to total Xe for both the element and capsule, and 3) the ratio of Xe isotopic content in the capsule to that in the element. All three parameters show similar variations for four of the five elements noted above (K-36B, K-45, K-46, and B-1-1), indicating a common mechanism may be the cause.

The ratio of total capsule fission gas to total element fission gas is an indication of the magnitude of the cladding failure. Elements K-36B, K-45, K-46, U 194, and B-1-1 have very small values for this ratio. The total quantity of fission gas in the capsules of these elements is less than 1×10^{-6} moles in each case. This small release of fission products is in line with the classification of these elements as slight failures based on visual and radiographic examinations. (An element classed as a slight failure is one in which the cladding breach that allowed fission products to escape cannot be found.) Thus all five elements have the common trait of releasing only a very small quantity of fission products.

The ratio of total Kr to total Xe should approximate the ratio of yields of these gases. This is the case for the element plenum data and some capsule plenum data, but four of the five elements noted above (K-36B, K-45, K-46, and B-1-1) have very low values for this ratio in the capsule (see Table 463-XXVII). In addition to these large

TABLE 463-XXVII

FISSION GAS DISTRIBUTION PARAMETERS

Element No.	Ratio of Capsule Fission Gas to Element Fission Gas[f]	Ratio of Total Kr/Total Xe		Ratio of Xe Isotopic Content in Capsule to Content in Element			
		Element	Capsule	^{131}Xe	^{132}Xe	^{134}Xe	^{136}Xe
He Bonded Carbides							
U 93[a]	0	0.157	-	-	-	-	-
U 94[a]	0	0.156	-	-	-	-	-
U 105[a]	0	0.155	-	-	-	-	-
U 187[a]	0	0.164	-	-	-	-	-
U 189[a]	0	0.170	-	-	-	-	-
U 200	0.029	0.155	0.156	0.99	0.98	1.01	1.01
U 206[a]	0	0.157	-	-	-	-	-
U 208[a]	0	0.157	-	-	-	-	-
U 101[c]	0.27	0.162	0.162	0.98	0.99	1.01	1.00
U 109[c]	0.30	0.151	0.159	0.99	1.01	1.00	1.00
Na Bonded Carbides							
K-36B[d]	9.5×10^{-5}	0.153	0.02	5.9	0.36	0.088	0.035
K-42B[d]	0	0.157	-	-	-	-	-
K-45	1.9×10^{-3}	0.157	<0.01	5.0	0.50	0.32	0.14
K-46	2.5×10^{-4}	0.156	0.01	5.8	0.36	0.15	0.035
K-49[e]	3.4	0.253	0.230	1.12	0.97	0.98	0.98
U 191[a]	0	0.179	-	-	-	-	-
U 192[a]	0	0.170	-	-	-	-	-
U 194	3.5×10^{-4}	0.156	0.156	1.7	2.4	0.38	0.26
U 195[a]	0	0.168	-	-	-	-	-
U 197[a]	0	0.161	-	-	-	-	-
U 198[a]	0	0.161	-	-	-	-	-
W 4F[a]	0	0.157	-	-	-	-	-
W 8F[a]	0	0.156	-	-	-	-	-
Na Bonded Nitrides							
B 1-1	2.7×10^{-3}	0.176	(b)	6.4	0.23	0.12	(b)
B 2-2	0.027	0.156	0.150	1.17	1.00	0.98	0.93
B 3-2	0.083	0.166	0.133	1.79	1.12	0.96	0.63
B 3-4	0.16	0.164	0.135	1.09	1.00	0.98	0.98
B 3-5	1.5	0.194	0.139	1.24	0.99	0.95	0.96

(a) Unfailed element - no fission gas found in capsule.
(b) Insufficient fission gas for complete analysis. Krypton not detected in capsule.
(c) Failed elements reported previously by Gulf United Nuclear Fuels Corp. (Ref. 3).
(d) Unfailed element reported previously by Los Alamos Scientific Laboratory (Ref. 4).
(e) Element contains ^{233}U.
(f) Method B Calculation.

differences, the ratio of total Kr to total Xe in the capsules of Na-bonded elements is always equal to or less than the ratio in the element. Thus, the same mechanism which produced abnormally low values in a few elements may be in operation in all Na-bonded elements.

The ratio of the Xe isotopic content in the capsule to that in the element (see Table 463-XXVII) is a parameter which is sensitive to the variation that was first observed, i.e., the grossly different Xe isotopic contents of some elements and capsules. Four of the five elements noted above (K-36B, K-45, K-46, and B-1-1) were highly enriched in ^{131}Xe and depleted in the other Xe isotopes in the capsule. The fifth (U 194) was enriched in ^{131}Xe and ^{132}Xe and depleted in the others. A closer examination

of all failed, Na-bonded elements indicated that all capsules were enriched to some extent in ^{131}Xe and depleted in ^{134}Xe and ^{136}Xe. This was even true when the capsule contained more total fission gas than the element (K-49 and B-3-5). The data for failed, He-bonded elements showed that the elements and capsules had essentially identical Xe isotopic compositions. A similar statement can be made here as was made for the total Kr to total Xe ratio data, i.e., a single mechanism may be operative in all Na-bonded elements which affects the distribution of fission gas between the element and capsule. In a few cases, this mechanism predominates and results in grossly different distributions.

A calculation of the ratio of the Kr isotopic content in the capsule to that in the element is not shown. This was omitted because many of the elements that would show significant variation did not have enough Kr in the capsule to allow an isotopic analysis (see Table 463-XXIV).

Some feeling for mechanisms which could explain the observations of Table 463-XXVII can be obtained from an examination of the calculated isotopic concentrations of fission product Xe and Kr and their precursors as a function of irradiation time. These calculations were performed using the RIBD code[8] and the fuel composition of U 194. (Small variations in the calculated fission product compositions would result from the different U and Pu compositions of different fuel elements but these differences would not change the conclusions.) Figures 463-5 through 463-10 show the isotopic concentration of fission product Xe, I, Te, Kr, Br, and Se as a function of irradiation time.

One possible mechanism, the release of newly-produced fission gas from the element to the capsule early in life or shortly after a prolonged shutdown, can be eliminated immediately by examining Fig. 463-5. Newly produced Xe is enriched in ^{136}Xe and depleted in ^{131}Xe. This is the opposite of what was observed.

Considering only the four elements which showed similar anomalous behavior (K-36B, K-45, K-46, and

Fig. 463-6. Isotopic concentration of iodine fission products vs irradiation time.

B1-1), a mechanism involving precursors can qualitatively explain the observations. In the range of 30 to 100 hours irradiation time, the isotopic concentrations of I precursors approximates the capsule Xe isotopic concentrations observed for these elements (see Fig. 463-6 and Table 463-XXIV). Thus the release of fission products from the elements could be a transfer of element bond sodium containing dissolved I (as NaI) from the element to the capsule. This I subsequently decays to Xe and is released to the capsule plenum. There is evidence that a sodium transfer in this direction occurs. The element sodium level of a number of fuel elements classed as

Fig. 463-5. Isotopic concentration of xenon fission products vs irradiation time.
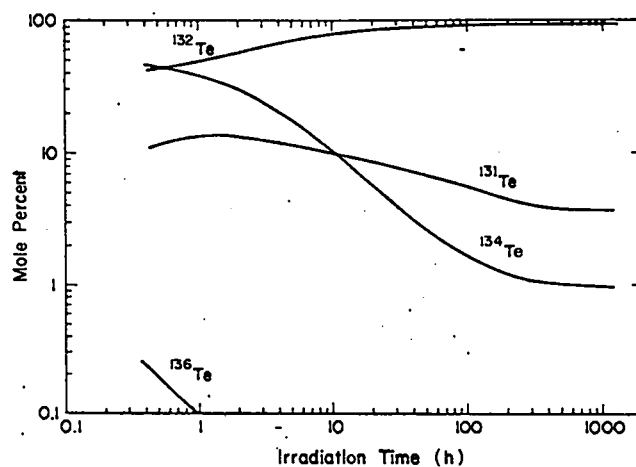
Fig. 463-7. Isotopic concentration of tellurium fission products vs irradiation time.
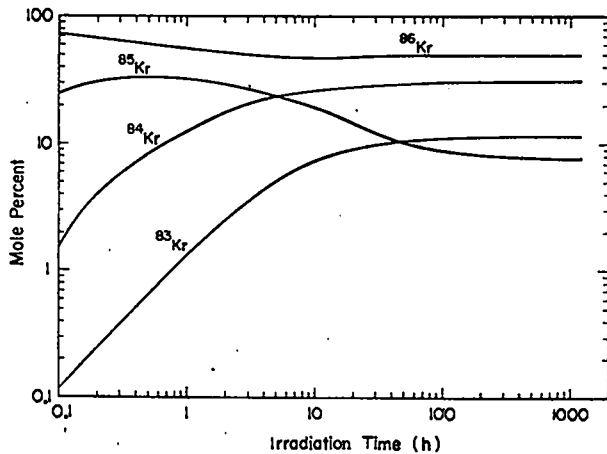
Fig. 463-8. Isotopic concentration of krypton fission
products vs irradiation time.
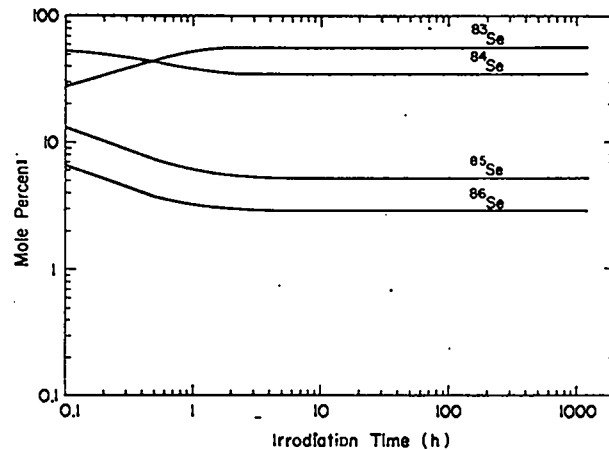
Fig. 463-10. Isotopic concentration of selenium fission
products vs irradiation time.

slight failures has been observed to be lower after ir-
radiation than as fabricated.[1] Estimates of the quantity
of sodium transferred from the element to the capsule are
in the range of 1/3 to 2 cm^3. The solubility of I (as NaI)
in sodium was estimated to be 4 x 10^{-6} moles/cm^3 at
$500°C$.[9] The quantity of Xe in the capsules of these four
elements ranged from 1 x 10^{-7} to 4 x 10^{-7} moles. Thus
sufficient sodium was transferred into the capsule to ac-
count for all the Xe found in the capsules.

This same mechanism can also explain the low values
of the total Kr to total Xe found in the capsules of these
four elements. Figure 463-11 shows a plot of the

Kr/Xe, Br/I, and Se/Te ratios as a function of irradia-
time time. These data came from the same calculations
used to produce Figs. 463-5 to 463-10. The Kr/Xe ratio
decreases monotonically with time, so that a low value
would not result from the transfer of newly produced gas.
If it is assumed that the Xe in the capsules of these four
elements comes mainly from the decay of I precursors,
a similar assumption can be made for the Kr, i.e., it
comes mainly from the decay of Br precursors. Thus
the final Kr/Xe ratio measured would be controlled by
the Br/I ratio in the sodium transferred into the capsule.
In the same range of irradiation times where I precursor
isotopic concentrations matched the Xe isotopic concentra-
tions observed (30 to 100 h), the Br/I ratio matches the
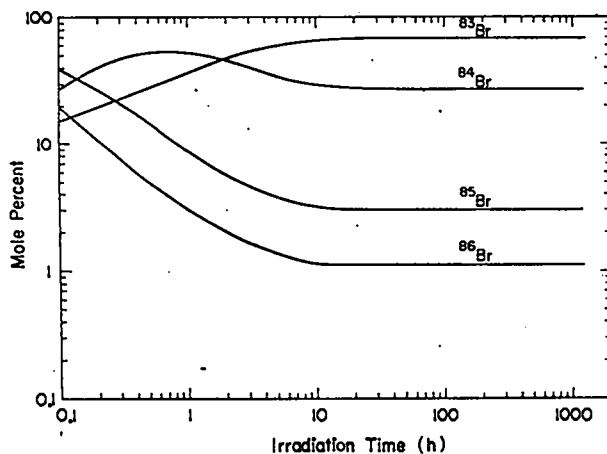
Fig. 463-9. Isotopic concentration of bromine fission
products vs irradiation time.
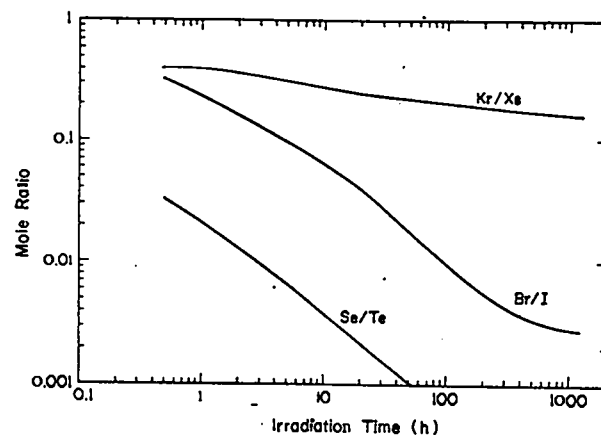
Fig. 463-11. Kr/Xe, Br/I, and Se/Te fission products
ratios vs irradiation time.

42

Kr/Xe ratio observed in the capsules of the four elements. Thus the observations for these four elements in Table 463-XXVII are consistent with the hypothesis that the fission gas in the capsules was transferred mainly as halogen precursors dissolved in the element bond sodium.

The observed Xe isotopic content and the total Kr/Xe ratio in the capsule of U 194 are not in agreement with this mechanism. The capsule fission product Xe is more highly enriched in ^{132}Xe than ^{131}Xe. The release of neither Xe nor I would result in a higher ^{132}Xe enrichment than ^{131}Xe (see Figs. 463-5 and 463-6), but the preferential release of Te could result in a high ^{132}Xe enrichment after decay (see Fig. 463-7). Also the total Kr/Xe ratio in the capsule is identical to that in the element. There does not appear to be any simple mechanism which can account for these two observations on U 194. This anomaly will continue to be studied.

The observation that all Na-bonded elements show some enrichment in ^{131}Xe and depletion in ^{134}Xe and ^{136}Xe in the capsule fission gas can be explained as a combination of the release of fission gas (Xe and Kr) directly from the element to the capsule through cladding cracks, and the transfer of some bond sodium between the element and capsule. This bond sodium would contain dissolved precursors of Xe and Kr which would skew the capsule fission gas isotopic compositions to some extent.

Of the 18 Na-bonded elements, K-49 requires special consideration. This element operated at a very high linear power (130 kW/m) and was a severe failure which showed evidence of fuel melting over much of the fuel column length. Thus the high gas release (see Table 463-XXV) is not unexpected, considering the operating history. Two of the Na bonded nitride elements (B 3-4 and B 3-5) were also severe failures. Although no fuel melting was observed, the fuel temperatures were higher than normal due to some gas blanketing of the element. Thus the fission gas release of these elements may be higher than normally expected for Na-bonded nitrides.

If the fission gas release of Na-bonded nitride elements is compared with Na-bonded carbides (excluding the three elements noted above, K-49, B 3-4, and B 3-5),

the nitride fueled elements show a lower release (0.86% to 7.1%) than the carbide elements (3.2% to 21.3%). It is not certain at this time whether this is a significant trend.

c. Gas Bubbles in the Fuel Element Sodium Bond

One of the advantages of sodium bonded high-performance fuel elements is the high thermal conductivity of the bond, which reduces fuel temperatures, and thus fuel swelling, at high power density. If gas bubbles exist in the fuel element sodium bond, the heat flux through the bubbles will be severely restricted, since the thermal conductivity of the gas is much lower (about an order of magnitude) than that of liquid sodium. Heat which would normally flow through the bubble area will be redistributed to flow through adjacent areas where a liquid sodium bond remains. The net result of a gas bubble in the sodium bond will be higher fuel temperatures under the bubble and a higher clad heat flux in the sodium-bonded region adjacent to the bubble.

Gas bubbles can exist in a fuel element sodium bond at fabrication or they could result from the release of fission gas from the fuel to the bond during irradiation. Bond bubbles or voids present after fabrication can be detected using eddy current measurements. Current technology allows voids or bubbles greater than 2 mm in diameter to be easily detected. If voids are indicated in a completed fuel element, the element can be rebonded until no voids or bubbles are detected, or rejected if they cannot be eliminated. Thus the size of gas bubbles in the sodium bond can be limited in new fuel elements.

During irradiation, fission gas (Kr and Xe) is generated in the fuel. For a typical fuel element with 8-mm-o.d. cladding, the fuel will generate about 70 mm^3 (STP) of fission gas per mm of fuel length for one at.% burnup. For a 0.5 mm diametral sodium bond, the bond volume is about 5 mm^3 per mm of fuel length. Even with the low fission gas release observed with sodium-bonded carbides (e.g.. 5%), enough fission gas is released within a few atom percent burnup to completely fill the sodium-bond volume. Thus if a mechanism is available to retain fission gas in the sodium bond, gas bubbles can form.

The behavior of gas bubbles in narrow, liquid-filled, gaps has been investigated by organizations interested in sodium-bonded fuel elements.[10-15] The general conclusions were that even without obstructions, stagnant bubbles can form in narrow gaps. When a system of stacked pellets in a cylindrical tube was tested,[12] relatively large bubbles formed under the edges of eccentrically located pellets. Mechanical vibrations were not effective in moving the bubbles located under pellet edges. Although there are many differences between these simulations and real fuel elements (for example, the simulations used liquids other than sodium in most cases, and were isothermal), they provide plausible mechanisms for the formation of gas bubbles in sodium bonds.

The effect of gas bubbles in a sodium bond on the temperature profile near the bubble has also been examined.[13,14] Bubbles which blanket small angles of the fuel surface (less than 30° or about 2 mm width in a fuel element with 8 mm o.d. cladding) do not increase the maximum fuel temperature very much. but the sector of fuel covered by the bubble can run at temperatures much higher than it would if no bubble were present. As the angle blanketed by the bubble increases, the location of the maximum fuel temperature moves from the center toward the fuel surface. For bubble angles greater than about 60°, the maximum fuel temperature is located near the fuel surface, at the center of the bubble. With large bubbles, a significant fraction of the fuel may operate at temperatures above the maximum temperature which would result if no bubbles were present.

In review, there is ample fission gas available to form bubbles in a sodium bond. Also, previous work has indicated a mechanism for trapping bubbles under edges of eccentrically located pellets and has described an observable consequence of large bubbles, i.e., high temperatures in the fuel under the bubble. In spite of this, there has been no clear evidence for the existence of gas bubbles in the sodium bond of fuel elements examined after irradiation. Levine, et al.[16] presented a section of a (U,Pu)C fuel element from a thermal irradiation (5 at.% burnup) in which one quadrant of the fuel showed much higher swelling than the other pieces. The high swelling

region was bounded by radial cracks in the fuel. They speculated that this region appeared as it did because it was free to swell unrestrained, while the other pieces of the fuel were restrained by the cladding and adjacent fuel fragments. In a later publication,[17] they mentioned the possibility of a gas bubble in the sodium bond outside this region. The boundary of the high swelling region did not follow the outline of isotherms that would result from a bubble in the bond. Thus a clear relation between the high swelling and a bond bubble cannot be made.

During the recent postirradiation examinations of sodium-bonded element at LASL, a number of asymmetric swelling patterns and asymmetric regions of $\beta - \gamma$ activity (in autoradiographs) were observed. The swelling patterns were particularly evident in fuel that was originally 98% of theoretical density. Figures 463-12 and 463-13 show photomosaics of two fuel sections. The high-porosity, asymmetric, regions exhibit grain-boundary swelling. The high-density areas visible within the grain-boundary swelling regions are large single grains which show little porosity within the grains. The

Fig. 463-12. Photomosaic of a high-density, sodium-bonded, carbide fuel element showing assymetric regions of grain-boundary swelling. (Fuel element U194, Section F; Mount No. 2C8).
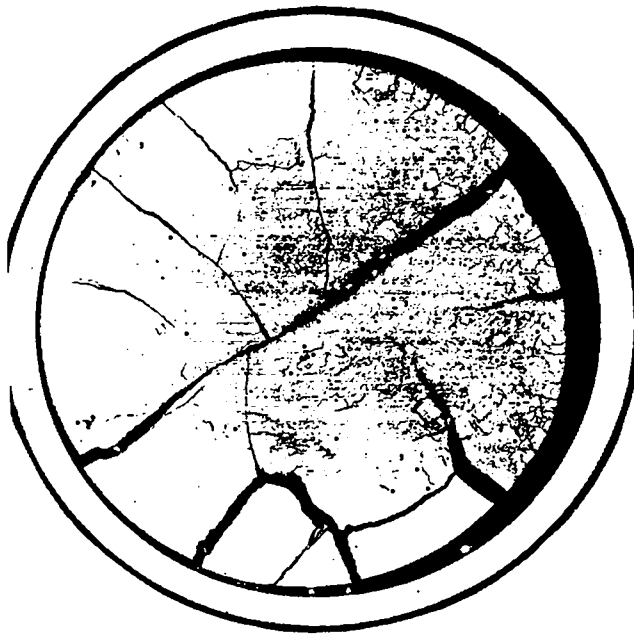
Fig. 463-13. Photomosaic of a high-density, sodium-bonded. carbide fuel element showing swelling resulting from a bubble trapped by an eccentrically-located pellet. (Fuel element U195, Section N; Mount No. 3C92T).
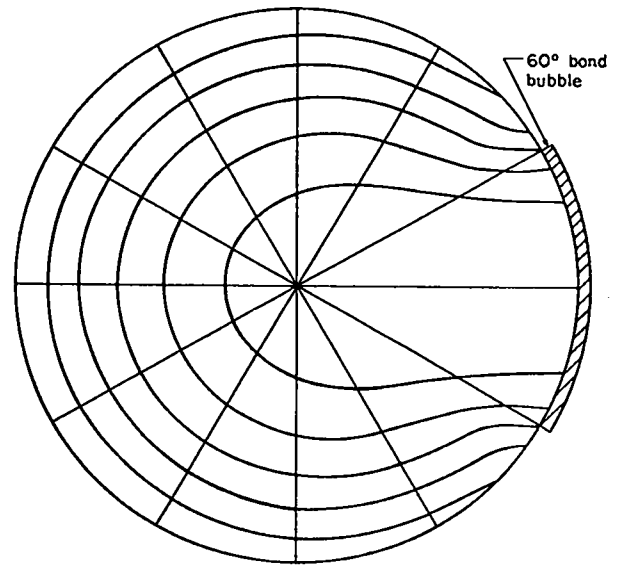
Fig. 463-14. Calculated isotherms at 80°C intervals in a carbide fuel pellet from an element with a very long, 60°, gas bubble in the sodium bond.

boundaries of the high-porosity regions are not influenced by the major cracks in the fuel pellets, i.e., the boundaries cross the cracks with little perturbation. If it is assumed that the observed grain-boundary swelling occurs only above some critical temperature, the boundary between the region of high swelling and the region of low swelling should parallel isotherms in the fuel.

Heat transfer calculations were performed to obtain the shape of isotherms in a transverse plane of a fuel element with various size gas bubbles in the sodium bond between the fuel and cladding. The fuel, bond, and cladding were divided into eight radial regions, 24 circumferential regions (15° each), and three axial layers for numerical heat transfer calculations. Sodium-bond bubbles subtending angles of 30° to 120° were simulated by replacing liquid sodium conductivity with argon gas conductivity in the bubble nodes. Radiation was allowed from the fuel surface to the inside cladding surface through the bubble. Calculations were performed for bubbles with a ratio of circumferential width to axial width of 2, 1, and 0 (infinitely long bubble). Figure 463-14 shows the isotherms at 80°C intervals in a fuel pellet

from an element with a very long, 60°, gas bubble in the sodium bond. A comparison of the isotherm shape with the shape of the high swelling region of Fig. 463-12 shows excellent agreement. Figure 463-15 shows the isotherms at 80°C intervals in a fuel pellet from an element with a short (axial/circumferential width = 1/2) 120° gas bubble in the sodium bond. The isotherms are from the central plane of the bubble. Their shape compares well with the high porosity region of Fig. 463-13. There is no unique correspondence between the bubble size (circumferential and axial widths) and the isotherm shape. Isotherms similar to those in Fig. 463-14 could also result from an approximately 75° square bubble in the sodium bond. Thus, for any observed high-swelling pattern, a unique bubble size cannot be determined, only a possible size range.

The high temperature in the fuel under a gas bubble can also affect fission product migration. Figure 463-16 shows a $\beta - \gamma$ autoradiograph (the dark areas are high activity) of the section shown in Fig. 463-13. There is a depletion of activity in the center, and in one sector the activity depletion approaches the fuel surface. This
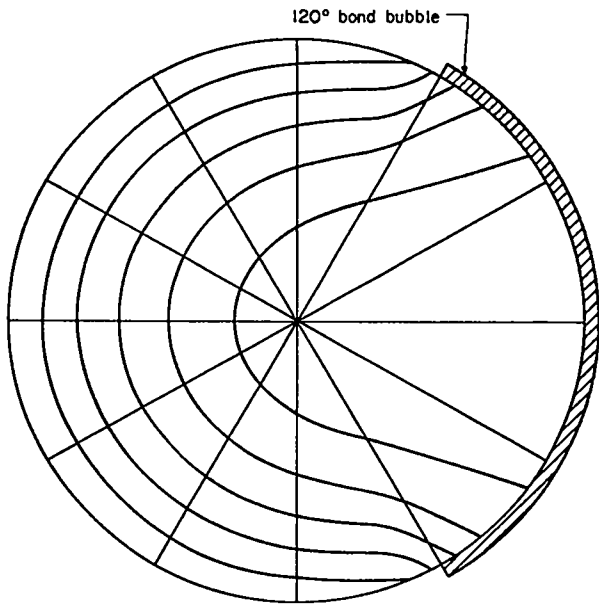
Fig. 463-15. Calculated isotherms at 80°C intervals in a carbide fuel pellet from an element with a short (axial/circumferential width = 1/2), 120°, gas bubble in the sodium bond.

Fig. 463-17. β-γ autoradiograph showing asymmetric depletion of activity. (Fuel element U191, Section M; Mount No. 3C71).

cut axially on a plane which bisected the region of high porosity. Figure 463-18 shows a photomosaic of the
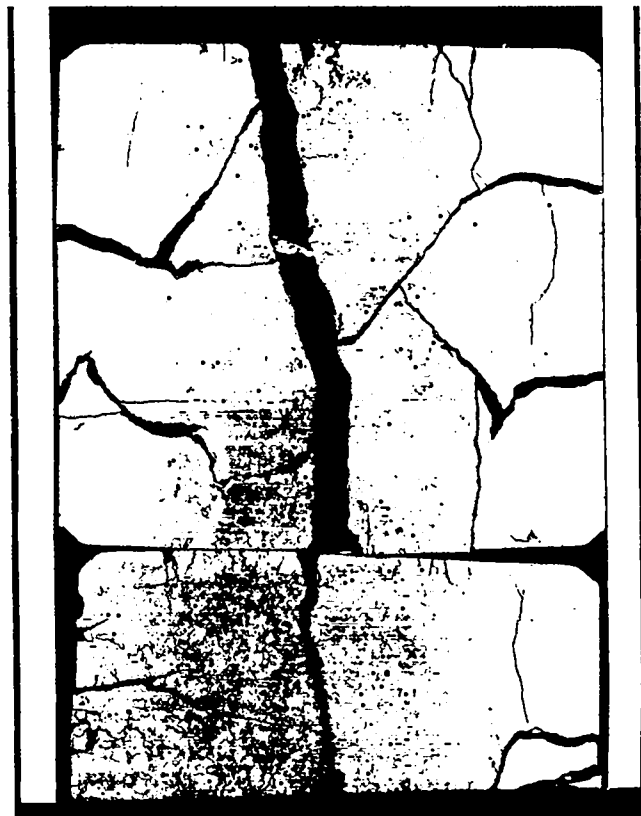
sector corresponds to the high porosity region seen in Fig. 463-13. Figure 463-17 shows another β-γ auto-radiograph with an asymmetric depletion in activity. In this case, the photomosaic of the section did not show a corresponding porosity variation.

The section shown in Fig. 463-13 was examined further to try to obtain some information about the axial variation of the high-porosity region. The section was

Fig. 463-16. β-γ autoradiograph of the fuel element section shown in Fig. 463-13. (Fuel element U195, Section N; Mount No. 3C92T).

Fig. 463-18. Photomosaic of the longitudinal section associated with the transverse section shown in Fig. 463-13. (Fuel element U195, Section N; Mount No. 3C92L).

longitudinal section obtained. The bottom corresponds to the plane shown in Fig. 463-13. About 1/3 of the pellet with the asymmetric high porosity region is visible on the bottom. The pellet above shows high porosity (grain-boundary swelling) in the center only. This would be expected from a pellet with a continuous sodium bond where the center was the hottest region. The discontinuity in the porosity variation across the pellet interface can be explained by assuming that a gas bubble blanketed a portion of the lower pellet but did not extend above the pellet interface. The porosity distribution probably resulted from a bubble trapped under the edge of the upper pellet (See Fig. 18 of Ref. 12.)

The photomosaics with asymmetric porosity distributions and the β-γ autoradiographs with asymmetric activity regions shown here are presented as evidence that relatively stationary gas bubbles exist in sodium bonds during irradiation. This conclusion is reached since: (1) there is an availability of fission gas; (2) there is a mechanism to hold bubbles in the bond under edges of eccentrically located pellets; and (3) the outline of the asymmetric swelling regions corresponds to the shape of isotherms in the fuel if bubbles were present in the bond. The term relatively stationary is difficult to define. The time constant for establishing an asymmetric temperature distribution in the fuel is only a few seconds. The time required for the fuel shown in Figs. 463-13 and 463-18 to swell cannot be determined at this stage of development of advanced fuels.

The pictures shown here represent a sample of more than 10 fuel element sections exhibiting the asymmetric swelling or asymmetric β-γ activity phenomenon. As stated earlier, the particular sections shown were chosen because the contrast between the original 98% theoretical density fuel and the high porosity regions is obvious. Other fuels with initial densities below 95% of theoretical also show asymmetric porosity regions resulting from gas bubbles in the sodium bond, but, in many cases, there is little contrast between the regions of high and low swelling. One observed trend is that the occurrences of asymmetric porosity or activity regions in fuel element sections were greater in elements with larger initial sodium-bond gap widths. Since larger gaps would lead to larger pellet offsets between eccentric pellets, elements having large fuel-cladding gaps may trap gas bubbles in the bond more often than elements with smaller gaps.

The relationship between gas bubbles in the sodium bond of fuel elements and the fuel element failures observed so far is not clear. It is obvious that a gas bubble perturbs the operation of the fuel element, and that large bubbles can cause a significant portion of the fuel to operate above the design temperature. The increased fuel swelling in the region covered by the bubble may decrease the design burnup limit of the element. But evidence of large (covering more than 90° of the fuel surface) gas bubbles has been observed in fuel elements which have not failed at 5 at.% burnup. Also evidence for sodium-bond gas bubbles has been observed in a number of elements classed as slight failures, but the occurrence of gas bubbles has not been related to the failures. Although bond gas bubbles can be considered as harmful to the ultimate potential of sodium-bonded elements, there is no evidence to indicate that they caused any of the initial failures observed to date. The incidence of sodium-bond gas bubbles may be reduced in the future if liner tubes are used. The very small gap between the fuel and the liner tube (less than 0.05 mm) does not permit significant pellet eccentricities. Thus, potential gas bubble traps under edges of eccentric pellets may be eliminated. This postulate should be verified by a comparison of the elements with and without liners in the U5100 Series currently being irradiated.

D. Safety Irradiation Testing
(J. F. Kerrisk and D. G. Clifton)

1. Series UL Tests

A series of four transient irradiations in TREAT, conducted as a joint effort of LASL and Gulf United Nuclear Fuels Corp., was designed to determine the effect of irradiation on the failure threshold of helium- and sodium-bonded, (U,Pu)C fuel elements. Table 463-XXVIII describes the fuel element parameters. Tests UL-1 and UL-2 were completed during the previous fiscal year.[1]

TABLE XXVIII

LASL SERIES UL TESTS

	TEST			
	LASL-UL-1	LASL-UL-2	LASL-UL-3	LASL-UL-4
Fuel Element[a]	263 (138 A)	264 (146 A)	265 (138)	266 (146)
Fuel Material[b]	90 vol% $(U_{0.85}Pu_{0.15})C$ + 10 vol% $(U_{0.85}Pu_{0.15})_2C_3$			
Fuel Pellet O.D., mm	6.25	6.09	6.25	6.09
Bond Material	He	Na	He	Na
Bond Thickness Diam. mm	0.36	0.77	0.36	0.77
Clad Material	316SS	304SS	316SS	304SS
Clad Thickness, mm	0.56	0.38	0.56	0.38
Smear Density, % Theoretical	90	77	90	77
Fuel Column Length, mm	349 ± 3			
Burnup, at.%[c]	0	0	4	4

[a]Fuel element numbers reassigned by Gulf United. Old numbers shown in parentheses.

[b]Uranium enriched to 60% in ^{235}U.

[c]Irradiated in EBR-II at 40 to 45 kW/m in subassembly X055.

Assembly of the capsules for tests UL-3 and UL-4 was completed by the Radiometallurgy Group of Hanford Engineering Development Laboratory. Both tests were performed at TREAT in mid-July, 1973. The reactor power and total reactor energy requested for these tests were the same as for tests UL-1 and UL-2. A preliminary review of the capsule temperatures and reactor power indicated that the tests were performed as requested.

The UL-3 and UL-4 capsules have been returned to the LASL hot cell facility for examination. The capsules had been neutron radiographed at TREAT, and the inner capsules have been x-radiographed and gamma scanned at LASL. An examination of the radiographs of UL-3 (the He-bonded element) indicates cladding cracks in a number of areas. An examination of the radiographs of UL-4 (the Na-bonded element) indicates a number of

areas which may have cladding cracks. There is no evidence of fuel melting in either radiograph. An analysis of the gamma scanning results indicates that the He-bonded element (UL-3) has failed since ^{137}Cs was detected outside the element cladding. There was no evidence of fission products outside the cladding of the Na-bonded element (UL-4).

2. **Future Tests**

Liaison with Argonne National Laboratory has been established for the purpose of planning future off-normal and transient irradiation tests.

III. QUALITY ASSURANCE
(L. E. Lanham)

General

1. A quality assurance presentation was made to AEC-RRD at the June 24-28, 1974, LASL Program Review

Meeting. Included was a discussion of the existing qual-ity assurance program, quality assurance problems, and future quality assurance plans.

2. The commitments made as a result of this meet-ing will require the quality assurance organization to per-form a maintenance overcheck for critical processing equipment and to plan and perform a quality assurance function in the certification of contractor fabrication facilities.

3. A Quality Assurance Engineer has been hired and is being trained to provide a quality assurance engineering function for fuel preparation and element fabrication. Two Quality Assurance Specialists have been hired and will report to work after July 1, 1974. They will provide the independent quality assurance overcheck for all fab-rication operations.

Fuel Pin Fabrication

1. Independent quality assurance surveillance has continued on the preparation of facilities, equipment,and procedures for pin fabrication. All quality assurance procedures have either been completed or are in the final stages of preparation.

2. A series of flow sheets have been prepared to cover all operations in pin fabrication. These documents give the sequence of operation, procedures to be used, including review or hold points.

3. Operators are being trained and the certification documentation is being prepared for all required pro-cedures.

Fuel Preparation

1. Independent quality assurance surveillance has continued on the development fuel preparations. The quality assurance requirements for quality control and documentation for development work are consistent and similar to those that will be required for the production of fuel.

2. Operator training is being conducted for new em-ployees who will perform the various operations in fuel preparation. The documented certification for each oper-ator is being prepared and will be in place before the start of fuel production.

3. All quality assurance procedures have been

prepared including those reflecting the latest production plans and technical adjustments in fuel preparation.

IV. REFERENCES

1. "Quarterly Report, Advanced Plutonium Fuels Pro-gram, April 1 through June 30, 1973,and Seventh Annual Report, FY 1973," Los Alamos Scientific Laboratory report LA-5390-PR (Sept. 1973).

2. "Quarterly Report, Advanced Plutonium Fuels Program, July 1 through September 30, 1973," Los Alamos Scientific Laboratory report LA-5477-PR (April 1974).

3. M. Montgomery and A. Strasser, "Irradiation of Low-Density Solid and High-Density Annular Pellet Uranium-Plutonium Carbide Fuel Rods to 77,000 Mwd/T," Trans. Am. Nuc. Soc. 15, 754 (1972).

4. J. O. Barner, "Behavior of Sodium-Bonded (U,Pu)C Fuel Elements After Moderate Burnup," Los Alamos Scientific Laboratory report LA-4669-MS (April 1971).

5. M. E. Meek and B. F. Rider, "Compilation of Fis-sion Product Yields, Vallecitos Nuclear Center, 1972," General Electric report NEDO-12154 (1972).

6. "Guide for Irradiation Experiments in EBR-II," Argonne National Laboratory, Chicago, Illinois, Appendix C.

7. F. L. Brown et al.. "Performance of Mixed-Car-bide Fuel Rods Under Fast Reactor Conditions." Trans. Am. Nuc. Soc. 10, 473 (1967).

8. R. O. Gumprecht, "Mathematical Basis of Computer Code RDBD," Douglas United Nuclear, Inc. report DUN-4136 (June 1968).

9. M. A. Bredig et al., "Miscibility of Liquid Metals with Salts, I. The Sodium-Sodium Halide System," J. Am. Chem. Soc. 77, 307 (1955).

10. "Quarterly Status Report on the Advanced Plutonium Fuels Program, April 1-June 30, 1968,and Second Annual Report, FY 1968." Los Alamos Scientific Laboratory report LA-3993-MS, p. 70 (1968).

11. "Quarterly Status Report on the Advanced Plutonium Fuels Program, October 1-December 31, 1967," Los Alamos Scientific Laboratory report LA-3880-MS, p. 37 (1968).

12. H. O. Schad and A. A. Bishop, "Stationary Gas Bubbles in Narrow Liquid-Filled Gaps," Nuclear Applications and Technology 8, 261 (1970).

13. E. H. Novendstern and A. A. Bishop," Temperature
Distribution Caused by Gas Bubbles in a Sodium
Bonded Fuel Rod," Chemical Engineering Progress
Symposium Series No. 92, Vol. 65, p. 131 (1969).

14. R. Schoneberg and H. Ernst, "The Behavior of Gas
Bubbles in a Sodium Bonded Carbide Fuel Element
in a Fast Reactor," Nuclear Engineering and Design
21, 65 (1972).

15. L. Rutland, B. H. Cherry, and S. Isreal, "Critical
Bubble Size in Sodium-Bonded Ceramic Fuels,"
Trans. Amer. Nucl. Soc. 10, 471 (1967).

16. P. J. Levine et al., "Postirradiation Observations
of Sodium-Bonded (U,Pu)C Fuels," Trans. Amer.
Nucl. Soc. 13, 606 (1970).

17. B. L. Harbourne et al., "The Irradiation Behavior
of Sodium-Bonded Mixed-Carbide Fuel Pins," in
Proceedings of the Conference on Fast Reactor Fuel
Element Technology, R. Farmakes, Ed. , American
Nuclear Society, p. 869 (1971).

PROJECT 472

FBR ANALYTICAL QUALITY ASSURANCE STANDARDS AND METHODS

RESEARCH AND DEVELOPMENT

Person in Charge: R. D. Baker
Principal Investigator: G. R. Waterbury

I.   INTRODUCTION

Necessary to the development of high quality fuels, control rods, and other reactor components required by the FBR program are highly reliable analytical methods for the chemical characterization of the source materials and products, and for the measurement of burnup, O/M ratio, and various gases on irradiated fuels. Tasks for ensuring the production of these materials are: (1) the continual preparation and distribution of carefully characterized calibration materials and quality control samples for use by and surveillance of the vendors and purchasers during periods of production, (2) the preparation and guidance in the use of quality assurance programs for chemical specification sampling and analysis, (3) the development of improved methods of analysis, as required, (4) the preparation of continually updated compilations of analytical methods, and (5) the analysis, in a referee capacity, of samples in dispute between vendors and purchasers. For the near future, these tasks are dedicated to the FFTF. They will be extended, as appropriate, to the LMFBR demonstration and large production facilities.

Tasks concerned with irradiated FBR fuel examinations are: (1) the development of burnup methods based on conventional mass spectrometry, on chemical analyses using inexpensive chemical apparatus, and on spark source mass spectrometry for rapid, precise measurements, (2) the prooftesting of developed methods for burnup jointly with the Allied Chemical Corporation (Idaho), (3) the development of methods for the measurement of the O/M ratio, and (4) the development of methods for

the measurement of gases including techniques to measure the release rates of various gases as a function of temperature-time cycling.

As a high priority item, a program has been initiated to establish a quality assurance program and to develop analytical methods, as necessary, for the chemical characterization of low-friction, hard surfaces to be applied to various FFTF core components. Also initiated is a task to prepare a manual of analytical methods for the chemical characterization of metallic core components for issuance as an RDT Standard.

II.   ANALYTICAL CHEMISTRY PROGRAM FOR LOW-FRICTION, HARD SURFACES

In August, 1973, LASL began a cooperative effort with HEDL to establish a program for the chemical characterization of low-friction hard surfaces to be applied to contacting components of the FFTF reactor. The hard surface is to be chromium carbide applied as a molten blend of Cr_3C_2 and nichrome powders.

A.   Development of Analytical Methods
(W. H. Ashley, D. W. Steinhaus, J. E. Rein, G. R. Waterbury)

Methods that have been used by a potential vendor for the chemical characterization of Cr_3C_2 powder, nichrome powder, and the hard surface have been evaluated. The methods for determining chromium, nickel, carbon, and impurity silicon were basically sound. Modifications were made to ensure improved precisions and increased analysis rates. The potential vendor had methods for characterizing the Cr_3C_2 and nichrome powders for

impurity iron, cobalt, and manganese. As it was expected that HEDL specifications would cover a wider variety of elements, an emission spectrographic method for determining general metal impurities and methods for measuring nitrogen and oxygen were developed. In addition, the dissolution of the hard surface was investigated. These methods are discussed individually below.

The hard surface sample prepared for chemical specification overcheck analyses will be an aluminum cylinder to which a relatively thick layer of hard surface will be applied at times when reactor components are surfaced. Removal of the hard surface as an analytical sample without adherent aluminum is impractical. Hence an analytical method was developed for measuring the aluminum to provide for material balance computations of major and minor components on an aluminum-free basis.

A sample of hard surface, prepared on a brass cylinder by the potential vendor, was extensively characterized by chemical and electron microprobe analyses to provide information to HEDL for establishing chemical composition specifications.

1. Dissolution of Samples (R. D. Gardner, R. E. Perrin).
The potential vendor's procedure for the dissolution of Cr_3C_2 and hard surface was based upon a Na_2O_2 fusion. Close attention of a skilled analyst was necessary to attain complete solubilization and recovery of all components.

Refluxing $12\underline{M}$ $HClO_4$ effectively dissolves nichrome powder, Cr_3C_2, and hard facing, producing a solution suitable for the determinations of chromium, nickel, and aluminum. Silica deposits quantitatively during the refluxing and the filtered residue provides the sample for the silicon determination.

2. Determination of Chromium (R. E. Perrin, R. D. Gardner).
The method for determining chromium was improved by incorporating the perchloric acid dissolution. Following this dissolution, the solution was diluted and traces of chlorine from perchloric acid decomposition were removed by boiling. Chromium then was completely oxidized to Cr(VI) by adding Ag^+ and $(NH_4)_2S_2O_8$ and boiling. Manganese, an impurity element, was also oxidized to Mn(VII), which would interfere,

but it was reduced to noninterfering Mn(II) by adding HCl and boiling the solution. The Cr(VI) was not reduced by HCl. A measured quantity of excess ferrous solution was added to the cooled solution, and the unreacted excess was titrated with standard ceric sulfate solution using Ferroin to indicate the endpoint.

3. Determination of Nickel (R. E. Perrin, R. D. Gardner).
The potential vendor's method, based on a gravimetric determination of nickel dimethylglyoximate, was slightly modified in procedural detail to improve precision.

4. Determination of Aluminum (R. D. Gardner).
An atomic absorption spectrophotometric method was developed for the determination of aluminum. The reference calibration was prepared using nichrome and Cr_3C_2 powders that were the source materials for the hard surface.

5. Determination of Carbon (R. E. Perrin, R. D. Gardner).
Conditions were established for this analysis using a commercial (LECO WR-12) carbon analyzer. These conditions included heating the particles (< 25 mg) of the sample plus iron chips, tin granules, and a copper ring at $1700^{\circ}C$ in an oxygen stream and measuring the produced CO_2 gas chromatographically. Results were equal for samples analyzed by this method and with a customized oxygen-combustion apparatus using a V_2O_5 flux and gravimetric measurement of the produced CO_2.

6. Determination of Nitride Nitrogen (R. E. Perrin).
A method was developed that is applicable to measurement of nitride nitrogen in the three materials. The sample is dissolved in $14\underline{M}$ H_2SO_4 in a sealed quartz tube at $500^{\circ}C$. After cooling, H_2O_2 is added to destroy SO_2 formed during dissolution, excess NaOH is added, the NH_3 is steam distilled into a boric acid absorber solution, and this solution is titrated with standard acid.

7. Determination of Oxygen (M. E. Smith, D. E. Vance).
A method[1] for the determination of oxygen in uranium carbide samples was adapted to Cr_3C_2 and hard facing. The samples were heated to > $2500^{\circ}C$ in a graphite crucible with a flow of argon carrying the generated CO through I_2O_5 to oxidize CO to CO_2 which was measured manometrically.

8. __Determination of Metal Impurities (O.R. Simi).__
An emission spectrographic method was developed in
which a sample is dissolved in H_2SO_4 plus HNO_3 in a Tef-
lon beaker, the solution is evaporated, and the residue is
ignited to an oxide matrix. A weighed portion is trans-
ferred to a cratered graphite electrode and dc-arc exci-
ted in a 60% Ar-40% O_2 atmosphere. Reference materi-
als, with graded levels of the various impurity element
oxides, are powder blends of chromium and nickel oxides
with Ni/Cr ratios matching those of the hard surface.

B. Chemical and Electron Microprobe Characterization of Hard Surface
(W. H. Ashley, D. W. Steinhaus, E. A. Hakkila)

The test sample provided by the potential vendor was
a hard surface on a brass cylinder. In the comprehensive
analysis of the physically separated hard surface with ad-
herent brass pieces, copper and zinc from the brass were
determined to provide a total material balance. Signifi-
cant impurities and their levels as micrograms per gram
of hard surface were 11 000 oxygen, 4400 N, 3300 Fe,
1100 Mn, 950 Si, 140 Ba, 125 Al, 125 Cu, 50 Ca, 25 Ti,
25 V, and 7 Mg. Major findings of the electron micro-
probe analysis were: (1) copper and zinc from brass had
not diffused into the hard surface, (2) chromium and nick-
el from the hard surface diffused to about a 10-μm depth
into the brass, and (3) the hard surface consisted of two
phases, a major heterogeneous phase of chromium, nick-
el and carbon, and a minor phase consisting of nickel and
chromium entities that were generally less than 5 μm in
width and void of carbon.

C. Analytical Method Manual

A manual of methods for the chemical characteriza-
tion of Cr_3C_2, nichrome powders, and hard surface ap-
plied to an aluminum substrate is nearing completion.
This manual will contain a general information section
and methods for sample dissolution and determination of
Cr, Ni, Al, C, N, O, Si, and metal impurities. Drafts
have been exchanged between HEDL and LASL and final
editing is under way at HEDL.

D. Round Robin Evaluations of Analytical Capabilities
(J.E. Rein, R.K. Zeigler, G.R. Waterbury)

Cooperatively with HEDL, plans have been formula-
ted for a round robin evaluation of analytical methods

with participating laboratories of the potential vendor,
HEDL, and LASL. Batches of Cr_3C_2 and nichrome pow-
ders and a thick deposit of hard surface have been de-
livered to HEDL for use as test materials. At LASL,
analyses of random portions of the hard surface for C,
Cr, Ni, Al, and general metal impurities indicate that it
is adequately homogeneous to serve as a round robin test
material. HEDL will pulverize the hard surface and sup-
ply the three materials to LASL for packaging and distri-
bution.

E. Reference and Quality Control Materials
(J. E. Rein, G. R. Waterbury)

Cooperatively with HEDL, a plan has been established
for reference and quality control materials to be used for
a production QA program. This plan has been outlined in
an earlier progress report.[2]

III. ANALYTICAL CHEMISTRY PROGRAM FOR METALLIC CORE COMPONENTS
(W. H. Ashley, E. A. Hakkila, M. E. Smith, J. E. Rein, G. R. Waterbury)

As a new task this fiscal year, LASL joined HEDL
to prepare RDT F11-3 "Analytical Chemistry Methods
for Metallic Core Components." This document will pre-
sent a series of detailed methods for the determination
of major and minor elements in various stainless steels
and Inconels. Drafts have been reviewed and HEDL is
preparing edited copies for a final review.

IV. ANALYTICAL CHEMISTRY PROGRAM FOR BORON CARBIDE

A. Status of Analytical Methods and Qualification of Analytical Laboratories
(J. E. Rein, R. K. Zeigler, W. H. Ashley, G. R. Waterbury)

Last year,[3] round robin results showed that nine
chemical methods were satisfactory for analysis of boron
carbide to be manufactured according to FFTF specifica-
tions. A tenth method, for nitride nitrogen, was evalua-
ted by a round robin with three potential vendors, HEDL,
and LASL as participants. Both the within-laboratory
and among-laboratory precision were satisfactory. This
completes the round robin testing of analytical methods.

B. Calibration and Quality Control Materials
(J. V. Pena, H. J. Kavanaugh, L. A. Maestas, J. E. Rein)

The calibration material previously specified for the total boron determination was NBS H_3BO_3, to be used only for standardizing the titrimetric reagent. Because a dominant source of error in this determination is incomplete sample solubilization by fusion with Na_2CO_3, a preferred calibration material is boron carbide pellets. Various pellet lots were tested for boron content homogeneity. A satisfactory lot was found, packaged, and sent to HEDL.

As quality control samples for surveillance of the nitride nitrogen determination, the desired material was also boron carbide pellets. As a pellet lot with homogeneous nitrogen content was not found, one lot was pulverized and the 200-mesh, screened fraction, satisfactorily tested for homogeneity, was packaged as quality control samples and sent to HEDL.

All calibration and quality control materials, deemed adequate for the HEDL QA Program covering the initial production of FFTF boron carbide pellets, have been sent to HEDL.

C. Status of RDT Standards
(J. E. Rein, G. R. Waterbury)

A supplement to RDT Standard F2-8 "Qualification and Control of Analytical Chemistry Laboratories for Control Rod Absorber Material Analysis" was prepared that provides coverage for the nitride nitrogen determination. The section concerned with the total boron determination was revised to include the use of boron carbide pellets as a calibration material. The revisions have been reviewed by HEDL prior to their addition to F-2.

D. Development of Analytical Methods
(W. H. Ashley, G. R. Waterbury)

An alternate method was developed for the determination of nitride nitrogen and evaluation of the sealed quartz tube technique was in progress for the dissolution of samples in the total boron determination.

1. Determination of Nitride Nitrogen (R. E. Perrin, A. Zerwekh). The present method, involving a fusion of the sample with LiOH followed by distillation and titration of the nitride nitrogen as ammonia, is not consistently reliable . The cause is a high resistance to complete

fusion by some boron carbide materials. Development was completed of an alternate method[4] in which a sample is dissolved with $14\underline{M}\ H_2SO_4$ in a sealed quartz tube at $500°C$; NaOH is added to make the resulting solution alkaline; and the nitride nitrogen, converted to ammonia, is distilled into a boric acid absorber solution and titrated with standard acid. No boron carbide material tested to date has required longer than 24 h for complete dissolution.

2. Dissolution of Samples for the Determination of Total Boron (R. E. Perrin, R. D. Gardner). The present dissolution procedure for boron carbide preceding the determination of boron is a fusion with Na_2CO_3 which is prone to erratic, low recovery and requires the close attention of experienced analysts. The sealed quartz tube technique described in the previous section is being evaluated for inclusion in the boron determination. A major advantage is that relatively large pellet pieces can be dissolved whereas the fusion with Na_2CO_3 requires powdered samples. Pulverization of the hard boron carbide pellets introduces significant amounts of the mortar thereby complicating the subsequent analysis. In general, the technique is compatible with the subsequent boron determination, giving results that agree or exceed those obtained by the same boron method following Na_2CO_3 fusion. For certain samples, however, the results are lower for reasons not yet established.

V. ANALYTICAL CHEMISTRY PROGRAM FOR FBR MIXED OXIDE FUEL

A. Calibration and Quality Control Materials
(J. V. Pena, H. J. Kavanaugh, L. A. Maestas, J. E. Rein)

Shipments designated A and B, each with quantities for a production quarter, have been supplied to the vendors of FFTF mixed oxide fuel, to ARHCO as the supplier of the PuO_2 to the vendors, and to HEDL as the fuel receiver. Shipments C and D have been prepared and sent to the facilities that were ready for them. Packaging of shipment E materials is under way. Some of the C, D, and E shipments are minus certain materials for which the supply was depleted.

A new supply of HEDL-prepared plutonium oxide and mixed oxide, to be used as matrix materials for the

preparation of blends to serve as calibration and quality control materials for metal and nonmetal impurities, has been analyzed to establish the levels of the various impurities. With one exception of a high level of calcium in the plutonium oxide, the materials are satisfactory for the intended purpose. An attempt by HEDL is under way to provide an additional plutonium oxide lot with a low calcium content. Blend preparation is under way with priorities given to those materials that are depleted. In addition, uranium oxide of high purity is being prepared at LASL for use in making additional metal and nonmetal blends in this matrix.

B. Reference Analysis
(R. G. Bryan, R. K. Zeigler, G. R. Waterbury)

Statistically selected numbers of mixed oxide pellets from lots supplied by a vendor to HEDL have been analyzed to provide plutonium assay referee values.

C. Quality Assurance Plan
(R. K. Zeigler)

A quality assurance program for the chemical characterization of FBR mixed oxide fuels was presented at a meeting of the American Society for Quality Control.[5]

D. Development of Analytical Methods

1. Determination of Burnup

a. Mass Spectrometric Procedures (S. F. Marsh, M. R. Ortiz, R. M. Abernathey, J. E. Rein). A two-column, ion-exchange procedure[6] was modified[7] to improve reliability and decrease analyst effort. In this procedure, the first column retains plutonium and uranium as anionic chloride complexes from $12\underline{M}$ HCl while neodymium and most other fission products pass through. The second column chromatographically separates neodymium from other fission products, including rare earths, as anionic nitrate complexes using a CH_3OH-HNO_3 mixed solvent. The plutonium and uranium are sequentially eluted from the first column with $0.1\underline{M}$ HI-$12\underline{M}$ HCl, followed by $0.1\underline{M}$ HCl.

The major modifications are: (1) substitution of macroporous anion exchange resin for the previously used conventional ion exchange resins in both columns, (2) a change in the composition of the CH_3OH-HNO_2 mixed solvent used in the chromatographic separation of neodymium, and (3) automation of the chromatographic column operation.

During the past year, the modified method was used to analyze a series of very low burnup (< 0.01% fissioned) samples of mixed uranium-plutonium fuel. Because the americium/neodymium ratio in these samples is several hundredfold higher than usual, an additional ion exchange separation was incorporated into the above procedure to separate americium from neodymium. The rare earth-containing effluent from the first column was converted to an C_2H_5OH-HCl medium and passed through a pellicular cation exchange column before the chromatographic ion exchange separation of neodymium. This separation, described in the next section, retains rare earth elements on the column while trivalent actinides pass through giving a 100-fold decrease in americium.[8] The rare earths then are eluted with $5\underline{M}$ HCl and fumed with HNO_3 to convert them to nitrates for the neodymium chromatographic separation.

b. Method Using Conventional Low-Cost Apparatus (S. F. Marsh, M. R. Ortiz, J. E. Rein). Development has continued on a method incorporating the ion exchange separation of uranium, plutonium, and total rare earths (as the fission product burnup monitor), followed by a spectrophotometric measurement of each. The separation, based in part on the two-column procedure described above, involves fuming the sample with $HClO_4$ to oxidize plutonium to Pu^{+6} prior to retention of U^{+6} and Pu^{+6} on a macroporous anion exchange column from $12\underline{M}$ HCl. The effluent, which contains trivalent actinides, rare earths, and most other fission products, is converted to an C_2H_5OH-HCl medium and transferred to a pellicular cation exchange resin column. The rare earths are sorbed while trivalent actinides (Am and Cm) and extraneous fission products pass through. The rare earths then are eluted with $5\underline{M}$ HCl.

Following the removal of the trivalent actinides from the initial anion exchange resin column, the plutonium is eluted with $0.1\underline{M}$ HI-$12\underline{M}$ HCl and the uranium with $0.1\underline{M}$ HCl.

Arsenazo III was selected as the chromogenic agent for the spectrophotometric measurement of the separated uranium, plutonium, and total rare earths. A mixture of rare earths plus yttrium, in proportions

simulating fission products from a fast reactor mixed uranium-plutonium fuel, has been used to develop the procedure. A mixed-oxide fuel, that had been irradiated in EBR II to 10.7% burnup as determined by the mass spectrometric procedure, is being used to test the procedure. Rare earth separation, recovery, and measurement were shown to be satisfactory. Uranium separation and measurement were shown to be satisfactory. Uranium separation and measurement were also satisfactory at moderate concentrations, but there was an unidentified interference at higher levels.

2. Determination of O/M Ratio in Solid Solution (U, Pu)O₂ (G. C. Swanson, G. R. Waterbury). The oxygen-to-metal atom ratio (O/M) of oxide reactor fuels affects such properties as: oxygen potential, melting point, thermal conductivity, actinide migration during irradiation, and fuel-clad interaction. Oxide fuels are most often analyzed for O/M by thermogravimetric methods in which the sample is weighed, exposed to conditions of temperature and gas oxygen potential designed to produce a known O/M, reweighed, and the initial O/M calculated from the weight changes. The most effective reference materials to date for determining the O/M produced by various analysis conditions are weighed samples of highly pure uranium and plutonium metals which are ignited to oxides under conditions which prevent loss of sample. A mechanical mixture of these two oxides has been used as a reference material to calibrate analysis conditions for solid solution (U, Pu)O₂ samples, but the suitability of this standard is questionable from theoretical as well as experimental considerations because it is not a solid solution as are the mixed oxide fuels.

The goals of this research are to develop a solid solution (U, Pu)O₂ reference material for O/M and to investigate the important thermodynamic properties of this material. These thermodynamic properties are determined by correlating the O/M of the reference material with the oxygen potential of the atmosphere in equilibrium with the reference material. A Mettler thermobalance has been modified to heat the materials in controlled oxygen-potential atmospheres. A solid-state, electrochemical oxygen concentration cell is being developed to allow

in situ measurement and confirmation of oxygen potential of the atmosphere equilibrated with the standard.

The oxygen potential of the thermobalance atmosphere is controlled by the H_2/H_2O ratio of the gas. Hydrogen is added either as the pure gas or as a calibrated $Ar-H_2$ mixture. Water is generated by recombining at a platinum catalyst the H_2 and O_2 produced by electrolysis of H_2O. A molecular sieve trap prior to the catalyst removes any water vapor to assure that the water introduced to the thermobalance is only that produced by the electrolysis. Use of the two H_2 gas sources and a constant-current, electrolysis power supply, which spans four orders of magnitude, produces oxygen potentials from -605 to -208 KJ mol^{-1} (-145 to -50 K cal mol^{-1}) at 1300°C.

The electrochemical oxygen concentration cell is prepared from ThO_2 doped with Y_2O_3 (YDT) to produce an oxygen-defect structure in which oxide ions move freely. Such an electrode produces an electrical potential between its interior and exterior surfaces proportional to the difference in oxygen potential. Several test cells were prepared using a YDT tube commercially fabricated to fit within the thermobalance. A configuration giving the best test results was prepared for insertion in the thermobalance, but failure of an epoxy seal led to loss of the ceramic tube and some damage to the thermobalance. A new concept for fabrication of a cell with only the tip as YDT and the remainder nonconducting thorium oxide is being tested with ceramic tubes fabricated at LASL. This configuration has the advantage of maintaining the sensor surface at constant temperature whereas the tube fabricated from YDT had the active surface passing through a thermal gradient with the result that data are much more difficult to interpret.

The methods of preparation of solid solution (U, Pu)O₂ reference material for O/M will involve either an in situ preparation of a U-Pu alloy by melting together highly pure U and Pu metals followed by oxidation to solid solution oxide or by in situ sintering of a mechanical mixture of U and Pu oxides prepared from highly pure metals. In a preliminary test, uranium metal was melted in an Al_2O_3 crucible in the thermobalance and ignited to oxide without

loss or interaction with the Al_2O_3. Presently, a highly pure uranium metal is being oxidized and will be equilibrated with various oxygen potentials and temperatures to confirm the system operation. The capability of the thermobalance furnace to maintain a temperature of $1600°C$ will be used in sintering a mechanical mixture of UO_2 and PuO_2 to prepare solid solution $(U, Pu)O_2$ should the alloy method of preparation fail.

   3. Determination of Sulfur in Uranium-Plutonium Oxides (L. E. Thorn, R. G. Bryan). The previously used method for this determination was improved by changing the reductant to produce H_2S. The major operations are dissolution with HCl in a sealed quartz tube, addition of a reducing acid mixture to produce sulfide, distillation of H_2S, and spectrophotometric determination of the sulfide. The reducing acid mixture was changed from $HI + H_3PO_2$ in water to $HI + NaH_2PO_2$ H_2O in acetic acid. Uranium, which previously precipitated, remains in solution and does not hinder complete recovery of sulfide. A more sensitive and stable chromogenic agent, N, N-diethyl-p-phenylenediamine, has been substituted for the previous agent of p-phenylenediamine. Precision of the new method, using 200-mg samples, is 10% relative standard deviation for 5 μg (25 ppm) of sulfur decreasing to < 2% for 20 μg (100 ppm) of sulfur.

   The method was verified by repeated measurements on sulfate reference materials. An unknown factor is the oxidation state of sulfur in calcined mixed oxide fuel. An investigation of this factor is planned.

E. Development of Gas Measurement Techniques
   (R. M. Abernathey, J. E. Rein)

   An apparatus was assembled with an end-design capability to measure gas components released from samples of fuel, boron carbide, or other reactor materials as a function of temperature. The major components are an induction-heated chamber with controllable atmospheres including vacuum, a gas processing train, and a mass spectrometer.

   Testing of the apparatus showed no major difficulties and its use for samples was scheduled to start next quarter.

VI. QUALITY ASSURANCE
   (L. E. Lanham)

   Independent Quality Assurance surveillance has been conducted on the operations for the preparation and shipment of quality control and calibration samples. This activity will be increased to include an independent quality assurance overcheck of these operations as soon as the Quality Assurance Specialist (who arrives July 1, 1974) can be trained.

   A very substantial effort this fiscal year was implementation of a QA plan that encompasses the preparation, packaging, shipment, and documentation of all calibration and quality control materials sent to vendors and to HEDL as part of HEDL's QA program for the FFTF. Included in this plan are all analytical methods that are used to characterize and overcheck the materials.

VII. REFERENCES

1. W. G. Smiley, "Determination of Oxygen in Metals Without High Vacuum by Capillary Trap Method," Anal. Chem. 27, 1098 (1955).

2. R. D. Baker, "Quarterly Report -- Advanced Plutonium Fuels Program, July 1 through September 30, 1974," Los Alamos Scientific Laboratory report LA-5477 (December 1973).

3. R. D. Baker, "Quarterly Report -- Advanced Plutonium Fuels Program, April 1 through June 30, 1973. and Seventh Annual Report, FY 1973," Los Alamos Scientific Laboratory report LA-5390-PR (August 1973).

4. R. D. Baker, "Quarterly Report -- Advanced Plutonium Fuels Program, January 1 to March 31, 1973," Los Alamos Scientific Laboratory report LA-5284-PR (May 1973).

5. R. K. Zeigler, "Quality Assurance Plan for Mixed Oxide Fuel for LMFBR," 20th Western Regional Conference, American Society for Quality Control, Portland, OR, September 27-29, 1973.

6. R. M. Abernathey, G. M. Matlack, and J. E. Rein, "Sequential Ion Exchange Separation and Mass Spectrometric Determination of ^{148}Nd, Uranium, and Plutonium for Burnup and Isotopic Distribution Measurements," in Analytical Methods in the Nuclear Fuel Cycle, Vienna, 1972 (IAEA), Paper IAEA-SM 149/37, SII/Pub/291, pp. 513-521.

7. S. F. Marsh, M. R. Ortiz, R. M. Abernathey, and J. E. Rein, "Improved, Two-Column, Ion Exchange Separation of Plutonium, Uranium, and Neodymium in Mixed Uranium-Plutonium Fuels for Burnup Measurement," Los Alamos Scientific Laboratory report LA-5568 (in print).

8. S. F. Marsh, M. R. Ortiz, and J. E. Rein, "Lanthanide-Trivalent Actinide Separation in Ethanol-Hydrochloric Acid," 17th Conference on Analytical Chemistry in Nuclear Technology, Gatlinburg, TN, October 23-25, 1973.

VIII. PAPERS PRESENTED

1. R. K. Zeigler, "Quality Assurance Plan for Mixed Oxide Fuel for LMFBR," 20th Western Regional Conference, American Society for Quality Control, Portland, OR, September 27-29, 1973.

2. S. F. Marsh, M. R. Ortiz, and J. E. Rein, "Lanthanide-Trivalent Actinide Separation in Ethanol-Hydrochloric Acid," 17th Conference on Analytical Chemistry in Nuclear Technology, Gatlinburg, TN, October 23-25, 1973.